UNIVERSITY OF MANCHESTER

Feedstock Recycling of Polymer by Hydrocracking

A Thesis submitted to the University of Manchester for the degree of Doctor of Philosophy in the Faculty of Engineering and Physical Science

Abdulrahman Zaid A Bin Jumah

2021

Department of Chemical Engineering and Analytical Science

Table of Contents

List of Figures

List of Tables

Abstract —PhD Thesis

With more stringent environmental regulation and taxation, rising landfill costs and the drive towards a circular economy, there is an increasing need to redirect polymer waste from landfill/energy recovery towards the enhanced recovery of chemicals and monomers. The most widespread approach to chemical recycling is pyrolysis (or cracking). However, a more effective option is that of hydrocracking, which offers the potential for the selective recovery of useful chemical fractions but is also tolerant of the presence of heteroatoms. The starting point for this study was to convert pure polymers representing around 70% of the total global production, namely, polyethylene (LDPE, HDPE), polypropylene (PP) and polystyrene (PS), into hydrocarbon gas and liquid, mostly in naphtha (C_5-C_{12}).

Reactions were carried out using a laboratory batch system at a relatively moderate temperature (≤330 ^oC), pressure (20 barg) and in the presence of zeolite catalysts of Beta and USY (typically loaded with Pt or Ni). The study was extended to test post-consumer polymers to simulate different types of waste streams, for example, solvent bottles (LDPE) and centrifuge tubes (PP) as well as consumer products by milk bottles (HDPE) and water drinking cups (PS). Typically, total conversion of pure polymers was achieved, and more importantly, a high proportion of the post-consumer polymers and blends tested were converted into gas (C_3-C_4) and naphtha fractions with a high proportion of branched isomers, which are valuable products in the petrochemical industry.

A kinetic study using a lumping model that describes the hydrocracking of LDPE was carried out. In developing kinetic model, mass transfer was taken into consideration and the results of the modelling project were compared with similar studies found in the literature but over thermal or catalytic cracking to prove the lower energy requirements of the hydrocracking.

Declaration

No portion of the work referred to in this thesis has been submitted in support of an application for another degree or qualification of this or any other university or other institute of learning.

Copyright Statements

i) The author of this thesis (including any appendices and/or schedules to this thesis) owns certain copyright or related rights in it (the "Copyright") and s/he has given The University of Manchester certain rights to use such Copyright, including for administrative purposes.

ii) Copies of this thesis, either in full or in extracts and whether in hard or electronic copy, may be made only in accordance with the Copyright, Designs and Patents Act 1988 (as amended) and regulations issued under it or, where appropriate, in accordance with licensing agreements which the University has from time to time. This page must form part of any such copies made.

iii) The ownership of certain Copyright, patents, designs, trade marks and other intellectual property (the "Intellectual Property") and any reproductions of copyright works in the thesis, for example graphs and tables ("Reproductions"), which may be described in this thesis, may not be owned by the author and may be owned by third parties. Such Intellectual Property and Reproductions cannot and must not be made available for use without the prior written permission of the owner(s) of the relevant Intellectual Propert and/or Reproductions.

iv) Further information on the conditions under which disclosure, publication and commercialisation of this thesis, the Copyright and any Intellectual Property and/or Reproductions described in it may take place is available in the University IP Policy (see http://www.campus.manchester.ac.uk/medialibrary/policies/intellectualproperty.pdf), in any relevant Thesis restriction declarations deposited in the University Library, The University Library‟s regulations (see http://www.manchester.ac.uk/library/aboutus/regulations) and in The University‟s policy on presentation of Theses

Acknowledgements

It is my pleasure to express my great thankful and deeply respectful to my supervisor, Prof. Arthur Garforth, for accepting me working in this interesting project, this work could not be successfully completed without his guidance and support. In addition, I would like to thank my co-supervisor Dr. Maryam Malekshahian for all the valuable time she has spent teaching and helping me to understand the modelling aspects in my project. Arthur and Maryam, thank you both for your constructive feedback throughout my PhD, and for encouraging me to give my best, even in my difficult times.

I would also like to acknowledge the effort and support of Dr. Aleksander Tedstone, Dr. Mohamed Aljamri and the technical support at the University of Manchester (Mr. Loris Doyle, Dr. Desmond Doocey and Mrs. Shahla Khan), and my friends and colleagues in the catalysis group.

I would like also to deliver my appreciation to my sponsor (King Saud University) for giving me this great opportunity to do a PhD degree in one of the top ranking Universities in the UK.

In addition, my inestimable appreciation goes to my parents, brothers and sisters for their permanent support over the distance. I am very thankful to my wife (Razan) for her exceptional support and encouragement during my study, and to my lovely daughter (Danah) for adding more happiness and pleasure to my life in Manchester.

List of Abbreviations

#	Number
3D	3 dimensional
APC	American plastic council
BET	Brunauer Emmett Teller
C	Concentration
Ce	Cerium
cm	Centimetre
Co	Cobalt
Cu	Copper
EFAL	Extra framework aluminium
FID	Flame ionization detector
g	Gram
G	Gas
GC	Gas chromatography
h	Hour
HDPE	High density polyethylene
HL	Heavy liquid
i-	Iso
k	Kinetic constant
La	Lanthanum
LDPE	Low density polyethylene
m	Mass
mm	Millimetre
Mo	Molybdenum

MOR	Mordenite
M_w	Molecular weight
N	Exchange flux
N	Naphtha
n-	Normal
Ni	Nickel
p-	Para
P	Pressure
PA	Area under the peak
PE	Polyethylene
PET	Polyethylene terephthalate
PP	Polypropylene
PS	Polystyrene
Pt	Platinum
PVC	Polyvinyl chloride
r_A	Reaction rate
RF	Response factor
rpm	Revolutions per minute
S	Exchange surface area
SEM	Scanning electron microscopy
T	Temperature
t	Time
TEM	Transmission electron microscopy
TGA	Thermogravimetric analysis
TPD	Temperature programmed desorption

USY	Ultrastable Y
V	volume
XRD	X-ray diffraction
α	Alpha
μm	Micrometer
η	Effectiveness factor

1 Introduction and Literature Review

1.1 Context and overview of the research problem

Polymers play a major role in enhancing living standards on a global scale. They contribute to facilitating human life in many different areas, including medicine, communication, transportation, agriculture, packaging, clothing, and construction.[1, 2] Their characteristics of light weight, low production cost, durability, and versatility make polymers commercially and economically attractive, and thus, they are now widely used in different applications.[3] Consequently, the dependency on polymer materials is growing.[3] The abovementioned characteristics have resulted in substituting many conventional materials, such as metal, paper and wood, and the demand for polymers has risen substantially and is expected to double in the next 20 years, reaching more than 600 million tonnes of production per year.[4, 5]

Synthetic polymers are primarily derived from oil and consist of long chains of repeating organic molecular units called monomers.[1, 5] The manufacture of polymers consumes about 8% of the total global oil production – 4% to synthesise the polymers, and 4% to generate the power for the manufacturing process. Polymers were first made in 1860 but were only developed by the industry in the 1920s, and polymer manufacturing is quickly becoming one of the fastest developing industries worldwide.[6] However, the increase in polymer production is inevitably leading to a greater accumulation of polymer waste.

Despite all the advantages of polymers, they have considerable adverse effects due to their slow degradation process and the irresponsible customer behaviour of using them only once. The effects have caused the environment to become heavily contaminated

by large volume of polymer waste, thereby endangering the biological equilibrium.[3] Synthesised polymers are not biodegradable, usually fragmenting slowly into smaller particles known as microplastics. These particles represent a major issue for the ecosystems, economy, and human health and have been found in the stomachs of different species, including earthworms, birds, turtles, and fishs.[7] It is almost impossible to collect them once they enter the environment since they are mixed with, e.g. sand. Hence, there are several worldwide initiatives to ban the production of single-use polymers, increase the efficient use of resources, and reduce resource dependency.[8, 9] These strategies mainly aim to prevent the environmental damage from single-use polymer being recklessly discarded.[8] A series of actions and strategies have been initiated to ensure the most efficient methods to reuse and recover the raw materials from which the polymers are made, thereby avoiding the linear utilisation of resources, and enhancing the circulation process. This circularity in producing and recovering polymer materials lies at the heart of the circular economy concept.[8]

On the other hand, one of the main challenges currently facing the petroleum industry is the need to start operating with non-traditional feedstocks, rather than crude oil only.[10] There are many reasons for this shift, including the high consumption of existing reserves, the fluctuating oil price, insecure supplies, and last but not least, environmental issues.[10] Against this backdrop, an efficient polymer waste management method could be used to achieve the global industrial target of a circular economy by utilising the waste and recovered feedstock material, sending it to oil refineries as a non-traditional feedstock.

1.2 Polymers

Polymers were first developed in the 1800s by Charles Goodyear when he discovered how to vulcanise natural rubber.[11] In 1909, and after several attempts to develop oil-based polymers, Leo Baekeland, a chemist scientist from Belgium, synthesised the first polymers to enter mass production, namely polystyrene (PS) and polyvinyl chloride (PVC).[12] The modern form of polymers emerged later in the 1900s, including PVC in 1926, PS in 1938, and high-density polyethylene (HDPE) and polypropylene (PP) in 1951.[13] A recent development in polymer manufacture has been the production of biodegradable polymers, including polyhydroxyalkanoates (PHA), polylactides (PLA), aliphatic polyesters, and polysaccharides, which are produced through the bacterial fermentation of biomaterials, such as sugars and lipids.[14]

Polymers are a generic group of natural or manufactured materials, including plastics and rubbers. They consist of numerous repeating structures called monomers, each consisting of a carbon chain accompanied by hydrogen, oxygen, nitrogen and other organic or inorganic elements; Figure 1-1 presents an example of the formation of polystyrene. The molecular weight of polymers is at least 100 times larger than that of smaller molecules, such as water or methanol, and therefore, polymers are known as macromolecules.[15, 16]

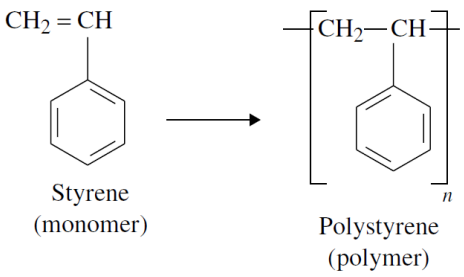

Figure 1-1 The formation of polystyrene from styrene; reproduced from [17].

Polymers have a variety of chemical structures, physical and mechanical properties, and thermal characteristics, among others. Synthetic polymers, for instance, have an

amorphous structure, low thermal conductivity, high electrical resistance, a low softening temperature and controllable elastic behaviour.[15] These polymers, which include polyolefins, are pre-formed in the liquid phase, then formed and moulded into different shapes by applying heat and pressure to be used in various applications. Polymers are divided into three classifications based on their structure and degree of polymerisation: linear polymers, where the monomers are single linear chains, such as polyester; branched polymers, where the monomers are linear chains with side chains, such as low density polyethylene; and cross-linked polymers, where two or more chains are joined by side chains, such as melamine and rubber.[17]

Polymers can also be divided into two groups based on their thermal behaviour, namely thermoplastics and thermosets. **Thermoplastics** are soft and flowing when heat is applied, and solidify upon cooling. Thermoplastics represent about 80% of plastic manufacturing output today.[17, 18] Polystyrene, nylon, polyvinyl chloride (PVC), and polyethylene are all thermoplastics. Thermoplastics can only be linear or branched polymers.[17, 18] In contrast, **thermosets** can only be formed once by applying heat and pressure, and they cannot be thermally reprocessed. Thermosets are usually cross-linked polymers.[17, 18]

1.2.1 Global polymer production

The global production of polymers continues to increase due to the huge demand based on their outstanding features compared to metal and wood. In 2019, the global production of plastic was reported to be 368 million tons, representing a 2.45% increase over 2018's production.[19] European plastic production reached 58 million tonnes in 2019, Figure 1-2 presents the distribution of the global production of plastic by region in 2019.[19]

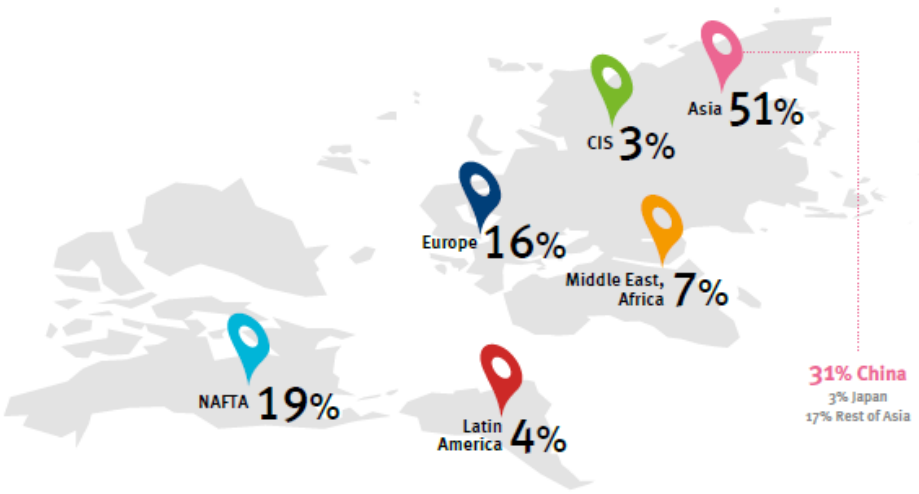

Figure 1-2 The global distribution of plastic production by region in 2019; reproduced from [20].

However, the continuous growth in the demand for and production of plastic inevitably leads to a greater accumulation of plastic waste, resulting in more serious environmental issues.

1.2.2 Global polymer waste

Polymer waste is a major concern for governments because if there is no efficient and safe waste management, the more polymers are produced, the more waste is accumulated. Polymers are intended to be lightweight and durable, yet many of them are only briefly in use. Geyer et al.[21] examined polymer production data to compare the product lifetime distributions for eight different product categories (Figure 1-3). The study aimed to estimate the time from a polymer being used to it reaching the end of its useful lifetime and disposal. Polymers used in packaging sectors have average lifetimes of less than a year, while those used in construction last for decades. Packaging is a recent application for polymers; occupying about 45% of the total global polymer production by volume, it remains essential to mainstream society.[22] Polymers used in packaging are mainly made of thermoplastic resins.[23] Different types of polymers are used for packaging, including polyethylene terephthalate (PET), high-

density polyethylene (HDPE), polyvinyl chloride (PVC), low density polyethylene (LDPE), polypropylene (PP) and polystyrene (PS).[23]

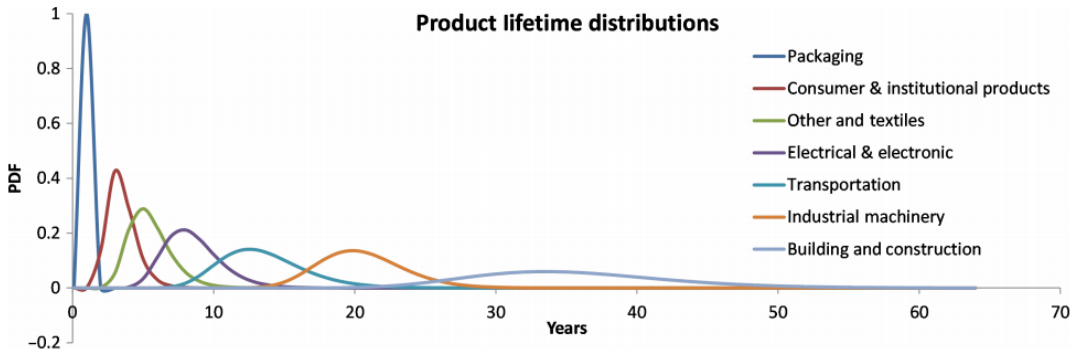

Figure 1-3 Product lifetime distributions for eight industrial use sectors, plotted as log-normal probability distribution functions (PDF); reproduced from [21].

From 2006-2018, the volume of the polymer waste collected in Europe increased by 19%, reaching 29.1 million tonnes. A large portion of that waste ended up in landfills (24.9%) or was incinerated (42.6%).[19] With the increase in polymer consumption and waste, serious action must be taken to develop eco-friendly methods of managing that waste and enhance the circular economy of polymer manufacturing. However, there are still some challenges associated with this kind of waste; these can be summarized in four following points:

Resistance to degradation: Polymers, in general, have poor biodegradability and they remain intact for hundreds of years, occupying considerable space in landfills. Apart from the economic loss due to the price of land for landfills, they are a developing environmental concern due to their effect on the atmosphere. The waste dumped in landfill generates greenhouse gases, such as methane, and may even pollute groundwater resources.[24]

Low density: Polymers are commonly used for packaging, and the discarded plastic items have a large volume and a large interior void. Hence, they occupy substantial space in landfills while incurring high transportation costs.[24]

Chemical additives: During the manufacture of polymers, chemical additives are incorporated with polymers to add certain features to the final products. Some of these additives are hazardous and must, therefore, be disposed properly.[25]

Difficult to separate: Polymer waste is usually a mixture of different types of polymer (e.g. labels and bottles are made of two different types of polymers). In addition, polymers are often co-extruded or laminated to provide bespoke properties, such as gas barrier membranes in PET bottles, making them difficult to separate.[26]

1.3 Circular economy

Moving towards a sustainable and circular economy, polymers play a major role due to their versatility and capacity for development and innovation. In the transport sector, for instance, lightweight polymers contribute to increased fuel-efficiency and a reduction in greenhouse gas emissions. In the construction sector, polymers are utilised as efficient and long-lasting insulators, such as in piping and water tanks, thereby saving the energy required to cool or heat a building. In addition, one of the main uses of polymers is for the safe packaging of goods and foods.[4, 27] However, to achieve a sustainable and resource-efficient economy, the core principles of the circular economy should be applied. These can be summarised in three activities: reuse at the product level, including repair and refurbishment; reuse at the component level by remanufacturing; and reuse at the material level by recycling. Extracting raw materials and processing them are energy and material-intensive processes and can cause significant harm to the environment. However, reprocessing post-consumer materials by any of the abovementioned creative methods of reuse would result in less (albeit non-negligible) environmental damage; see Figure 1-4.[28] In addition, when the primary production of polymer is minimised, natural resources, such as fossil fuels,

are preserved to ensure a sustainable future, thereby avoiding the dumping of polymer waste in landfills.[28]

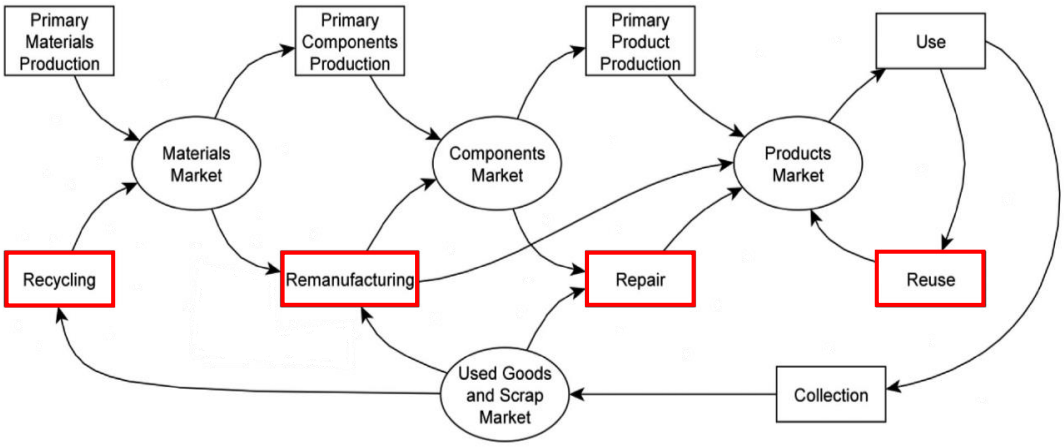

Figure 1-4 The circular economy system of interconnected markets, modified from [28].

The polymer circular economy is a closed process that avoids the single use of polymer products, and aiming to generate value from waste. Polymer waste is considered as a valuable resource that can be recovered and reproduced in the form of a new polymer, as feedstock material for petrochemical refineries, or to generate energy when recycling is not viable.[27]

The ideal solution to polymer waste is recycling; however, this requires significant advances in the chemistry of the thermoset resin to produce a chemical structure that can be reverse-polymerised.[4] Additionally, more legislation should be enacted to ensure the appropriate collection and disposal of domestic or industrial post-consumer polymers, since more than half of waste materials currently enter the mixed-waste stream.[27] Most recycled polymers now come from recycling bins (Figure 1-5), proving the crucial role of legislation and consumer behaviour.[27]

Figure 1-5 Statistical data of the source of recycled polymers; reproduced from [27]

1.4 Polymer waste management

The solution to the increase in accumulated polymer waste can be approached in three ways, namely substitution, reuse and recycling.[29, 30] Substitution proposes replacing polymer with a biodegradable material that is less harmful to the environment. However, polymers have developed to substitute various materials, especially for packaging, such as metal and wood, due to its lightweight character and relatively cheaper production cost. Currently, there are no effective alternative materials offering the same benefits as polymers. Another proposed method is managing the polymer waste by reusing the material, which would lead to a reduction in the waste volume. That is merely a partial solution as there is still polymer waste that needs to be managed, that is, discarded broken polymer products or those polymers at the end of their lifetime. The final approach is recycling, referring to the reclaiming of the chemicals used in polymers for reuse.[29, 30] Regardless of the approach, a sustainable future demands the consideration of the issue of polymer waste to prevent accumulation in landfills everywhere and to make the best use of it. Figure 1-6 summarises the growth in polymer waste and the treatment methods used in Europe

between 2006 and 2018.[20] The different recycling methods for polymer waste are discussed in detail in the next section.

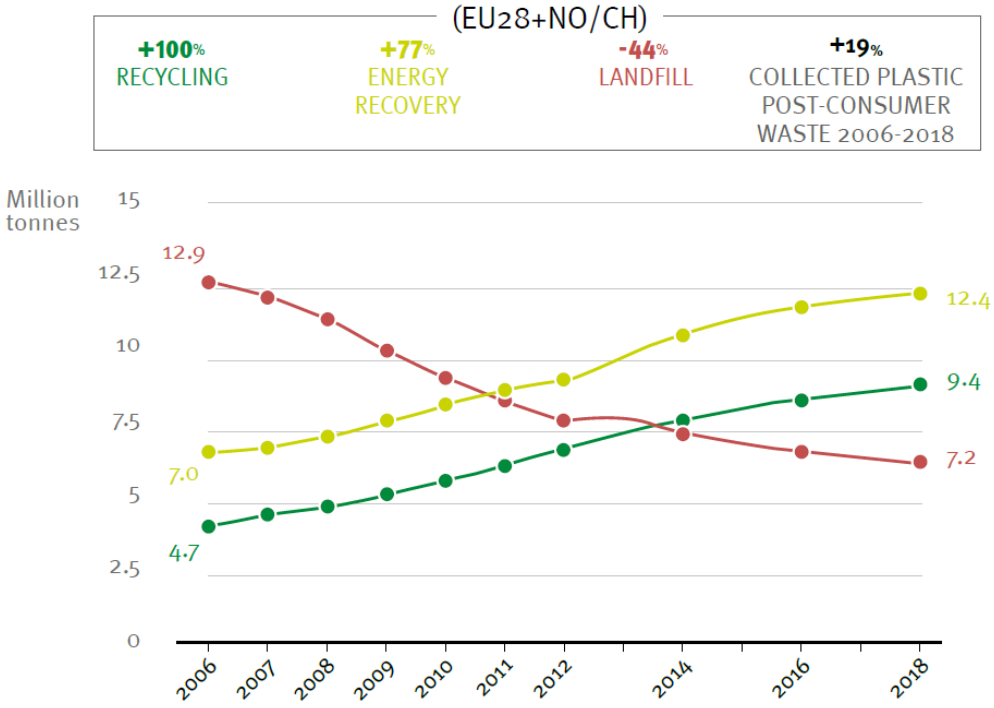

Figure 1-6 Evolution of plastic waste treatment in Europe (2006-2018); reproduced from [19].

1.4.1 Polymer recycling

Polymers can be recycled using many different techniques; these can be classified according to the final products as following:

Primary: The waste is processed to be reused again with the same characteristics and quality of the original material. This is only viable for thermoplastics, when the waste comprises of very pure polymers, and when there is no contamination.[31]

Secondary: The waste is used as a feedstock to produce lower quality polymer products. Mixed streams can be used, albeit limited by the compatibility of the polymer types in the feed stream. However, this method is not economically viable due to the high operation cost, the limited market, and the low price for the final products.[31]

Tertiary: Also known as chemical or **feedstock recycling**, the polymer waste is processed under high temperature and pressure to be decomposed into a basic hydrocarbon feedstock.[17] The thesis focuses on this type of recycling, and this method is discussed in more detail in the next section.

Quaternary: The waste is used as fuel to recover energy, e.g. as a heat source or to produce electricity via incinerators, due to the high caloric value (CV) of the polymers, which can match that of conventional fuels such as petrol and diesel, they can be used efficiently as fuel. However, the main concern for polymer waste **incineration** is the emission of complex pollutants and the environmental damage from greenhouse gas emissions.[31] Figure 1-7 summarises the various recycling techniques.

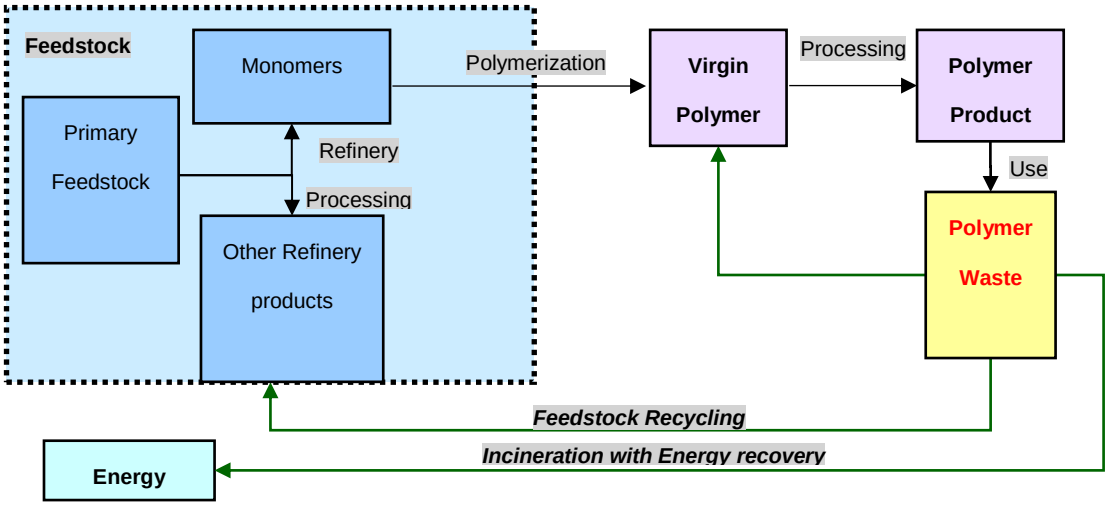

Figure 1-7 Recycling techniques; modified from [30].

1.4.2 Feedstock recycling

Feedstock recycling involves the decomposition of polymers into the original monomers or/and other hydrocarbon molecules by applying heat, pressure and/or chemical agents. The product can be used as a feedstock for polymer production or be added to refinery products, or be used directly as fuel. This recycling method is described as the most effective alternative mechanism for managing polymer waste.

However, it still has low contribution in the industry in that only 0.2% and 0.1% of the total collected post-consumer polymers were chemically recycled in Germany and Italy, respectively, in 2018.[19] For this method to be applied broadly, the total operational efficiency should be maximised by solving the technical issues, such as the high temperature and pressure requirements; this aspect forms the basis for the main objective of this thesis. Feedstock recycling can be approached via three pathways: depolymerisation, partial oxidation and cracking (thermal, catalytic and hydrocracking).

1.4.2.1 Depolymerisation

The depolymerisation, also known as chemolysis, of used polymers is a reversible reaction that involves a chemical agent to yield the starting monomers. Many processes have been developed and classified based on the chemical agent in the reaction, such as glycolysis and methanolysis.[29]

Polymers are divided into two categories based on the monomers they are made of, namely condensation polymers and addition polymers. Depolymerisation is only suitable for condensation polymers, such as polyamides, polyesters, nylons and polyethylene terephthalate (PET).[32] However, a study carried out by Kaminsky et al. [33] resulted in a yield of 98% monomers from the depolymerisation of polymethylmethacrylate (PMMA) at 450 ^{o}C. The restriction of this method to condensation polymers further limits its use due to the difficulties in separating the waste and the fact that the vast majority of polymer waste cannot be processed using this technique. Moreover, this technique is very sensitive to the impurities in the form of additives, and thus a high conversion rate can only be obtained for pure polymers.[32]

1.4.2.2 Partial oxidation

As stated earlier, the direct combustion of polymer waste causes significant damage to the environment due to greenhouse gas and possibly particulate emissions. Partial oxidation using oxygen and/or steam can overcome this issue to produce a mixture of hydrocarbons and syngas (H_2 and CO). The product of this method (syngas) is widely used in the chemical industry, both as a feedstock and a fuel. This mechanism has shown great success for the treatment of coal, heavy petroleum fractions, biomass and waste (including polymer waste).[32] For example, Wallman et al.[34] reported a hydrogen production of 60-70% from polymer waste using two-stage pyrolysis and partial oxidation. However, this method operates at very high temperatures (1200-1500 $^{\circ}$C), and requires an extensive amount of energy and expensive construction materials for the reactor unit, making it economically unviable. Moreover, it usually yields low-quality products requiring further upstream processing, and there is still a possibility of environmentally harmful emissions resulting from this process.[32]

1.4.2.3 Cracking

Cracking plastic waste is a similar concept to that utilised in petroleum refineries. It refers to the process of breaking large compounds into smaller ones, in terms of their molecular weight, as well as more valuable compounds. This approach can be achieved by heating and pressurising the waste in an inert atmosphere (pyrolysis) or by using hydrogen (hydrocracking). Pyrolytic methods can be either thermal or catalytic cracking.

1.4.2.3.1 Thermal cracking

Thermal pyrolysis is the process of heating polymers in the absence of oxygen (in an inert atmosphere, usually N_2) to decompose polymers, generating carbonised char and volatile fractions. The volatile fraction can be separated by condensing the liquid oil from the high calorific gas. The proportion of each of these mixtures depends on the waste nature and the process conditions;[29, 35-37] Figure 1-8 illustrates the mechanism of the thermal cracking of polystyrene.

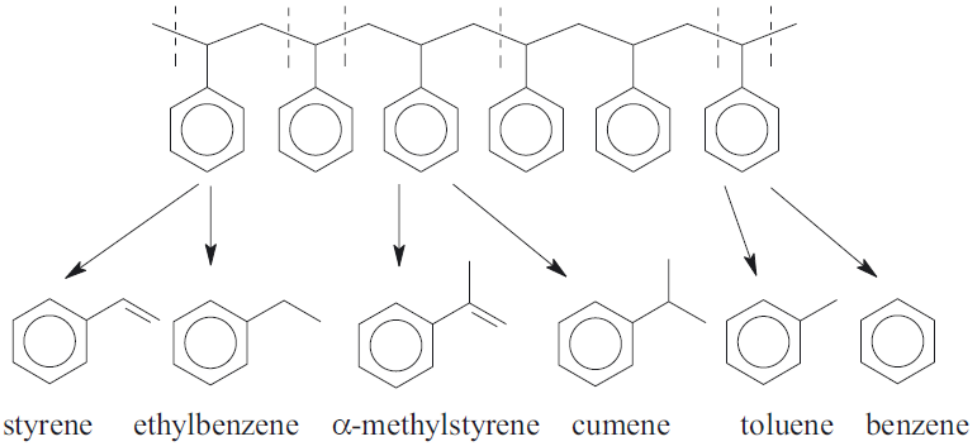

Figure 1-8 The reaction mechanism of cracking PS; reproduced from [38].

Polymer pyrolysis is performed at high temperatures of 500-800 °C and a complex polymer mixture can be processed without prior separation. However, this method has had little commercial success due to the high operating costs resulting from the intense energy demands.[29, 35, 37] Furthermore, the products are of low quality and require further treatment, leading to a reduced market price.

1.4.2.3.2 Catalytic cracking

There are numerous review articles on the topic of catalytic cracking,[39-47] and typically the work is carried out in batch[41, 42, 48, 49] and packed bed[39, 49, 50] reactors. Catalytic cracking was developed to mitigate the intensive energy demands of thermal pyrolysis by involving a microporous catalyst in the reaction, meaning it occurs at a lower

temperature of 350-500 ˚C.[35, 51, 52] Furthermore, the catalyst enhances the product selectivity toward a narrower distribution of hydrocarbons and a greater market value. Another advantage of catalytic cracking is that it avoids the formation of undesired species, such as halogenated materials from waste containing PVC.[35, 51, 52] Catalytic cracking typically occurs over acidic zeolites, such as ZSM-5, USY and Beta. The advantage of using zeolite is regarding the corresponding properties of zeolites structure including acid sites, micro/meso porous open structure, and relatively high specific surface area.[53-56]

Catalytic cracking can be carried out in a single or dual-step process. In the former, the polymer and the catalyst are in close contact inside the reactor at all times. In the latter, the polymer is initially cracked thermally and then the volatile product is exposed to the catalyst to boost the quality.[29, 57, 58] A two-stage laboratory batch reactor for catalytic cracking is presented in Figure 1-9.

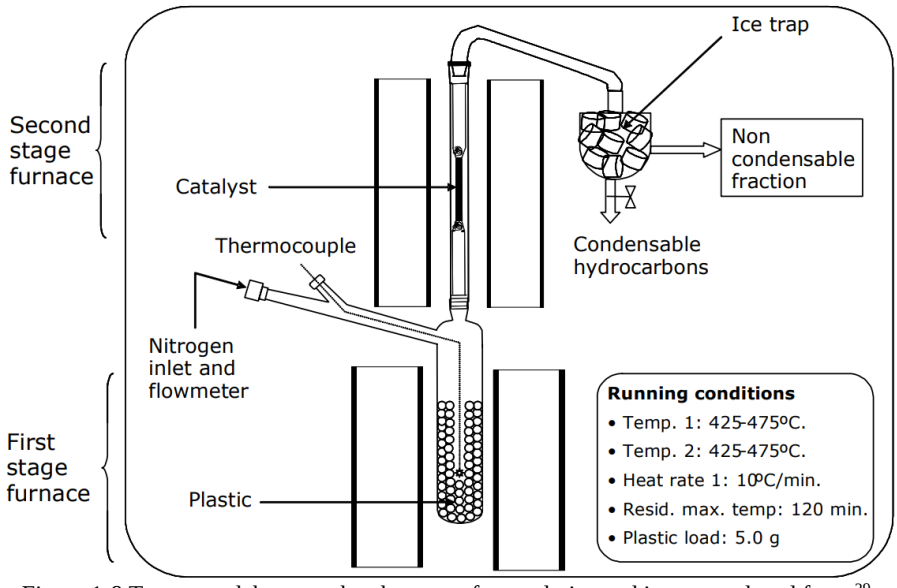

Figure 1-9 Two-stage laboratory batch reactor for catalytic cracking; reproduced from [29].

However, this process has some disadvantages, such as the high cost of the catalyst and its recoverability as well as the high energy requirements due to the highly endothermic reaction of catalytic cracking.[59, 60]

1.4.2.3.3 Hydrocracking

In this method, polymers are degraded under relatively mild heat and hydrogen pressure. This process overcomes most of the disadvantages of the previous methods as it is exothermic, in contrast to the highly endothermic reactions of thermal or catalytic cracking. The hydrogen pressure also contributes to a reduction in coke formation, which would otherwise deactivate the catalyst. This process consists of two reactions, namely cracking of the large polymer molecules and hydrogenation of unsaturated products. The hydrogenation, for fuel applications, ensures better quality and more valuable hydrocarbons with fewer aromatics and olefins and more isomerised alkanes.[61-64] However, the main drawback of this method is the need for high hydrogen pressure, which is mainly obtained by an expensive process of steam reforming in petroleum refineries.[65] Hydrocracking forms the core in this thesis and is discussed later in more detail.

1.4.3 Visible technologies for tertiary recycling

The following presents a brief summary of some of the facilities in use in Europe for the chemical recycling of post-consumer polymers.

1.4.3.1 Hamburg University, Ebenhausen

A small plant with a capacity of 5,000 tonnes per year was built based on Hamburg University's pyrolysis technology. The plant demonstrated great success in converting polyolefin (PE/PP), yielding 51% gas and 42% liquids. However, due to the instability of the oil price and its direct effect on the product price, the plant was not economically profitable to run on a small scale.[30]

1.4.3.2 BASF, Ludwigshafen

A large pilot plant with a capacity of 15,000 tonnes per year was designed to recycle mixed plastic waste supplied by Duales System Deutschland (DSD). In 1994, the BASF initiated a full-scale industrial plant, but two years later the plant was shut down due to the uncertainty of the long-term supply.[15, 17]

The plant consisted of three units that converted waste into petrochemical products. The plastic was melted in the first stage and then liquefied in an agitated tank. Meanwhile, a water washer absorbed the hydrochloric acid from the PVC at a temperature of >300 ˚C. Following that, the liquefied plastic was fed into a tubular reactor to be cracked at a high temperature of 400 ˚C. In the last stage, the product was separated into gases, oil and high-boiling point oil in a distillation column (Figure 1-10). The product distribution for this processes was typically 20–30% gas and 60–70% oil.[15]

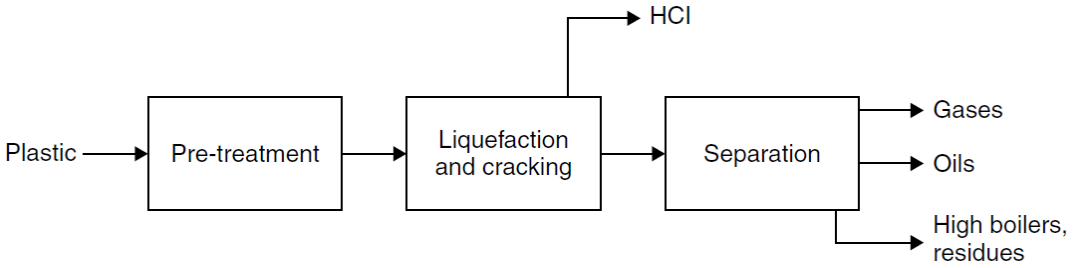

Figure 1-10 Operating schematic of BASF plant; reproduced from [15].

1.4.3.3 BP, Grangemouth

In 1998, BP Chemicals, in collaboration with VALPAK and Shanks & McEwan, started the POLSCO project to examine the profitability of recycling 25,000 tonnes of polymer waste per year.[15] This process required some pre-treatment of the feed, including a reduction in size and the removal of non-polymeric materials. After that,

the shredded polymer was fed into a fluidized bed reactor and heated to 500 ˚C in an inert atmosphere. When the polymer were thermally cracked, the produced hydrocarbons left the bed in gaseous form and the solid impurities with the formed coke remained in the reactor to be collected by the cyclone.

Figure 1-11 presents the flowsheet of the BP process. The process recovered light and heavy hydrocarbon fractions of about 85 wt.%. Moreover, success was achieved in removing chlorine, whereby the product stream contained only around 10 ppm of Cl. However, the process was not profitable due to the considerable amount of energy used for both the pre-treatment and the operation.[15]

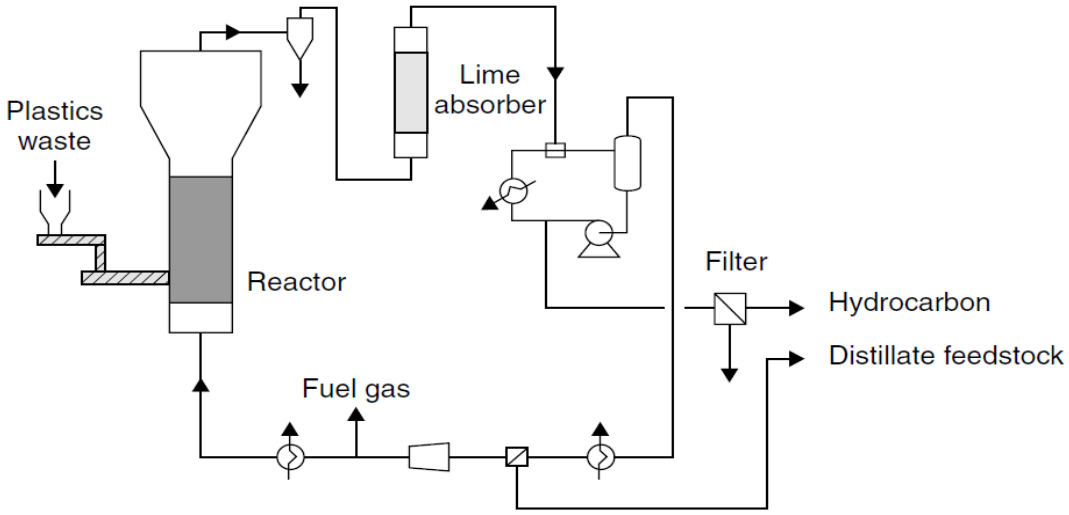

Figure 1-11 Process flowsheet of BP plant, reproduced from [15].

Those three examples highlighted the challenges facing the chemical recycling of polymers including intensive operation cost as well as the instability of feedstock supply caused by the inefficient collection of solid waste. However, the recent global movement toward a cleaner environment, by addressing stricter regulations against landfilling polymer waste and applying proper collections technologies of solid waste with encouraging individuals to separate their waste, has made chemical recycling of polymer waste visible. In the UK alone, number of companies are planning to build or

have already existing facilities for chemical recycling of polymers; examples of those companies are listed in Table 1-1.

Table 1-1 Chemical recycling plants or plants under construction in the UK

Company	Description
Recycling Technologies[66]	Pyrolysis recycling machine was developed to convert household and commercial polymer wastes into wax and liquid oil fractions, and patented by *Recycling Technologies, RT7000.*[67] A pilot plant using this technology is already established in Swindon and the full-scale commercial RT7000 plant with a capacity of 7,000 tonnes per annum is being constructed in Scotland to be on stream by 2021.
ReNew ELP[68]	*ReNew ELP* planning to construct the world's first commercial-scale Cat-HTR™ plastic recycling plant in 2021. The technology is based on hydrothermal upgrading using supercritical water to convert plastic waste into smaller and stable hydrocarbons (naphtha). The first phase of construction will have a capacity of 20,000 tonnes per annum and due to be completed by 2022.
Enval[69]	*Enval treats plastic better*, has developed a full commercial scale pyrolysis plant for low density packaging waste containing laminated materials and aluminium laminates feedstock.
Plastic Energy[70]	*Plastic Energy* already run two commercial polymers into oil recycling plants in Spain, which have been in operation since 2017. The technology used is based on a patented Thermal Anaerobic Conversion (TAC) technology.[71] In addition, an agreement have been signed with Viridor in May 2020 to build a new 30,000 tonnes per annum capacity chemical recycling plant in Scotland by 2023.
Quantafuel[72]	*Quantafuel UK Ltd* is going to build four chemical recycler plants based on a patented pyrolysis technology.[73] The capacity of each plant is going to be 80,000 tonnes per annum and to be run by 2024.

1.5 Hydrocracking of polymer waste

Hydrocracking is the process of converting high-boiling molecules into more valuable and lower molecular weight substances, with a high selectivity towards iso/normal paraffins and low olefin yields. This process breaks the carbon bonds of large hydrocarbons and simultaneously hydrogenates unsaturated cracked products;[74] the overall mechanism of hydrocracking is shown in a simplified form in Figure 1-12. Hydrocracking is a complex process, and it remains difficult to predict the real molecule kinetics of the process or the accurate distribution of the outputs.

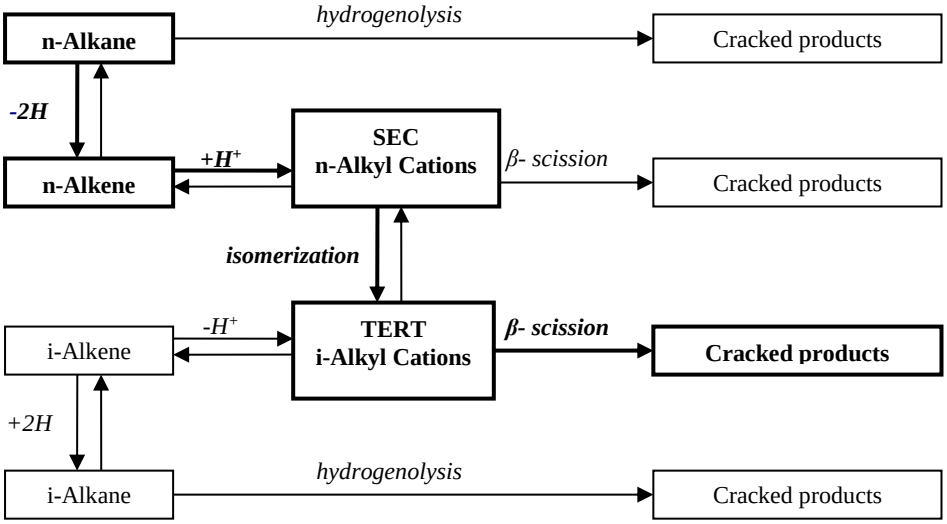

Figure 1-12 Overall mechanism of the hydrocracking reaction; reproduced from [75].

Hydrocracking is the most versatile process in modern petroleum refineries due to its flexibility and operational tolerance regarding both feedstock and products, enabling refineries to achieve an economical balance in terms of demand and supply.[76, 77] This flexibility is a reflection of advances in catalyst development, whereby the process design allows catalysts to operate efficiently, facilitating the optimal integration between hydrocracking and other refining processes.[77] In addition to being a vital process in modern refineries, hydrocracking also shows great promise for recycling polymer waste. The advantages of polymer hydrocracking are as follows:[78, 79]

- Polymers can be converted in a single stage without prior treatment or heating.
- The presence of hydrogen promotes the removal of any heteroatoms in polymer waste, such as chlorine, sulfur and sodium.
- The separation requirement for the product is less than for the pyrolysis process due to the narrower range of hydrocarbons produced by hydrocracking.
- The product stream is rich in valuable high-quality saturated hydrocarbons (more paraffins and less olefins).

- The catalyst can be regenerated in situ during the reaction, thereby minimising the deactivation caused by coke formation.

The hydrocracking of polymers usually occurs in the presence of a bifunctional catalyst at moderate temperatures (300-450 °C) and a relatively high cold hydrogen pressure (20-150 bar).[24] Thermal cracking and hydrocracking reactions are complementary, whereby cracking is endothermic and hydrogenation is an exothermic reaction.[24] Elevated hydrogen pressure is required to enhance the hydrogenation reactions, decrease the formation of coke, and prevent polymerisation.[24] The following sections review the potential catalysts and reaction conditions based on the existing literature.

1.5.1 Effect of reaction parameters on the hydrocracking of polymers

Numerous parameters can affect the reaction rate in the hydrocracking of polymer. Essentially, the cracking activity depends on, the reaction temperature and pressure, the quality of the feedstock, and the activity and selectivity of the catalyst.[75] This section focuses on those four main parameters.

1.5.1.1 Effect of reaction temperature

Reaction temperature plays a major role in the hydrocracking performance and product distribution, and many researchers have discussed the influence of the hydrocracking temperature. Luo and Curtis[80] and Joo and Curtis[81] reported similar conclusions, namely that increasing the hydrocracking temperature enhances the conversion rate. In the case of Luo and Curtis, [80] increasing the temperature from 400 to 440 °C doubled the degradation of LDPE over an alumina catalyst. Joo and Curtis[81] found that it is inefficient to operate the reaction of LDPE (over $NiMo/Al_2O_3$) at 400

℃ compared to 430 ℃ based on the large difference in the degradation rate. These two studies underline the importance of the hydrocracking temperature and how a small change can make a remarkable difference in certain critical temperature ranges.

Venkatesh et al.[82] found a significant increase in the conversion rate of HDPE over a 0.5%Pt/ZrO_4/SO_4 catalyst by increasing the temperature from 325 to 375 ℃. At the lower temperature, the conversion was only 25% for a reaction time of 60 min, and almost full conversion was achieved at 375 ℃ for a shorter reaction time (25 min). Furthermore, the authors reported that at the higher temperature, the selectivity was toward the liquid product, which was the most desirable product. Another study carried out by Rothenberger et al.[83] observed a similar finding regarding the positive effect of high temperature on the hydrocracking of HDPE and polymer mixtures consisting of 50% PE, 35% PS and 15% PET. The conversion of HDPE and mixed polymers increased from 5% and 38% at 430℃ to 15% and 65% at 445 ℃, respectively, over an aged Ni-Mo supported alumina catalyst (known as AO-60). However, the study reported increased selectivity towards gaseous products at the higher temperature. Liu[84] showed that prolonging the reaction time or reaction temperature enhances the total hydrocracking activity, but minimises the yields of C_9-C_{15} (jet fuel range hydrocarbons) due to further cracking. Therefore, maximising the hydrocracking temperature leads to a higher conversion rate but not necessarily the preferred selectivity to a valuable product. The rate of thermal cracking is increased at high temperatures, yielding lighter products and more coke decomposition, resulting in increased deactivation of the catalyst.

On the other hand, Zmierczak et al.[85] concluded that an increase in temperature could be effective until a point where any further increase only effects in a negligible

difference in the conversion rate. Their study was on the degradation of PS over a Fe_2O_3/SO_4 catalyst, and the conversion increased from 71 to 89% in the temperature range of 350-400 ℃ and then remained almost constant at 425-450 ℃ with a conversion of 92%.

In practice, the optimum temperature is difficult to predict due to the change in the feed composition in each polymer waste batch. Therefore, literature and experiments reported later in this thesis suggests a moderate hydrocracking temperature to achieve a balance between enhancing the conversion, improving the selectivity of liquid products, retaining the catalyst activity by reducing the coke formation, and most importantly, lowering the operational costs.

1.5.1.2 Effect of hydrogen pressure

The presence of the hydrogen, as stated earlier, enhances the total activity of the polymer hydrocracking process as well as the quality of the products. Ding et al.[74] investigated the effect of hydrogen pressure on the conversion of American Plastics Council (APC) waste over Ni supported an activated silica alumina (Ni/HSiAl) catalyst at 375 ℃. The finding was that the initial increase of hydrogen pressure from 18.3 to 52.2 bar H_2 enhances the reaction performance, while the effect becomes negligible with a further increase, as shown in Figure 1-13. In terms of the product distribution, the liquid yield followed the conversion trend and a relatively small change was observed in the gas yield with a pressure difference.

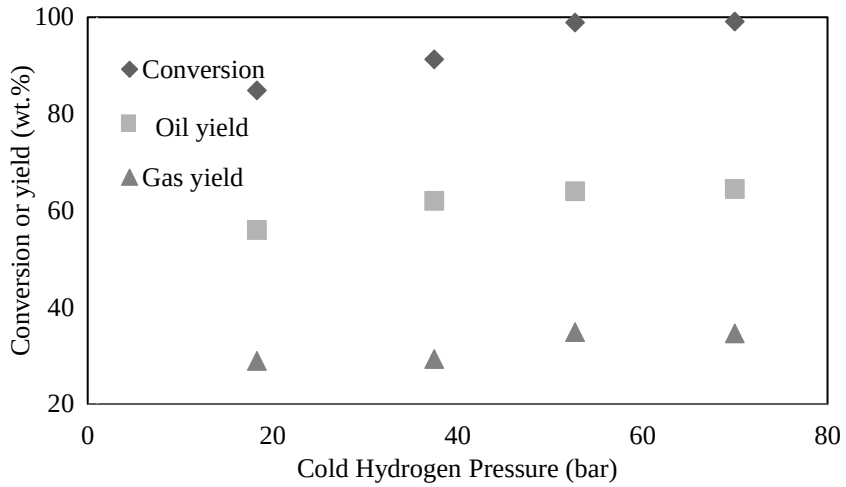

Figure 1-13 Effect of hydrogen pressure on hydrocracking of APC plastic waste over Ni/HSiAl; adapted from [74].

Conversely, Venkatesh et al.[82] claimed that a change in pressure does not affect the degradation rate but rather the product distribution. The study was carried out on the hydrocracking of HDPE at 375 °C over a $0.5Pt/ZrO_2/SO_4$ catalyst and with a reaction time of 25 min. With a lower hydrogen pressure of 53 bar, there was more liquid product, namely 80%, whereas the liquid yield at 84 bar H_2 was 69%. Linking this work with Ding et al,[74] it supported the conclusion made by Ding that varying the hydrogen pressure does not lead to a visible difference in the conversion rate at high pressure (i.e. >50 bar). According to Edwin G et al.[86], in their study on the transport phenomenon in the catalytic hydrocracking of PS in solution, observed no significant improvement in the PS reaction rate even at a pressure of 140 bar H_2. One explanation might be due to the saturation of sites on the catalyst surface with hydrogen, contributing to the absence of a gas−liquid mass transfer limitation.[87] Regarding the effect of hydrogen pressure on coke formation, Akah et al.[88] measured the difference in the coke formed under different pressures. They found that increasing the pressure decreased the coke formation rate.

To summarise, hydrogen pressure enhances the conversion of polymer hydrocracking and increases the selectivity toward liquid products, although these effects decrease

when the pressure is elevated too high. Moreover, the product can be modified by maximising the pressure, which could be useful to remove impurities as well as reduce coke formation, resulting in a more active and reliable catalyst. However, from an economical and safety point of view, lower hydrogen pressures are preferred to reduce safety risks as well as the operational and capital costs.

1.5.1.3 Effect of reaction time

Reaction time is an important factor that can vary the extent of polymer degradation as well as the quality of the products. Shabtai et al.[89] studied the effect of reaction temperature in the hydrocracking of PP over a ZrO_2/SO_4 catalyst under reaction conditions of 410 ℃ and 104 bar H_2. Their observation was that the degradation continued to increase with time, but not with the same increment. At low reaction time (30 minutes), the conversion increased rapidly to 87%, however, it then increased slowly to reach full conversion at 60 min. therefore, it is expected that if the reaction is thermal, the conversion will continue but the rate falls as the concentration of the polymer decreases (Figure 1-14).[90]

$$(-r_A)_P = kC_A \quad (1)$$

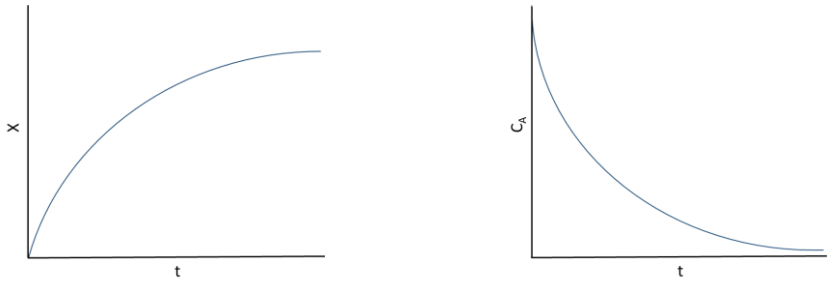

Figure 1-14 Typical conversion and concentration profiles against reaction time for batch reactor.

However, when a more active catalyst is used, Venkatesh et al.[82, 91] found that after a short reaction time, the effect of time on the conversion was insignificant, but the

product distribution changed significantly by lengthen the reaction time. After a 20 minutes of reaction time, the liquid yield from degrading PP over a 0.5%Pt/ZrO_4/SO_4 catalyst at 325 ℃ and 84 bar H_2 was 90%, and almost all that liquid was converted into gas over a reaction time of 60 min. Therefore, the original product (liquid) was converted over extended reaction time in a series type of reactions into gas (Figure 1-15)

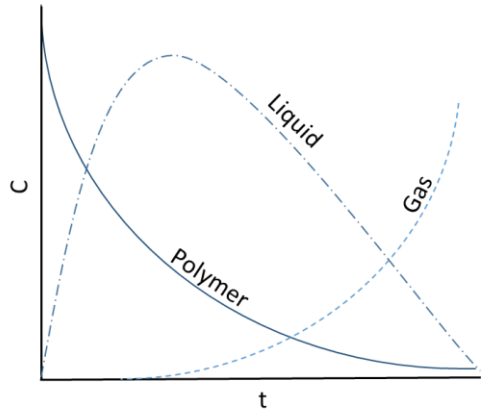

Figure 1-15 Typical concentration profile for liquid and gas products against reaction time in polymer hydrocracking.

To summarise, if the hydrocracking procedure occurs over a bifunctional catalyst, the cracking reaction is rapid compared to thermal hydrocracking, which increases gradually with time. Therefore, lengthening the reaction time over a bifunctional catalyst results in more cracking, leading to the conversion of the initial product, liquid, to lighter gaseous products. Therefore, a short reaction time is recommended if the catalyst is active enough to avoid over-cracking the desired product; this would be economically beneficial and reduce the operation cost. A rapid reaction time would also allow the process to be considered for continuous operation, reducing significantly reactor operational cost (e.g. heating, cooling, emptying and cleaning).

1.5.1.4 Effect of type of feed

One of the biggest challenges facing the hydrocracking of polymer waste is that the composition of the materials in the feedstock varies between batches. The reaction performance and the quality of the products rely heavily on the type of polymer fed to the reactor. Various types of virgin and waste polymer were tested in the literature to observe which conditions produce the best performance. Ali et al.[92] tested five different types of polymers (PS, PET, PP, LDPE and HDPE) over different catalysts to study hydrocracking. They found that PS was fully converted and produced the highest amount of liquid under the study conditions (430 °C and 83 bar), while HDPE and LDPE were the most difficult to be degraded and produced the highest gas yield. Similarly, Venkatesh et al.[82] degraded HDPE, PP and PS over two different metal-supported catalysts and observed that PS required the lowest temperature of 300 °C for complete degradation. Following that, PP converted completely at 325 °C, while only 25% of HDPE was converted at the same temperature. However, the selectivity of gasoline was the highest in the HDPE degradation. Venkatesh et al.[91] stated that the high conversion of PP was due to the alternating of carbon atoms in the branched structure of the PP.

Kohli et al.[93] observed that by adding waste polymer to heavy crude feeds, the hydrocracking yield of saturated hydrocarbons and aromatic increases, and the amount of asphaltene and resin is minimised over reaction condition of 420-450 °C, 60 bar and 2 h. This indicates that the polymer is hydrocracked at high temperatures into smaller molecules to yield a hydrogen-rich hydrocarbon stream and reactive hydrogen. This hydrogen typically takes part in hydrogenation reactions, thereby increasing the H/C ratio and decreasing coking.

To sum up, some polymers are more easily cracked than others, broadly PS > PP > HDPE + LDPE, based on their chemical structure, and the selectivity and quality of the liquid products vary based on the type of polymers in the feedstock. Moreover, the impurities present in the waste mixture can substantially affect the performance of the reaction with much reduced rate and heavier products (waxes, tars). Therefore, a reliable catalyst should be developed to tolerate the variety of chemicals which are added to or contaminate polymer waste and thus enhance the hydrocracking process.

1.5.1.5 Effect of type of catalyst used

Catalyst plays a major role in polymer hydrocracking as it enhances the cracking under modest reaction conditions. A hydrocracking catalyst must be bifunctional to functionalise both the cracking of high molecular weight hydrocarbons and the hydrogenation of the unsaturated products formed during the cracking steps.[94] A typical cracking catalyst support is silica-alumina incorporated with a base or a noble metal as the hydrogenating catalyst. Hydrogenation enhances cracking as it hydrogenates coke precursors, such as aromatics, as well as the coke deposited on the catalyst, thus slowing deactivation and lengthening catalyst lifetime. The coordination of these activities is based on the amount of metal placed on the acidic support, and this enhancement achieves when a certain metal loading is reached.[94] The literature usually describes cracking catalysts that are a combination of silica and alumina, including acid-treated aluminosilicates, amorphous synthetic silica-alumina, and crystalline, synthetic silica-alumina, also known as zeolites or molecular sieves. All of these are thermally stable acid catalysts and their cracking activity is based on their acidity. Lewis and Brønsted acid sites are present and active in the case of silica-alumina catalysts, and their ratio is dependent on the hydration degree of the catalyst.[95]

The silica-alumina ratio determines the number of active sites and their specific activity.[96] The rest of this section reviews several studies on the hydrocracking of polymers over different catalysts.

Huffman et al.[97] and Shah et al.[98] compared the performance of thermal hydrocracking with catalytic hydrocracking using a very small amount of catalyst. The comparison was carried out for a mixture of washed waste (APC plastic waste) over ZSM-5 for 60 min at 445 ℃ and 14.8 bar H_2. The results showed that the addition of 1% catalyst enhanced the quality of the liquid products, with the gasoline selectivity was increased. In line with this, Rothenberger et al.[83] investigated the effect of catalytic hydrocracking over a molecular sieve catalyst (13X) compared to thermal hydrocracking. The conversion over the catalyst was increased by 16% compared to thermal hydrocracking at 430 ℃ and 70 bar H_2. The improvement with using catalyst was further supported by the findings of Liu and Meuzelaar[99] and Ding et al.,[74] who showed that the presence of a NiMo/SiO_2-Al_2O_3 catalyst was advantageous to the reaction rate compared to thermal hydrocracking. The addition of the catalyst increased the conversion rate from 63% to 71%, and the liquid product yield from 40% to 47%.

As mentioned earlier, catalyst acidity is required for hydrocracking reactions and thus, knowledge of the necessary type and quantity of acid sites is essential. Ochoa et al.[100] studied the effect of the acidity characteristics of different catalysts on the degradation of medium-density polyethylene (MDPE) at 420 ℃ and 55 bar H_2; the catalysts they used and their properties are listed in Table 1-2. Their study showed similar conversion rates over pure SiO_2 and Al_2O_3 compared to thermal hydrocracking. There were no changes in the hydrocracking activity by using pure SiO_2 and Al_2O_3, and that is

because the former has negligible acidity, while the latter does not contain any strong acid sites, which are essential for the cracking reaction.[101] However, the increase in total acidity in the SiO_2-Al_2O_3 catalysts does not affect the liquid production, and the liquid yield is found to be solely a function of Brønsted acidity. Meanwhile, the gas yield is not a function of the acid site type, and the difference in all cases was less than 1%.

Table 1-2 Properties of the catalysts used by Ochoa et al.[100] and the concentration of pentane-soluble oils products from the hydrocracking reaction of MDPE at 420 °C, 55 bar and 15 min.

Catalyst	Surface area m^2/g	Total acidity mmol/g	Brønsted/Lewis ratio	Concentration of pentane-soluble oils %
SiO_2	187	0.001	0	26
25%SiO_2-75%Al_2O_3	238	0.5	0.2	73
50%SiO_2-50%Al_2O_3	250	0.4	0.3	84
75%SiO_2-25%Al_2O_3	277	0.3	0.7	82
Al_2O_3	150	0.3	0	-
No catalyst	-	-	-	22

Moreover, Ali et al.[92] tested HDPE, LDPE, PS, PP and PET over four catalysts (ZSM-5, presulfided NiMo/γ-Al_2O_3, presulfided NiW/SiO_2-Al_2O_3 and metal-supported zeolite Y) for 60 min at 430 °C and 83 bar H_2. The results showed that the highest conversion and selectivity towards liquid product was over ZSM-5, Table 1-3. Moreover, the authors concluded that alumina was not as active as amorphous SiO_2-Al_2O_3 or zeolites because of its lower acidity. This observation was also supported by Mosio-Mosiewski et al.[60] who tested the recycling of LDPE using NiMo/Al_2O_3 as a catalyst. They demonstrated that the addition of the non-acidic catalyst did not change the conversion compared to the thermal hydrocracking. However, less isomerised hydrocarbons and no aromatics were produced over the NiMo/Al_2O_3 catalyst compared to the liquid produced by the thermal process; this is due to the strong metal

sites provided by the NiMo, which enhance the hydrogenation of non-saturated products.

Table 1-3 Conversion and liquid selectivity of hydrocracking different types of polymers done by Ali et al.[92] over ZSM-5 catalyst at reaction conditions of 430 ℃, 83 bar H_2 and 1 h

Polymer type	Conversion %	Liquid selectivity %
LDPE	55	88
HDPE	55	63
PS	100	91
PP	70	91
PET	74	90

Regarding the effect of the metal loading on the catalyst, Venkatesh et al.[82] hydrocracked HDPE, PP and PS over different catalysts (ZrO_2/SO_4, 0.5%Pt/ZrO_2/SO_4, 2%Ni/ ZrO_2/SO_2 and 1%Pt/ γ-Al_2O_3) at 375 ℃ and 83.8 bar H_2. The conversion over 0.5%Pt/ZrO_2/SO_4 and 2%Ni/ZrO_2/SO_4 was almost the same and a high iso/n-alkane ratio was obtained over both catalysts. On the other hand, an insignificant conversion of PP was obtained over a weak acidic catalyst of 1%Pt/γ-Al_2O_3, and the non-metal-functionalised ZrO_2/SO_4. Moreover, Hesse and White[102] and Akah et al.[88] investigated the function of Pt over zeolite USY in the hydrocracking of HDPE at 310 ℃ and 55 bar H_2. Compared to the USY catalyst, the 1%Pt/USY obtained a higher conversion and higher gas product, while three times less coke was formed. The absence of the hydrogenation function in the USY catalyst promotes the formation of aromatics and polyaromatics in large pores, resulting in high coke formation and catalyst deactivation. That finding demonstrated that the loading of Pt enhanced the hydrocracking reaction and increased the stability of the catalyst through the hydrogenation of precursors and coke formed. A study by Aljabri et al.[48] on the catalytic cracking of PS over 3%FeCu/ Al_2O_3 and at a low temperature of 250 ℃ showed the full degradation of PS with 60% liquid yield.

To sum up, the catalyst facilitating hydrocracking of polymers requires both acidic and hydrogenation-dehydrogenation functions. It is also desirable to have a hydrotreating ability in order to tolerate the presence of impurities in the used polymers.[103] Metal-supported zeolites are good examples of successful hydrocracking catalysts, and it is that type of catalyst will be utilised in this thesis. Finally, to make the process commercially feasible, it is recommended that the amount of the catalyst to dry polymer is as low as possible, for example 3-10 wt.%.

1.6 Zeolites as catalysts

Zeolites have been shown to be active catalysts for the hydrocracking of polymers. Zeolite types and their pore structure have a significant impact on hydrocracking activity, selectivity and stability. The following sections focus on zeolite properties as a catalyst for the hydrocracking reaction.

1.6.1 Definition and structure

Zeolites were discovered by the Swedish mineralogist Axel Cronstedt in 1756 when he found minerals containing hydrated aluminosilicates, occupied by cations and water. He named those materials zeolites, a Greek word derived from the words “zeo” (to boil) and “lithos” (stone), because he observed that intumescent crystals formed after heating the material with a blowpipe flame.[104-107]

Zeolites are well-defined crystalline aluminosilicate consisting of aluminium, silicon and oxygen in a regular framework. Their structure is formed by silicon and aluminium sharing oxygen atoms, and it represents a regular structure of $[SiO_4]^{4-}$ and $[AlO_4]^{5-}$ tetrahedral units. These tetrahedral units form frameworks with small pores

and cages, and these voids have different sizes, ranging from 0.1 to 1.0 nm.[108] The general chemical formula of a zeolite is:

$$M_2/nO.Al_2O_3.ySiO_2.wH_2O \quad (2)$$

Where, "n" represents the cation valence number, "y" is in the range of 2-10, and "w" is the number of water molecules that the zeolite's voids contain.[108] Zeolites are commonly classified based on their pore dimensions, as shown in Table 1-4.

Table 1-4 Classification of zeolites based on pore size; adapted from [109, 110]

Classification	Channel diameters	Pore opening of tetrahedral units	Example
Small-pore zeolites	up to 0.43 nm	8-MRs	Erionite and A
Medium-pore zeolites	up to 0.55 nm	10-MRs	ZSM-5 and ZSM-11
Large-pore zeolites	up to 0.75 nm	12-MRs	Y, Beta and Mordenite
Extra-large-pore zeolites	> 0.75 nm	14 or more MRs	ITQ-33 and ITQ-37

1.6.2 Zeolite structures

This section focuses on zeolite USY and Beta because they are classified as large-pore, highly acidic zeolites and hence more suitable for catalysing large molecules, such as polymers.

1.6.2.1 Faujasite (zeolite USY)

Faujasite, discovered in 1842 by French geologist Damour, is a zeolite family that can be synthesised industrially.[111] The faujasite family includes zeolites X, Y, ECR-4, ECR-32, EMC-1 and CSZ-3. Zeolite USY has the most open zeolite structure with the widest channel system among zeolites. It has a three-dimensional pore structure based on sodalite cages (β-cages) that consist of 24 T atoms. The sodalite cages are connected through double 6-ring windows, known as "hexagonal prisms", creating a larger cavity with a pore opening (12 T atoms) and a diameter of 0.74 nm and the large

cavity being called α-cage (1.5 A°), which interconnects with the 12-membered T atoms (Figure 1-16).[112] Zeolite USY is commonly used in petroleum refineries, such as in hydrocarbon cracking, due to its activity and stability at high reaction temperatures.[113, 114]

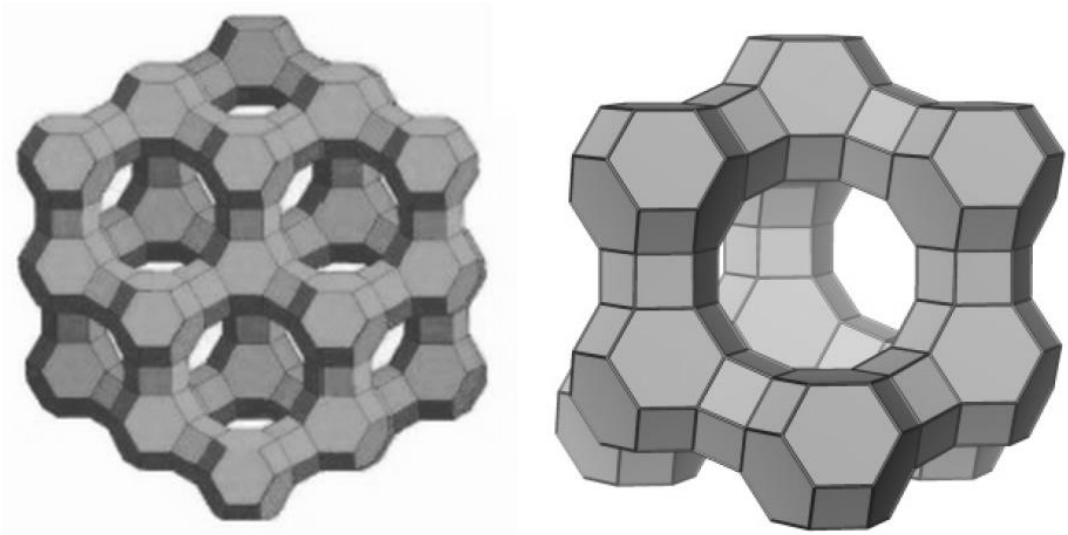

Figure 1-16 The framework structure of zeolite USY, formed by interconnecting sodalite cages through double 6 rings and creating large α-cage; adapted from [115].

1.6.2.2 Beta

Zeolite Beta was first synthesised in 1967 by Robert Wadlinger and has a three-dimensional intersecting channel system with 12-membered T atoms.[116] The pore dimensions are 0.66 × 0.67 nm for the straight channels and 0.56 × 0.56 nm for the sinusoidal channel. The primary building unit is composed of 16 T units sell: four fused 6-rings or eight fused 5-rings (Figure 1-17).[117]

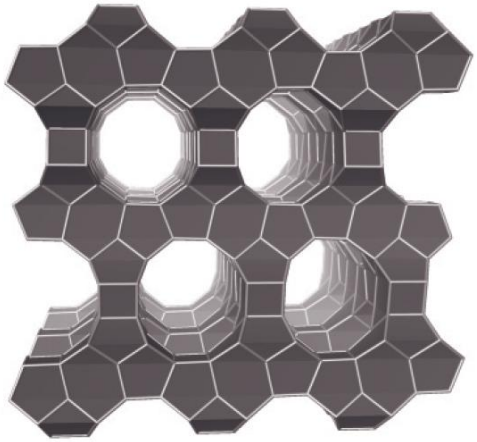

Figure 1-17 The framework structure of zeolite Beta, showing 12-membered T atoms and three-dimensional channels; adapted from [115].

The thermal stability and strong acidity of zeolite Beta makes this catalyst an attractive agent with increased application in the petrochemical industry, such as in aromatic alkylation,[118] and the nitration of aromatic compounds.[119]

1.6.3 Zeolite physical properties

Zeolites are used in a wide range of applications due to their unique properties as catalysts; these are described in this section.

1.6.3.1 Acid properties

The acidity of zeolites is one of the key features for their use as catalysts in the hydrocracking processes. Brønsted acid sites are formed by hydroxyl bridge between aluminium and silicon atoms. The higher the number of aluminium atoms in the zeolite structure, the higher the number of these sites; furthermore, the lower the Si/Al ratio, the more Brønsted acid sites a zeolite has as the hydroxyl bridge acts as a proton donor.[120] On the other hand, Lewis acidity is present as extra framework aluminium (EFAL), which migrates to the surface from the framework, creating a defect. These aluminium species are non-tetrahedral. This electron-pair-accepting EFAL (Lewis acid sites) can be formed by high temperature steaming zeolites.[120]

Zeolites are also available commercially in ammonium form, or protonated form (or H form), and sometimes in sodium form. Zeolite are mainly manufactured using silica, alumina, water and sodium hydroxide. To obtain the acidic hydrogen-form, it is necessary to exchange the sodium cation (compensating for the framework charge) with ammonium ions and then heat to generate the protons acid sites.

1.6.3.2 Shape selectivity

Zeolites are well known as selective materials, and the selectivity of products formed over zeolites is influenced by the pore dimensions and the channel system. Therefore, the internal pores of the zeolite structure should have similar dimensions to the desired product molecules. The shape selectivity of zeolites can be classified into three types: reactant selectivity, product selectivity, and transition state selectivity.[121-123]

1.6.3.2.1 Reactant selectivity

The diffusion of the reactants to the zeolite's active sites is limited by the size of the zeolite pores. Thus, the reactant molecules should have a smaller diameter than the pores of the zeolite; otherwise, they will be prevented from entering. For instance, a normal or straight chain paraffin diffuses more easily through numerous zeolites than iso- or branched chain paraffin, as shown in Figure 1-18.

1.6.3.2.2 Product selectivity

Inside the zeolite pores, various intermediate molecules are likely to be formed via a chemical reaction. The results can be either smaller molecules than the reactant (cracked), the same molecular weight (isomerised) or larger molecules that can block the pores and resulted in deactivation of the catalyst, or subentry reaction. As a result, a variety of reaction pathways may be present for any individual product, potentially

complicating the kinetics of the process. For example, the alkylation reaction of toluene with methanol produces xylene isomers; however, only para-xylene can diffuse out through the ZSM-5 type zeolite, as shown in Figure 1-18.

1.6.3.2.3 Restricted transition state selectivity

This selectivity limits or prevents some bulkier molecular compounds from being formed inside the catalyst pore during the intermediate reaction. For example, it prevents the transalkylation of dialkylbenzenes, where an alkyl group undergoes intermolecular transfer, as shown in Figure 1-18.

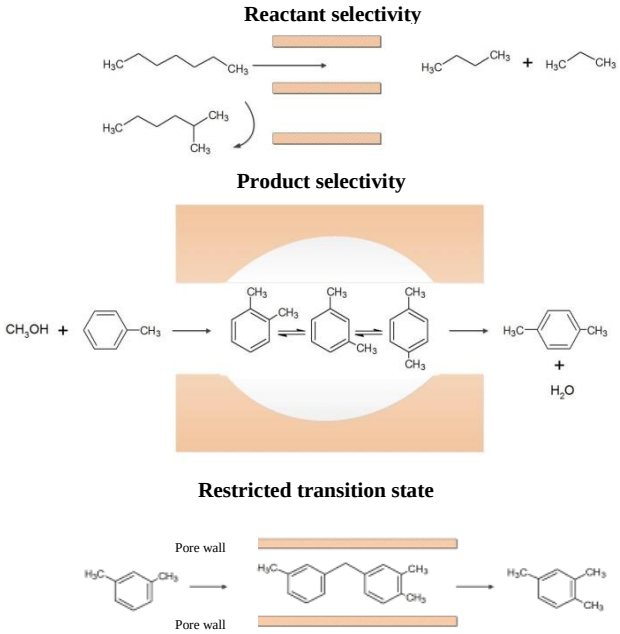

Figure 1-18 Schematic representation of the three types of shape-selectivity of zeolites; adapted from [124].

1.6.3.3 Zeolites as support

The microporous structure of the different zeolites and ion exchange capabilities make them the material of choice for supporting other catalytic functions, especially metals. The addition of metals to zeolite catalysts is widely used in commercial chemical plants, as discussed earlier. This technique can be done by two different methods, namely ion exchange or impregnation. These metals can adjust the zeolite structure as

well as change some of the physical properties of the zeolite[125]. Moreover, new catalytic active sites may be formed, which could enhance the catalytic activity by incorporating metal cations.[126]

1.7 Aims and objectives

The aim of this project is to develop an efficient chemical process using a highly active catalyst to tolerate the complexity of the polymer waste stream and hydrocrack it into high-value feedstock materials. This development will contribute to addressing the global challenge of polymer waste, as chemical recycling offers a method of recapturing the value of this rich hydrocarbon source more effectively and is a key step towards circular economy avoiding landfilling or incineration of polymers where direct reuse or mechanical recycling is not possible. The objectives to achieve these aims are to:

- Understand the behaviour of the hydrocracking reaction over a metal-supported acidic catalyst and determine the best reaction conditions by testing a model compound of squalene.
- Design, characterise and test suitable heterogeneous catalysts using zeolite for the depolymerisation of pure and mixed polymer streams in batch reactors.
- Characterise product slates from the batch reactor studies using pure and mixed polymer streams.
- Modify the catalyst by altering the acidity and metal functionality by using different Si/Al ratios of different zeolites and different metals, such as Ni and Pt, to enhance the hydrocracking rate and increase the selectivity of liquid oil.

- Extend the study using an actual mixture of post-consumer polymer as the feed stream and applying the optimised catalyst formulation to increase the practicality level of this research.
- Develop an appropriate modelling approach to study the kinetics of polymer hydrocracking, taking into account both mass transfer and diffusion limitation.
- Propose a reaction network that describes polymer hydrocracking and demonstrates its capabilities and limitations.
- Determine the kinetic constants of the hydrocracking reaction of pure polymer and estimate the apparent activation energies.

1.8 References

1. Namazi, H., Polymers in our daily life. *BioImpacts* **2017,** *7* (2), 73.
2. Elias, H.-G., *An introduction to polymer science*. 1st ed.; Weinheim: New York, 1997; p 492.
3. Bodzay, B.; Bánhegyi, G., Polymer waste: controlled breakdown or recycling? *International Journal of Design Sciences Technology* **2016,** *22* (2), 109-138.
4. Ayre, D., Technology advancing polymers and polymer composites towards sustainability: a review. *Current Opinion in Green Sustainable Chemistry* **2018,** *13*, 108-112.
5. Comăniță, E.-D.; Hlihor, R. M.; Ghinea, C.; Gavrilescu, M., Occurrence of plastic waste in the environment: ecological and health risks. *Environmental Engineering Management Journal* **2016,** *15* (3), 675-685.
6. Gourmelon, G. Global Plastic Production Rises, Recycling Lags http://vitalsigns.worldwatch.org/vs-trend/global-plastic-production-rises-recycling-lags (accessed 30/07/2020).
7. Costa, J. P. D.; Rocha-Sanyos, T.; C.Duarte, A. *The environmental impacts of plastics and micro-plastics use, waste and pollution: EU and national measures*; 2020.
8. Bucknall, D. G., Plastics as a materials system in a circular economy. *Philosophical Transactions of the Royal Society A* **2020,** *378* (2176), 20190268.

9. Van Eygen, E.; Laner, D.; Fellner, J., Circular economy of plastic packaging: current practice and perspectives in Austria. *Waste Management* **2018,** *72*, 55-64.

10. RoyalDutch/ShellGroupOfCompanies *The Shell Sustainability Report 2006. Meeting the energy challenge*; Shell International B.V.: 2006.

11. White, J. L., *Principles of polymer engineering rheology*. John Wiley & Sons: 1990; p 336

12. Vlachopoulos, J.; Strutt, D., Polymer processing. *Materials Science Technology* **2003,** *19* (9), 1161-1169.

13. Hammer, J.; Kraak, M. H.; Parsons, J. R., Plastics in the marine environment: the dark side of a modern gift. *Reviews of Environmental Contamination Toxicology* **2012**, 1-44.

14. Reddy, C.; Ghai, R.; Kalia, V. C., Polyhydroxyalkanoates: an overview. *Bioresource Technology* **2003,** *87* (2), 137-146.

15. Scheirs, J.; Kaminsky, W., *Feedstock recycling and pyrolysis of waste plastics*. John Wiley & Sons Chichester, UK: 2006; p 785.

16. Carraher Jr, C. E., *Seymour/Carraher's polymer chemistry*. CRC Press: 2003; p 952.

17. Ali, M. F.; Siddiqui, M. N. In *The conversion of waste plastics/petroleum residue mixtures to transportation fuels*, Proceedings of the first international conference on environmentally sustainable development v. 1-3, 2005.

18. Halden, R. U., Plastics and health risks. *Annual Review of Public Health* **2010,** *31*, 179-194.

19. PlasticsEurope Plastics - the facts 2020 An analysis of European plastics production, demand and waste data. https://www.plasticseurope.org/en/resources/publications/4312-plastics-facts-2020 (accessed 01/04/2021).

20. PlasticsEurope Plastics –the facts 2017 An analysis of European plastics production, demand and waste data. https://www.plasticseurope.org/application/files/5715/1717/4180/Plastics_the_facts_2017_FINAL_for_website_one_page.pdf (accessed 10/02/2021).

21. Geyer, R.; Jambeck, J. R.; Law, K. L., Production, use, and fate of all plastics ever made. *Science Advances* **2017,** *3* (7), e1700782.

22. Rouch, D. *Plastic future: How to reduce the increasing environmental footprint of plastic packaging*; Clarendon Policy & Strategy Group: Melbourne, Australia, 2019.

23. Hahladakis, J. N.; Iacovidou, E., Closing the loop on plastic packaging materials: What is quality and how does it affect their circularity? *Science of the Total Environment* **2018,** *630*, 1394-1400.

24. Munir, D.; Irfan, M. F.; Usman, M. R., Hydrocracking of virgin and waste plastics: A detailed review. *Renewable and Sustainable Energy Reviews* **2018,** *90*, 490-515.

25. Plastic waste: ecological and human health impacts. *Science for Environment Policy, In-depth Report* **2011**.

26. Sharuddin, S. D. A.; Abnisa, F.; Daud, W. M. A. W.; Aroua, M. K., A review on pyrolysis of plastic wastes. *Energy Conversion and Management* **2016,** *115*, 308-326.

27. PlasticsEurope The circular economy for plastics: a European overview. https://www.plasticseurope.org/en/resources/publications/1899-circular-economy-plastics-european-overview (accessed 01/04/2021).

28. Zink, T.; Geyer, R., Circular economy rebound. *Journal of Industrial Ecology* **2017,** *21* (3), 593-602.

29. Aguado, J.; Serrano, D. P.; San Miguel, G., European trends in the feedstock recycling of plastic wastes. *Global NEST Journal* **2007,** *9* (1), 12-19.

30. Hernandez-Martinez, J. Feedstock recycling of plastic waste by hydrocracking. The University of Manchester, United Kingdom, 2008.

31. Al-Salem, S. M.; Antelava, A.; Constantinou, A.; Manos, G.; Dutta, A., A review on thermal and catalytic pyrolysis of plastic solid waste (PSW). *Journal of Environmental Management* **2017,** *197*, 177-198.

32. Garforth, A. A.; Ali, S.; Hernández-Martínez, J.; Akah, A., Feedstock recycling of polymer wastes. *Current Opinion in Solid State and Materials Science* **2004,** *8* (6), 419-425.

33. Kaminsky, W.; Predel, M.; Sadiki, A., Feedstock recycling of polymers by pyrolysis in a fluidised bed. *Polymer Degradation and Stability* **2004,** *85* (3), 1045-1050.

34. Wallman, P. H.; Thorsness, C. B.; Winter, J. D., Hydrogen production from wastes. *Energy* **1998,** *23* (4), 271-278.

35. Mangesh, V.; Padmanabhan, S.; Ganesan, S.; PrabhudevRahul, D.; Reddy, T. D. K. In *Prospects of pyrolysis oil from plastic waste as fuel for diesel engines: A review*, IOP Conference Series: Materials Science and Engineering, IOP Publishing: 2017; p 012027.

36. Aguado, J.; Serrano, D. P., *Feedstock recycling of plastic wastes*. Royal Society of Chemistry: 2007; p 192.

37. Pielichowski, K.; Njuguna, J., *Thermal degradation of polymeric materials*. iSmithers Rapra Publishing: 2005; p 324.

38. Kijenski, J.; Kaczorek, T., Catalytic degradation of polystyrene. *Polimery* **2005,** *50* (1), 60-63.

39. Sakata, Y.; Uddin, M. A.; Muto, A., Degradation of polyethylene and polypropylene into fuel oil by using solid acid and non-acid catalysts. *Journal of Analytical and Applied Pyrolysis* **1999,** *51* (1), 135-155.

40. Gobin, K.; Manos, G., Polymer degradation to fuels over microporous catalysts as a novel tertiary plastic recycling method. *Polymer Degradation and Stability* **2004,** *83* (2), 267-279.

41. Park, D. W.; Hwang, E. Y.; Kim, J. R.; Choi, J. K.; Kim, Y. A.; Woo, H. C., Catalytic degradation of polyethylene over solid acid catalysts. *Polymer Degradation and Stability* **1999,** *65* (2), 193-198.

42. Aguado, J.; Serrano, D. P.; Escola, J. M.; Garagorri, E.; Fernández, J. A., Catalytic conversion of polyolefins into fuels over zeolite beta. *Polymer Degradation and Stability* **2000,** *69* (1), 11-16.

43. Attique, S.; Batool, M.; Yaqub, M.; Gregory, D. H.; Wilson, C.; Goerke, O.; Shah, A. T., Synthesis and catalytic performance of cesium and potassium salts of aluminum substituted tungstoborate for pyrolysis of polyethylene waste to petrochemical feedstock. *Materials Chemistry Physics* **2020,** *246*, 122781.

44. Yu, H.; Li, F.; He, W.; Song, C.; Zhang, Y.; Li, Z.; Lin, H., Synthesis of micro–mesoporous ZSM-5 zeolite with microcrystalline cellulose as co-template and catalytic cracking of polyolefin plastics. *RSC Advances* **2020,** *10* (37), 22126-22136.

45. Muhammad, I.; Manos, G., Simultaneous pretreatment and catalytic conversion of polyolefins into hydrocarbon fuels over acidic zeolite catalysts. *Process Safety Environmental Protection* **2021,** *146*, 702-717.

46. Tae, J.-W.; Jang, B.-S.; Kim, J.-R.; Kim, I.; Park, D.-W., Catalytic degradation of polystyrene using acid-treated halloysite clays. *Solid State Ionics* **2004,** *172* (1), 129-133.

47. Çelikgöğüs, Ç.; Karaduman, A., Thermal-catalytic pyrolysis of polystyrene waste foams in a semi-batch reactor. *Energy Sources, Part A: Recovery, Utilization, and Environmental Effects* **2015,** *37* (23), 2507-2513.

48. Aljabri, N. M.; Lai, Z.; Hadjichristidis, N.; Huang, K.-W., Renewable aromatics from the degradation of polystyrene under mild conditions. *Journal of Saudi Chemical Society* **2017,** *21* (8), 983-989.

49. Adnan; Shah, J.; Jan, M. R., Polystyrene degradation studies using Cu supported catalysts. *Journal of Analytical and Applied Pyrolysis* **2014,** *109*, 196-204.

50. Williams, P. T.; Bagri, R., Hydrocarbon gases and oils from the recycling of polystyrene waste by catalytic pyrolysis. *International Journal of Energy Research* **2004,** *28* (1), 31-44.

51. San Miguel, G.; Serrano, D. P.; Aguado, J., Valorization of waste agricultural polyethylene film by sequential pyrolysis and catalytic reforming. *Industrial Engineering Chemistry Research* **2009,** *48* (18), 8697-8703.

52. Serrano, D.; Aguado, J.; Escola, J.; Rodríguez, J.; Morselli, L.; Orsi, R., Thermal and catalytic cracking of a LDPE–EVA copolymer mixture. *J Journal of Analytical Applied Pyrolysis* **2003,** *68*, 481-494.

53. Miskolczi, N.; Angyal, A.; Bartha, L.; Valkai, I., Fuels by pyrolysis of waste plastics from agricultural and packaging sectors in a pilot scale reactor. *Fuel Processing Technology* **2009,** *90* (7-8), 1032-1040.

54. Syamsiro, M.; Saptoadi, H.; Norsujianto, T.; Noviasri, P.; Cheng, S.; Alimuddin, Z.; Yoshikawa, K., Fuel oil production from municipal plastic wastes in sequential pyrolysis and catalytic reforming reactors. *Energy Procedia* **2014,** *47*, 180-188.

55. Kassargy, C.; Awad, S.; Burnens, G.; Upreti, G.; Kahine, K.; Tazerout, M., Study of the effects of regeneration of USY zeolite on the catalytic cracking of polyethylene. *Applied Catalysis B: Environmental* **2019,** *244*, 704-708.

56. Wang, J.; Jiang, J.; Sun, Y.; Zhong, Z.; Wang, X.; Xia, H.; Liu, G.; Pang, S.; Wang, K.; Li, M., Recycling benzene and ethylbenzene from in-situ catalytic fast pyrolysis of plastic wastes. *Energy Conversion Management* **2019,** *200*, 112088.

57. Bagri, R.; Williams, P. T., Catalytic pyrolysis of polyethylene. *Journal of Analytical Applied Pyrolysis* **2002,** *63* (1), 29-41.

58. La Mantia, F., *Handbook of plastics recycling*. iSmithers Rapra Publishing: 2002; p 460.

59. Venkatesh, K.; Hu, J.; Tierney, J.; Wender, I., Hydrocracking of polyolefins to liquid fuels over strong solid acid catalysts. *Preprints of Papers, American Chemical Society, Division of Fuel Chemistry* **1995,** *40*, 788-788.

60. Mosio-Mosiewski, J.; Warzala, M.; Morawski, I.; Dobrzanski, T., High-pressure catalytic and thermal cracking of polyethylene. *Fuel Processing Technology* **2007,** *88* (4), 359-364.

61. Scheirs, J., Polymer recycling: science, technology and applications. *Wiley & Sons Ltd* **1998**, 591.

62. Utami, M.; Wijaya, K.; Trisunaryanti, W., Pt-promoted sulfated zirconia as catalyst for hydrocracking of LDPE plastic waste into liquid fuels. *Materials Chemistry Physics* **2018,** *213*, 548-555.

63. Hauli, L.; Wijaya, K.; Syoufian, A., Hydrocracking of LDPE plastic waste into liquid fuel over sulfated zirconia from a commercial zirconia nanopowder. *Oriental Journal of Chemistry* **2019,** *35* (1), 128-133.

64. Samperio, J. A. S. Alternative catalytic processes for the valorization of plastic wastes to fuels. Universidad del País Vasco-Euskal Herriko Unibertsitatea, 2016.

65. Rana, M. S.; Samano, V.; Ancheyta, J.; Diaz, J., A review of recent advances on process technologies for upgrading of heavy oils and residua. *Fuel* **2007,** *86* (9), 1216-1231.

66. RecyclingTechnologies We want to make plastic a more sustainable material. https://recyclingtechnologies.co.uk/technology/ (accessed 12/04/2021).

67. Griffiths, A. E. Apparatus for treating waste comprising mixed plastic waste. US10717934B2, 2020.

68. ReNewELP A new solution for recycling waste plastic. https://renewelp.co.uk/wp-content/uploads/2020/02/ReNew-ELP-Brochure-.pdf (accessed 12/04/2021).

69. Enval The enval process. http://www.enval.com/process/ (accessed 12/04/2021).

70. PlasticEnergy Our technology. https://plasticenergy.com/technology/ (accessed 12/04/2021).

71. McNamara, D.; Murray, M. Conversion of waste plastics material to fuel. US10131847B2, 2011.

72. Quantafuel Plants & Projects. https://www.quantafuel.com/plants-and-projects (accessed 12/04/2021).

73. Fareid, E.; Fareid, L. E.; Larsen, T. T.; Kaalstad, P.; Norheim, A. Production of hydrocarbon fuels from waste plastic. WO2020008050A1, 2019.

74. Ding, W.; Liang, J.; Anderson, L. L., Hydrocracking and hydroisomerization of high-density polyethylene and waste plastic over zeolite and silica alumina supported Ni and Ni Mo sulfides. *Energy & Fuels* **1997,** *11* (6), 1219-1224.

75. Weitkamp, J., Hydrocracking and Hydrotreating. In *ACS Symp*, 1975; Vol. 20, p 1.

76. Anderson, R. B., *Experimental methods in catalytic research*. 1st ed.; Academic Press: 1968; Vol. 1, p 512.

77. Mohanty, S.; Kunzru, D.; Saraf, D., Hydrocracking: a review. *Fuel* **1990,** *69* (12), 1467-1473.

78. Aguado, J.; Serrano, D. P., *Feedstock recycling of plastic wastes*. Royal society of chemistry: 2007.

79. Fuentes-Ordóñez, E. G.; Salbidegoitia, J. A.; González-Marcos, M. P.; González-Velasco, J. R., Transport phenomena in catalytic hydrocracking of polystyrene in solution. *Industrial & Engineering Chemistry Research* **2013,** *52* (42), 14798-14807.

80. Luo, M.; Curtis, C. W., Thermal and catalytic coprocessing of Illinois No. 6. coal with model and commingled waste plastics. *Fuel Processing Technology* **1996,** *49* (1-3), 91-117.

81. Joo, H. K.; Curtis, C. W., Catalytic coprocessing of LDPE with coal and petroleum resid using different catalysts. *Fuel Processing Technology* **1998,** *53* (3), 197-214.

82. Venkatesh, K.; Hu, J.; Tierney, J.; Wender, I., Hydrocracking of polyolefins to liquid fuels over strong solid acid catalysts. *PREPRINTS OF PAPERS-AMERICAN CHEMICAL SOCIETY DIVISION FUEL CHEMISTRY* **1995,** *40*, 788-788.

83. Rothenberger, K. S.; Cugini, A. V.; Thompson, R. L.; Ciocco, M. V., Investigation of first-stage liquefaction of coal with model plastic waste mixtures. *Energy & Fuels* **1997,** *11* (4), 849-855.

84. Liu, Y., Hydrocracking of polyethylene to jet fuel range hydrocarbons over bifunctional catalysts containing Pt-and Al-modified MCM-48. *Reactions* **2020,** *1* (2), 195-209.

85. Zmierczak, W.; Xiao, X.; Shabtai, J., Depolymerization-liquefaction of plastics and rubbers. 2. Polystyrenes and styrene-butadiene copolymers. *Fuel Processing Technology* **1996,** *49* (1-3), 31-48.

86. Fuentes-Ordóñez, E. G.; Salbidegoitia, J. A.; González-Marcos, M. P.; González-Velasco, J. R., Transport phenomena in catalytic hydrocracking of polystyrene in solution. *Industrial Engineering Chemistry Research* **2013,** *52* (42), 14798-14807.

87. Xu, D.; Carbonell, R. G.; Kiserow, D. J.; Roberts, G. W., Kinetic and transport processes in the heterogeneous catalytic hydrogenation of polystyrene. *Industrial Engineering Chemistry Research* **2003,** *42* (15), 3509-3515.

88. Akah, A.; Hernandez-Martinez, J.; Rallan, C.; Garforth, A. A., Enhanced feedstock recycling of post-consumer plastic waste. *Chemcal Engineering Transactions* **2015,** *43*, 2395-2400.

89. Shabtai, J.; Xiao, X.; Zmierczak, W., Depolymerization− liquefaction of plastics and rubbers. 1. Polyethylene, polypropylene, and polybutadiene. *Energy & Fuels* **1997,** *11* (1), 76-87.

90. Fogler, H. S., *Elements of chemical reaction engineering*. 5th ed.; Prentice Hall: Philadelphia, PA, 2016; p 992.

91. Venkatesh, K. R.; Hu, J.; Wang, W.; Holder, G.; Tierney, J.; Wender, I., Hydrocracking and hydroisomerization of long-chain alkanes and polyolefins over metal-promoted anion-modified zirconium oxides. *Energy & fuels* **1996,** *10* (6), 1163-1170.

92. Ali, M. F.; Nahid, M.; Redhwi, S. S. H. H., Study on the conversion of waste plastics/petroleum resid mixtures to transportation fuels. *Journal of Material Cycles Waste Management* **2004,** *6* (1), 27-34.

93. Kohli, K.; Prajapati, R.; Maity, S. K.; Sharma, B. K., Hydrocracking of heavy crude/residues with waste plastic. *Journal of Analytical Applied Pyrolysis* **2019,** *140*, 179-187.

94. González-Marcos, M. P.; Fuentes-Ordóñez, E. G.; Salbidegoitia, J. A.; González-Velasco, J. R., Optimization of supports in bifunctional supported Pt catalysts for polystyrene hydrocracking to liquid fuels. *Topics in Catalysis* **2020**, 1-19.

95. Paterson, W. S. In *Advances in hydrocracking*, 7th World Petroleum Congress, 1967; pp 98-111.

96. Amenomiya, Y.; Cvetanović, R., Active sites of alumina and silica-alumina as observed by temperature programmed desorption. *Journal of Catalysis* **1970,** *18* (3), 329-337.

97. Huffman, G.; Rockwell, J.; Shah, N.; Anderson, L. L.; Ding, W. In *Catalytic liquefaction of waste plastic*, Proceedings of the 1997 Coal Liquefaction & Solid Fuels Contractors Review Conference, 1997.

98. Shah, N.; Rockwell, J.; Huffman, G. P., Conversion of waste plastic to oil: direct liquefaction versus pyrolysis and hydroprocessing. *Energy & Fuels* **1999,** *13* (4), 832-838.

99. Liu, K.; Meuzelaar, H. L., Catalytic reactions in waste plastics, HDPE and coal studied by high-pressure thermogravimetry with on-line GC/MS. *Fuel Processing Technology* **1996,** *49* (1-3), 1-15.

100. Ochoa, R.; Van Woert, H.; Lee, W.; Subramanian, R.; Kugler, E.; Eklund, P., Catalytic degradation of medium density polyethylene over silica-alumina supports. *Fuel processing technology* **1996,** *49* (1-3), 119-136.

101. Lin, L. F.; Zhao, S. F.; Zhang, D. W.; Fan, H.; Liu, Y. M.; He, M. Y., Acid strength controlled reaction pathways for the catalytic cracking of 1-pentene to propene over ZSM-5. *ACS Catalysis* **2015,** *5* (7), 4048-4059.

102. Hesse, N. D.; White, R. L., Polyethylene catalytic hydrocracking by PtHZSM-5, PtHY, and PtHMCM-41. *Journal of Applied Polymer Science* **2004,** *92* (2), 1293-1301.

103. Munir, D.; Irfan, M. F.; Usman, M. R., Hydrocracking of virgin and waste plastics: a detailed review. *Renewable Sustainable Energy Reviews* **2018,** *90*, 490-515.

104. Byrappa, K.; Yoshimura, M., *Handbook of hydrothermal technology*. 2nd ed.; William Andrew: 2012; p 800.

105. van Bekkum, H., *Introduction to zeolite science and practice*. 2nd ed.; Elsevier: Amsterdam, New York 2001; Vol. 137, p 1078.

106. Breck, D. W., *Zeolites molecular sieves, chemistry and use*. Wiley: New York, 1974; p 771

107. Smith, J. V., Definition of a zeolite. *Zeolites* **1984,** *4* (4), 309-310.

108. Flanigen, E. M., Zeolites and molecular sieves: an historical perspective. *Studies in Surface Science and Catalysis* **1991,** *58*, 13-34.

109. van de Runstraat, A., *Adsorption effects in acid catalysis by zeolites*. Technische Universiteit Eindhoven: Eindhoven, The Netherlands, 1997.

110. Perego, C.; Pollesel, P., Advances in aromatics processing using zeolite catalysts. *Advances in Nanoporous Materials* **2010,** *1*, 97-149.

111. Flanigen, E. M., Molecular sieve materials: their synthesis, properties, and characterizations. *Catalysis Reviews Science and Engineering* **1984,** *26* (3-4), 483-483.

112. Naidu, B.; Bhat, S. D.; Sairam, M.; Wali, A. C.; Sawant, D. P.; Halligudi, S. B.; Mallikarjuna, N. N.; Aminabhavi, T. M., Comparison of the pervaporation separation of a water–acetonitrile mixture with zeolite-filled sodium alginate and poly (vinyl alcohol)–polyaniline semi-interpenetrating polymer network membranes. *Journal of Applied Polymer Science* **2005,** *96* (5), 1968-1978.

113. Thomas, J. M.; Thomas, W. J.; Anderson, J. R.; Boudart, M., Principles and practice of heterogeneous catalysis. *Angewandte Chemie-English Edition* **1997,** *36* (23), 2689-2689.

114. García-Martínez, J.; Johnson, M.; Valla, J.; Li, K.; Ying, J. Y., Mesostructured zeolite Y—high hydrothermal stability and superior FCC catalytic performance. *Catalysis Science & Technology* **2012,** *2* (5), 987-994.

115. Kulprathipanja, S., *Zeolites in industrial separation and catalysis*. Wiley-VCH: 2010; p 620.

116. Wadlinger, R. L.; Kerr, G. T.; Rosinski, E. J. Catalytic composition of a crystalline zeolite. US36431664A, 1967.

117. Baerlocher, C.; McCusker, L. B.; Olson, D. H., *Atlas of zeolite framework types*. 5th ed.; Elsevier Science: 2001; p 298.

118. Bellussi, G.; Pazzuconi, G.; Perego, C.; Girotti, G.; Terzoni, G., Liquid-phase alkylation of benzene with light olefins catalyzed by β-zeolites. *Journal of Catalysis* **1995,** *157* (1), 227-234.

119. Smith, K.; Musson, A.; DeBoos, G. A., Superior methodology for the nitration of simple aromatic compounds. *Chemical Communications* **1996,** (4), 469-470.

120. Mirodatos, C.; Barthomeuf, D., Superacid sites in zeolites. . *Journal of the Chemical Society, Chemical Communications* **1981,** *2*, 39-40.

121. Weitkamp, J., Zeolites and catalysis. *Solid State Ionics* **2000,** *131* (1), 175-188.

122. Stöcker, M., Gas phase catalysis by zeolites. *Microporous and Mesoporous Materials* **2005,** *82* (3), 257-292.

123. Tanabe, K.; Misono, M.; Hattori, H.; Ono, Y., *New solid acids and bases: their catalytic properties*. 1st ed.; Elsevier: 1990; Vol. 51, p 364.

124. Busca, G., Zeolites and other structurally microporous solids as acid–base materials. In *Heterogeneous Catalytic Materials*, Elsevier: 2014; pp 197-249.

125. Townsend, R. P., Ion exchange in zeolites. *Studies in Surface Science and Catalysis* **1991,** *58*, 359-390.

126. Venuto, P. B.; Habib Jr, E. T., *Fluid catalytic cracking with zeolite catalysts*. 2nd ed.; Marcel Dekker: United States, 1979; Vol. 26, p 156.

2 General Methodology

2.1 Materials used

The zeolite catalysts (Beta and USY) were obtained from Zeolyst International, the related details are shown in Table 2-1.

Table 2-1 Summary of the zeolites used

Zeolite	Form	Si/Al ratio	Zeolyst code
Beta	NH_4^+	12.5	CP814C*
	H	175	CP811C-300
USY	NH_4^+	6	CBV712
	H	15	CP811C-300

The catalysts were metal-loaded using the following platinum and nickel salts, namely, tetraammineplatinum(II) chloride hydrate metal salts, with a purity of 98% ($Pt[NH_3]_4Cl_2 \cdot H_2O$, Mw 334.11, code no. 323330) was supplied by Sigma Aldrich. Nickel (II) nitrate hexahydrate, ($Ni(NO_3)_2 \cdot 6H_2O$, Mw 290.8g/mol, code no. 1750/50) was supplied by Fisher Scientific.

Hexamethyltetracosane (Squalane, $C_{30}H_{62}$) supplied by Sigma-Aldrich (purity >95%, bpt=350 °C), was used as a model compound. Squalane was selected as a branched hydrocarbon (Figure 2-1), with the branches being similar to that of a cross-linked polyolefin, and being a liquid at ambient temperature.

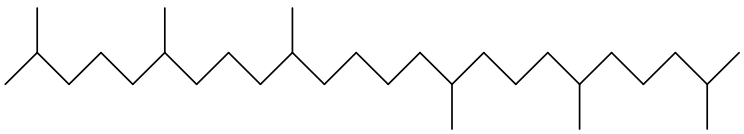

Figure 2-1 Molecular structure of Squalane.

High-purity virgin polymers were received from Goodfellows in powder (< 400 μm) or pellet form. Those polymers including low density polyethylene (LDPE, M_w ~ 150,000 g/mol, code no. ET316031), polypropylene (PP, M_w ~ 300,000 g/mol, code

no. PP306312), and polystyrene (PS, M_w ~ 167,000 g/mol, code no. ST316003). The post-consumer polymers used in this study are shown in Figure 2-2, and they were laboratory solvent wash bottles (LDPE, M_w ~ 57,800 g/mol centrifuge tubes (PP, M_w ~ 28,900 g/mol), household milk bottles (HDPE, 1L, typical of supermarket retailers), and clear drinking cups (PS, M_w ~ 161,320 g/mol).

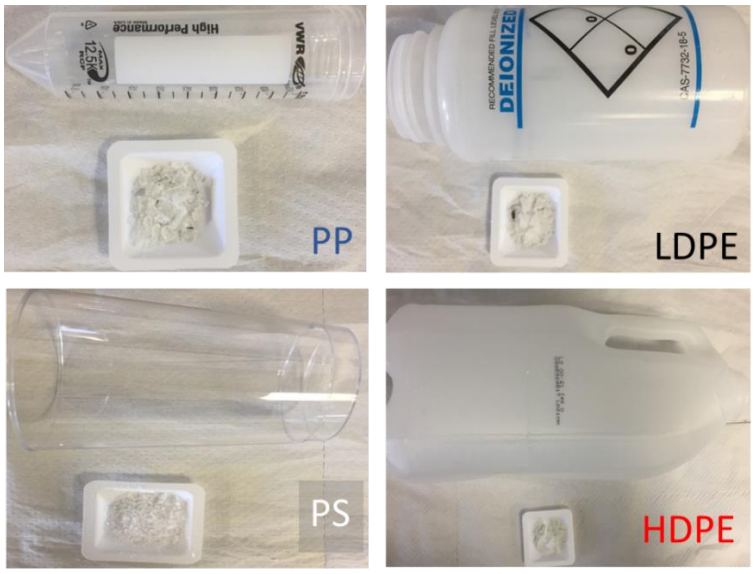

Figure 2-2 Post-consumer polymers used.

2.2 Catalyst preparation

2.2.1 Zeolite only as a catalyst

The ammonium-exchanged Beta and USY zeolites with Si/Al_{bulk} ratios of 12.5 and 6 were first calcined in an oven at 500 °C for 16 h at a ramping rate of 2.5 °C/min under atmospheric pressure. This step was necessary to transfer the catalyst to the active hydrogen form; as the Beta and USY zeolites with Si/Al_{bulk} ratios of 175 and 15 were supplied in the hydrogen-form, calcination was not required. Subsequently, the catalyst powder was pelleted, using a 1 cm diameter pressing die, under pressure by applying 5 tonnes of weight for 30 seconds. Then, the catalyst was crushed and sieved to 150-600 µm particles prior to loading using the tools shown in Figure 2-3.

Figure 2-3 Catalyst preparation using press, die, mortar and pestle, and molecular sieves.

The pelleted catalyst was then loaded into the middle of a tubular reactor for activation. A layer of glass beads (425–600 µm) was placed below the catalyst, and separated from the catalyst layer by glass wool plugs, as shown in Figure 2-4. The catalyst was activated in a three-zone tubular furnace at 450 °C for 16 h with a ramping rate of 2.5 °C/min under an H_2 flow of 50 ml/min. The activated catalyst was stored in a desiccator under a vacuum atmosphere to prevent oxidation and moisture uptake.

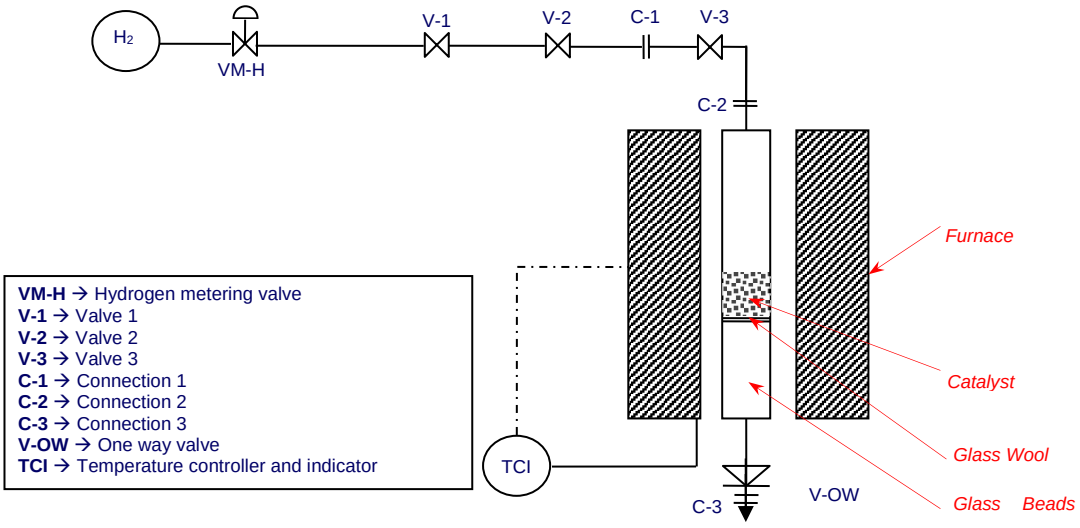

Figure 2-4 Scheme of the catalyst activation rig.

2.2.2 Bifunctional zeolites

Pt and Ni-impregnated zeolites were prepared using incipient wetness impregnation.[1] After conversion to its hydrogen-active form, the zeolite was mixed with the appropriate amount of metal salt dissolved in deionized water at a zeolite-to-solution ratio of 10 g : 100 ml, (for example, 0.1713 g of Pt salt in 100 ml of water to prepare 10 g of 1%Pt-zeolite). The mixture was then stirred for at least 12 h at an average temperature of 65 °C to ensure adequate dispersion of the metal on the surface of the catalyst and to allow slow evaporation of water, gradually forming a thick paste. The slurry was then dried in a carbolite furnace at 110 °C for 12 h. The pressing, sieving and loading into the tubular reactor were performed as described in section 2.2.1. The modified catalyst was then activated/reduced under the conditions outlined in section 2.2.1 to reduce the metal and activate the catalyst, making it ready for use.

2.3 Hydrocracking autoclave reactor

The hydrocracking experiments were carried out in a 300 mL stainless steel Parr Instruments stirred autoclave equipped with a U-shaped flat bar anchor agitator driven by an electronic motor. The reactor was heated using a jacket heater and controlled by an on/off controller monitored by a thermocouple placed between the jacket and the outside wall of the reactor. Another thermocouple placed inside the reactor was used to monitor the temperature of the reactants. The pressure was monitored by a pressure gauge (0-50 barg) with an accuracy of ± 1 bar installed on the top of the vessel. Figure 2-5 schematically illustrates the autoclave reactor setup.

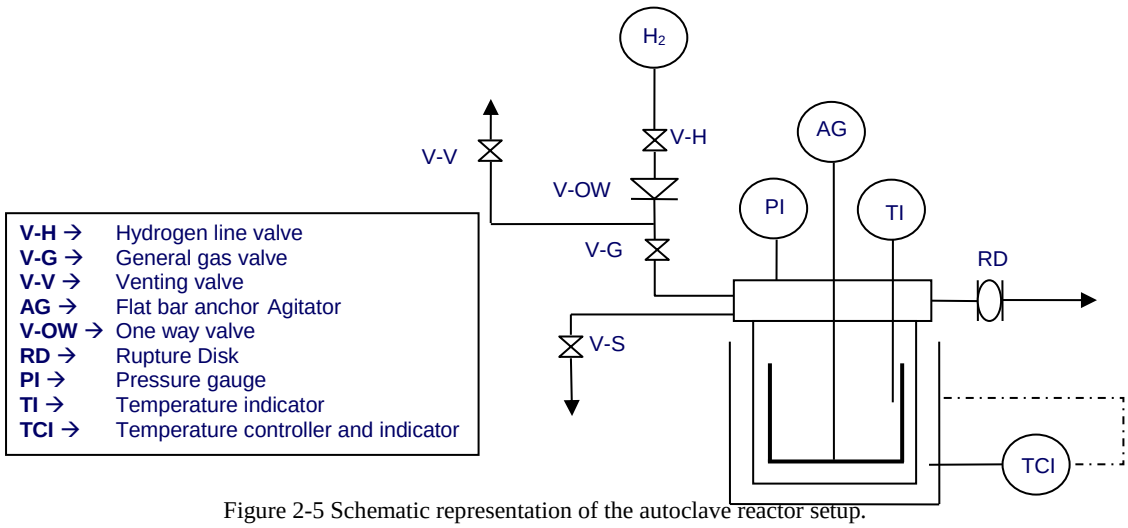

Figure 2-5 Schematic representation of the autoclave reactor setup.

2.3.1 Reactor operation procedure

The reactor was loaded with typically 20 g of polymer and 2 g of catalyst to achieve a feed-to-catalyst mass ratio of 10:1. To prevent the oxidation or deactivation of the metal function or the catalyst, it was important to store it in an H_2 atmosphere or under a vacuum; thus, both the reactant and catalyst were loaded into the reactor with minimal exposure to ambient air and humidity. When the reactor was loaded, the lid was fitted and the bolts were firmly tightened to avoid leaks. A PTFE gasket situated between the steel surfaces provided a seal. Following that, the reactor was flushed with H_2 at least three times under gentle agitation to remove any remaining air, thus preventing the deactivation or oxidation of the catalyst. Then, the reactor was pressurised to the reaction pressure and a leak test was performed for at least 1 h. If there was no leak, the thermocouples were connected and the vessel was positioned inside the heating jacket. At this point, all valves were closed and the reactor was ready for use.

To start the experiment, the autoclave was heated using a jacket heater and controlled using the wall temperature. The required set point temperature was initially not set due to the poor temperature feedback loop, leading to frequent temperature overshoots.

Therefore, a ramping rate of 10 °C/min was carried out manually until the inside temperature had reached the reaction temperature. At this point, the temperature was held isothermally for the required batch time. During the whole experiment, the pressure and all temperatures (inside, wall and set) were recorded each minute. When the reaction time was completed, the heater was switched off and cooling air was circulated around the autoclave to cool down the reactor and stop the reaction.

When the temperature had dropped to room temperature, all the gas products were collected using 600 mL Tedlar gas bags (supplied by Sigma-Aldrich), and the reactor pressure dropped to atmospheric pressure. The number of collected gas bags indicated the volume of gas produced. After that, the reactor was opened, and the liquid and solid yields were collected and weighed to determine the mass balance. The solid was washed using a solvent (dichloromethane or acetone, supplied by Sigma-Aldrich and Fisher Scientific, respectively) to extract any remaining liquid; then, the solvent was separated from the extracted oil by slow evaporation at ambient temperature. The final step comprised analysing the gas and liquid products using gas chromatography (GC) and gas chromatography and mass spectrometry (GC-MS).

2.4 Products analysis

To identify the conversions and yield of each different product of interest, GC-FID was used for analysing gas products and GC-MS for liquid products.

2.4.1 Gas chromatography basics

GC analysis is a widely used technique to determine the quantity of the different compounds present in a gas sample. It works by vaporising a liquid sample or injecting a gaseous unknown sample and passing it through a long column with an inert gas

flow (mobile phase) installed inside an oven that is heated in a prescribed manner.[2] The column is packed or coated with adsorbent materials (stationary phase, typically He or N_2), which adsorb different molecules with different strengths (partition coefficient). The adsorbed molecules are effectively separated and exit the column at different times based on their affinity for the stationary phase; the compounds with higher affinity take longer to exit the column.[3] An installed detector, typically a flame ionisation detector, measures parameters of the mixture exiting the column to quantify the results. However, the column type and the operation condition of the oven temperature ramp are key parameters affecting the quality of the separation of the compounds. [3] Thus, those factors should be optimized to obtain a good separation of the substances with a uniform response by the detector.

The GC presents the results in a chromatogram that plots time versus the detector response. In other words, it is a graph with a series of peaks with different areas at different times, each peak representing one compound, if full separation has been achieved. The main two key parameters which are the focus of the analysis are the **retention time** and **peak area**. The quantity of a certain compound in the sample is identified by calculating the peak area via the integration of the detector response versus the retention time. However, a calibration against standards of known concentration should be used to accurately quantify the fraction of the components present in the sample mixture.

2.4.1.1 Analysis of the gas products by GC-FID

The gas samples were analysed using a Varian CP 3800 GC fitted with a 50 m length, 0.32 mm inner diameter and 5 μm film thickness i.d. PLOT Al_2O_3/KCl capillary column and an FID detector. Table 2-2 illustrates the oven temperature method used

for analysing the gas samples by GC-FID. For the analysis, the gas bag containing the gas sample was connected to the inlet of the GC sample valve (250 μL) and pressed constantly and gently to release a constant 20 mL/min flow, measured by a bubble-meter connected to the GC injector outlet. When the flow was constant, the start button of the GC was pressed and the gas sample was injected into the GC using the gas sample valve (GSV).

Table 2-2 Oven temperature method used for gas analysis by GC-FID

Varian CP 3800 - control method	
Oven program	
T (°C)	time/ramp
70	1.5 min
70-225	10 °C/min
225	35 min

2.4.1.1.1 Identification and quantification of the gas samples

An appropriate calibration gas mixture (C_1-C_5 saturated hydrocarbons) with known composition was provided by Linde Gas and used to quantify unknown samples, known as the external standard method technique, (Table 2-3 presents the mole composition of each compound present in the calibration gas sample).

Table 2-3 Mole composition of the GC calibration gas

Compound	Mole fraction (%)	Compound	Mole fraction (%)
Methane	1.006	i-pentane	1.005
Ethane	0.999	n-pentane	1.007
Propane	0.998	Nitrogen	BALANCE
i-butane	0.987		

The retention time of the hydrocarbons using the PLOT Al_2O_3/KCl column was based on the number of carbon atoms, the level of chain branching and the level of unsaturation. Effectively, the retention time increased with increasing carbon number, and branched compared to linear hydrocarbons with the same carbon number had

shorter retention time. In addition, unsaturated hydrocarbons were retained more slowly on the column and had larger retention times than linear saturated hydrocarbons with the same carbon number.

In order to quantify the GC-FID, a response factor (RF) is calculated for each compound in the standard mixture, as shown in the following equation:

$$RF_i = C_{i\ std} / PA_{i\ std} \quad (1)$$

Where RF_i is the response factor for component i (mol%/area units); $C_{i\ std\ is}$ the concentration of component i in the standard mixture (mol%); and $PA_{i\ std}$ is the area of the peak identifying component i in the chromatogram of the standard mixture.

The RF was calculated to be used to estimate the correct composition of the sample. However, only the RFs for the components of the calibration gas were available, and thus an extrapolation was needed to quantify the other component such as alkenes and larger than C_5s. To do so, two assumptions were made: first, RF is the same for the compounds with the same number of carbon atoms and second, RF vs. carbon number (C#) representation is linear in a log-log plot. An example of applying the above equation to a standard sample to find the response factor is shown in Table 2-4.

Table 2-4 Calibration injection results example

Name	PA_i	RF_i	log (RF_i)	log (C#)
Methane	5535.85	0.000181	-3.74	0.00
Ethane	10599.75	0.000094	-4.03	0.30
Propane	15298.75	0.000065	-4.18	0.48
iso-butane	19254.65	0.000052	-4.28	0.60
n-butane	18786.55	0.000053	-4.27	0.60
iso-pentane	21467.90	0.000047	-4.33	0.70
n-pentane	19937.15	0.000050	-4.30	0.70

A typical plot of log RF_i versus log C# is shown in Figure 2-6 using real data from Table 2-4.

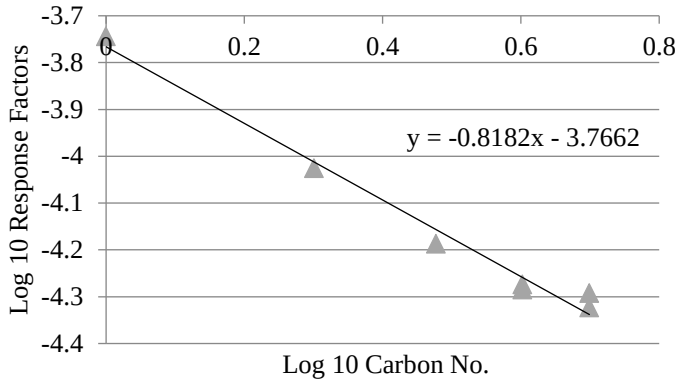

Figure 2-6 GC calibration curve for the standard gas sample (log RF vs. log C#).

Using the straight-line equation enables an extrapolation to find RF of the heavier compounds present in the calibration gas, but likely to be present in the reaction product mixture, as shown in Table 2-5.

Table 2-5 Response factors with extrapolations

Name	C#	RF_i extrapolated
C1	1	0.000172
C2	2	0.000097
C3	3	0.000069
C4	4	0.000055
C5	5	0.000045
C6	6	0.000039
C7	7	0.000034

These approximated response factors can be used to calculate the mole fraction of each molecule present in the gas sample by using the equation below.

$$c_i^{mol*} = RF_i \cdot PA_i \tag{2}$$

Where *i* is product *i* in the gas sample (excludes hydrogen); c_i^{mol*} is the concentration of component *i* in the gas sample, expressed as a mole fraction as obtained from the GC analysis; RF_i is the response factor for component *i*; PA_i is the peak area related to component *i*; and the rest of the total mol fraction represents the composition of H_2 in the gas bag, as shown in the equation below.

$$c_{H_2}^{mol*} = 1 - \sum c_i^{mol*} \tag{3}$$

Where $c_{H_2}^{mol*}$ is the concentration of H_2 in the gas sample, expressed as a mole fraction.

2.4.1.1.2 Calculation of the individual component masses in the sample

A GC chromatograph of an actual gas product sample is shown in Figure 2-7.

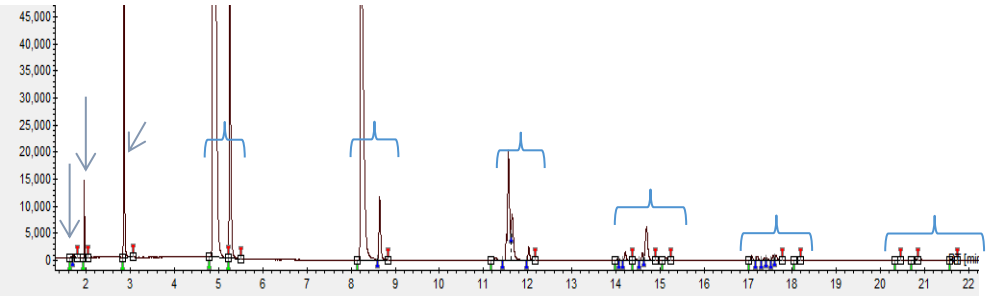

Figure 2-7 A GC chromatogram of an actual gas sample

Based on the GC analysis, the mole fraction of the gas sample can be estimated, which represents the composition of the total gas produced. Therefore, the concentration of each component present in the sample can be calculated using the equation below.

$$c_i^{mol} = \frac{c_i^{mol*}}{\sum c_i^{mol*}} \tag{4}$$

Where c_i^{mol*} is the mole fraction of component *i* in the gas sample as obtained from the GC analysis while taking hydrogen into account; and c_i^{mol} is the concentration as a mole fraction of component *i* in the gas sample (hydrogen-free basis).

To define the actual yield of the products, the total and individual masses of each component are required. Thus, the molar composition of each component needs to be transferred to a weight composition by using singular and average molecular weight, as shown in the equations below. The next step is calculating the total number of moles, which leads to estimating the total mass. To do this, the ideal gas law can be applied since the sample contains a mixture of non-polar gasses.

$$c_i^{wt} = \frac{c_i^{mol} \cdot Mw_i}{\sum c_i^{mol} \cdot Mw_i} \quad (5)$$

$$\overline{M_w} = \frac{\sum c_i^{mol} \cdot Mw_i}{\sum c_i^{mol}} \quad (6)$$

$$\frac{P_f V_{GS}}{RT_f} = n \quad (7)$$

Where c_i^{wt} is the concentration of component *i* in the gas sample, expressed as a weight fraction (hydrogen-free basis); c_i^{mol} is the concentration of component *i* in the gas sample, expressed as a mole fraction (hydrogen-free basis); Mw_i is the molecular weight of component *i*; $\overline{M_w}$ is the average molecular weight of the hydrocarbon products (g/mol); P_f is the pressure at which the gas bags are filled (Pa = 1 atm = 101325 Pa); V_{GS} is the volume of the total gas sample (m^3); *n* is the quantity of gas in the sample (mol); *R* is the gas constant of 8.31 $J.mol^{-1}.K^{-1}$; and T_f is the temperature at the end of the experiment (room temperature, K).

Finally, the total mass of the total gas produced can be estimated and the individual mass for each product can be calculated using the equations below.

$$n \cdot \sum c_i^{mol*} \cdot \overline{M_w} = W_G \quad (8)$$

$$m_{i=c_i^{wt}.W_G} \quad (9)$$

Where W_G is the mass of hydrocarbon gaseous products (g); and m_i is the sample mass of component *i* in the gas sample (g)

2.4.2 Mass spectrometry basics

Mass spectrometry (MS) is used to unequivocally identify single compounds present in a liquid sample. It works by ionising and breaking the molecules contained in the injected sample into several fragments. These fragments are then separated based on their mass-to-charge ratio and the resulting signals are recorded.[4] The results of MS are illustrated in a spectrum, indicating the masses of the fragments and the relative abundance of each mass, as shown in Figure 2-8 for the spectrum of n-decane and i-pentane.

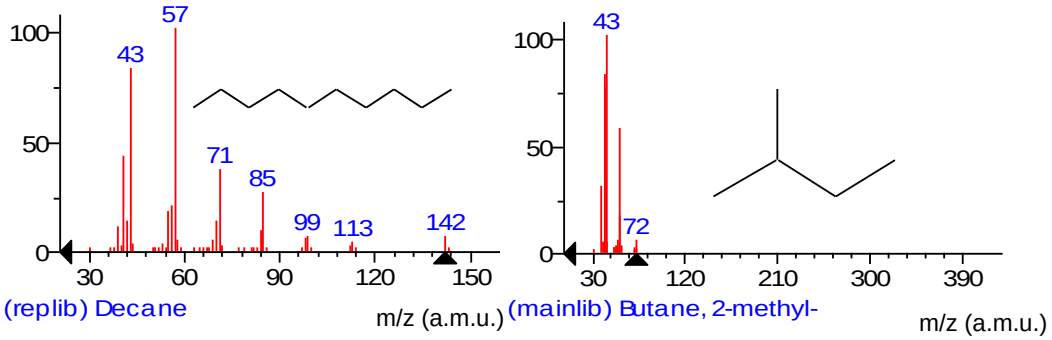

Figure 2-8 Mass spectra of n-decane and i-pentane. Abundance vs. mass (a.m.u.), reproduced from [5].

In MS, the molecules are ionised in a unique way, and this constitutes a fingerprint for the compound. The MS working parameters are standardized, and large spectra libraries containing over 100,000 known compounds exist, facilitating a comparison with the obtained spectra. In general, MS is a common analyser of pure components, while GC is more effective in terms of separation; thus, combining the techniques is very powerful where MS is used to identify components once they have been separated by GC.[6]

2.4.2.1 Liquid analysis by GC-MS

The GC-MS system used was an Agilent Technologies 6890N Network GC fitted with a 100 m x 0.25 mm i.d. PONA CB column. The GC-MS method is shown in Table 2-6.

Table 2-6 GC method for the GC-MS system

Agilent 6890N GC setup			
Oven program		Injector	
T (ºC)	Time/ramp	Injection vol (µl)	1.0
40	10 min	T (ºC)	250
42-260	2.25 ºc/min	Split ratio	75:1
260	60 min	Total flow (ml/min)	112.0
		Detector (MS)	
		T (ºc)	250
		Air flow (ml/min)	450
		H_2 flow (ml/min)	40

This method and the GC column used optimises the separation and run time to allow identification of a significant number of the compounds formed from polymer degradation in the range C_4-C_{34}. By identifying correctly these components in the liquid samples generated, they can be summarised with confidence into the amounts of linear alkanes, branched (mono- and multibranched) alkanes, cyclic alkanes, olefins and aromatics.

2.4.2.2 Identification and quantification

The GCMS software provides a chromatogram of the sample, whereby the mass spectrum related to that peak is obtained and can be matched against a library. The identification is not always accurate because samples often contain too many compounds and the column may not be able to separate them effectively. Given that all the components in the sample are supposed to be hydrocarbons, their spectra are

similar and identification can be problematic. Therefore, in this study a standard sample containing predominantly a series of n-alkanes with toluene, p-xylene and squalane was prepared and analysed as a reference to identify the compounds in the liquid samples, and help assign by carbon number. The components contained in the standard sample used are listed Table 2-7.

Table 2-7 GC-MS standard sample

Component	Represent	Component	Represent
n-pentane	C_5	Tridecane	C_{13}
n-hexane	C_6	Tetradecane	C_{14}
n-heptane	C_7	Pentadecane	C_{15}
Toluene	--	Hexadecane	C_{16}
n-octane	C_8	Heptadecane	C_{17}
p-xylene	--	Octadecane	C_{18}
n-decane	C_{10}	n-Eicosane	C_{20}
n-dodecane	C_{12}	Squalane	C_{30}

Figure 2-9 illustrates an example of a liquid sample chromatogram overlapped with a standard chromatogram to demonstrate the method of identifying of the involved compounds.

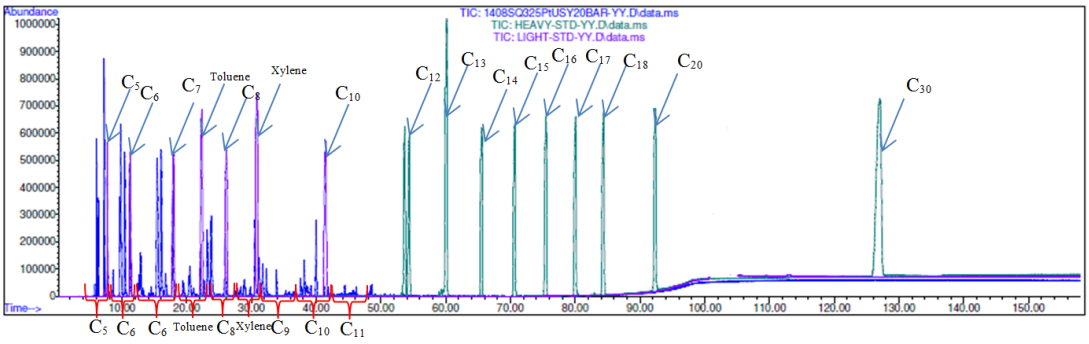

Figure 2-9 An example of a chromatogram sample overlapped with the standard chromatogram.

The GC-MS integrating the area for each peak in the chromatogram generated from GC-MS and the resultant area fractions were assumed to be representative of the weight composition of each substance. Based on the results of the standard sample the liquid products were quantified in carbon number groups (e.g. C_5, C_6 etc), as shown in Figure 2-9.

2.5 Catalyst characterisation

The following techniques were used to characterise the catalysts used in this study: X-ray diffraction (XRD), scanning electron microscopy (SEM) and energy dispersive X-ray spectroscopy (EDX), BET surface area, thermogravimetric analysis (TGA), temperature programmed desorption (TPD), and X-ray fluorescence (XRF). This section highlights the basic theory of each technique along with the experimental methods used for the catalyst characterisation.

2.5.1 X-ray diffraction (XRD)

X-ray diffraction (XRD) is an analytical instrument used to identify the purity and crystallinity of solid samples. In XRD, every crystalline pure substance has a unique pattern which works as a 'fingerprint'.[7] Each zeolite framework, such as Beta and USY, has a unique structure, and that structure can be detected using its X-ray diffraction pattern, allowing the crystallinity degree of the parent/modified zeolites to be determined.[8] The structural diffraction patterns of the ideal known zeolites can be taken from the International Zeolite Association (IZA) website.[9] The variation in the crystallinity of the modified samples can be compared and quantified based on the reference pattern. The principal equation used in XRD is Bragg's law, which measures the distances between the planes of the sample's atoms.[10]

$$n\lambda = 2d \cdot sin\theta \tag{10}$$

where n is an order of diffraction (n= 1,2,…); λ is the wavelength of the incident X-ray beam; d is the spacing between the planes in the atomic lattice; and θ is the angle between the incident ray and the scattering planes. Figure 2-10 illustrates the parameters of the XRD experiment.

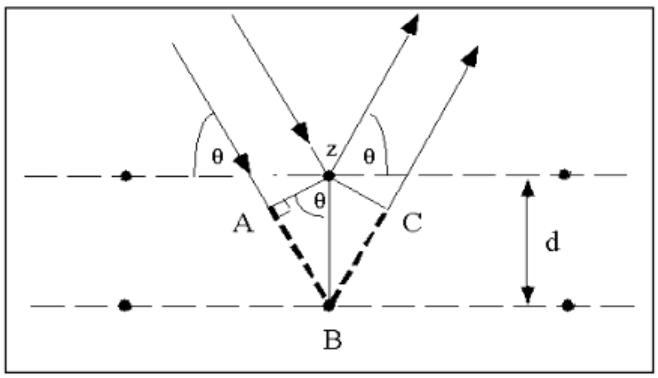

Figure 2-10 Diffraction of X-rays by a crystal; reproduced from [11].

To run the XRD, a powder sample of 0.5 g was pressed and packed to obtain a 2 mm wafer disk. After that, the sample was carefully loaded into the diffraction chamber to collect the XRD patterns of the samples using a Bruker D2 Phaser and a Rigaku MiniFlex X-ray powder diffractometer, which was equipped with nickel-filtered copper K alpha radiation, with generator settings of 30 mA and 40 kV.

The powder sample was scanned with an interval 2θ of (5° to 70°), a step size of 0.05° and a step time of 6 sec. The divergent slit was 1/8° and the scatter slit was 1/4°. The XRD patterns were then plotted via "Origin" software (Figure 2-11).

To identify the structures of the XRD patterns found for the unmodified (commercial) zeolites, these were compared to those reported in the literature; the following equation was used to compute the relative crystallinity of the modified zeolites with metals against its parent sample.[12]

$$\text{Relative crystallinity}(\%) = \frac{\sum_{i=1}^{n} \text{Peak Intensity of the modified sample}}{\sum_{i=1}^{n} \text{Peak Intensity of the parent (Ref.sample)}} \qquad (11)$$

where *i* is the peak number.

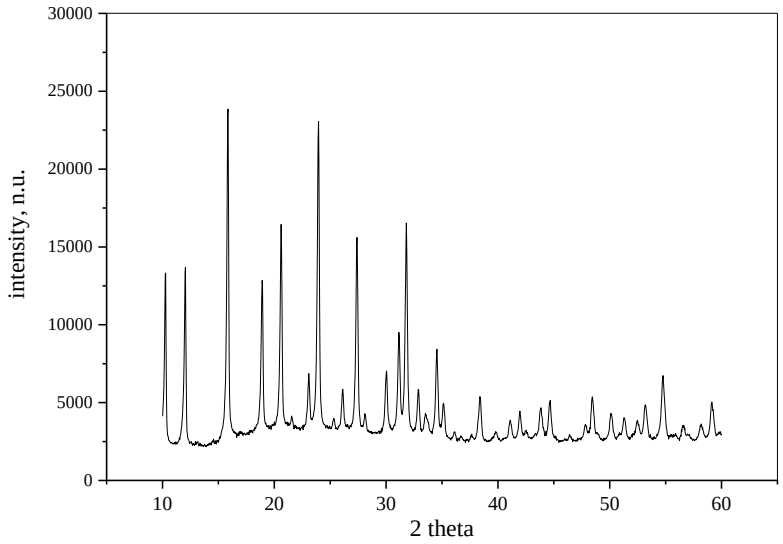

Figure 2-11 Typical XRD diffraction patterns of USY zeolite.

2.5.2 Scanning electron microscopy (SEM) and energy dispersive X-ray spectroscopy (EDX)

Scanning electron microscopy (SEM) was utilized to record the samples' surface topology, chemical composition, morphology, and crystalline structure on nanometer (nm) and micrometer (μm) scales. The elemental composition of the catalysts were determined via energy dispersive X-ray spectroscopy (EDX); this technique enables elements with an atomic number ranging from 4 to 92 to be detected.[13] A Quanta 250 system SEM/EDX was used, equipped with an Oxford Instruments XMaxN EDX detector; the setup operates in a vacuum and includes an objective lens, an electron gun, an electron detector, two condenser lenses, and a set of deflectors (Figure 2-12).

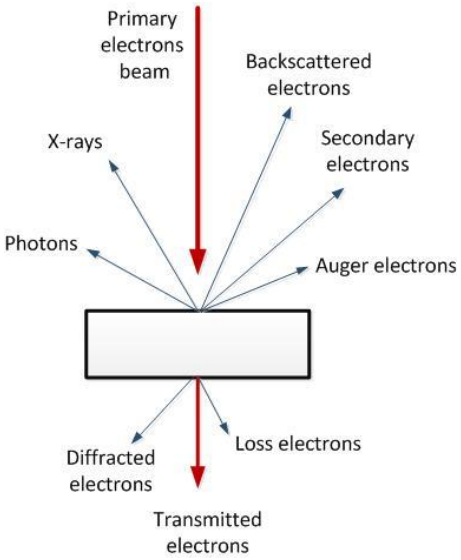

Figure 2-12 Interaction of the primary electron beam with the sample; reproduced from [14].

For the SEM analysis, some zeolite powder was briefly sonicated (~1 min) following suspension in acetone, and subsequently scattered on a metal plate. Meanwhile, to conduct the EDX analysis, the zeolite powder was dispersed onto a carbon tape and lightly pressed. Next, to prevent an electrostatic charge when scanning, an ultrathin layer of an electronically conductive material (gold) was used to coat the SEM/EDX sample. Figure 2-13 shows an example of an SEM image of zeolite Pt-Beta along with its EDX spectrum.

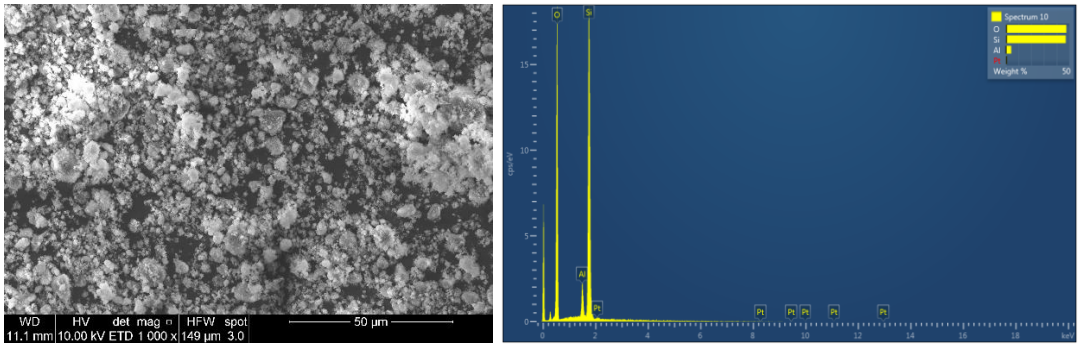

Figure 2-13 Example of an SEM micrograph of a Beta zeolite catalyst (left) along with the EDX spectrum (right).

2.5.3 Gas adsorption measurement with N_2 (BET isothermal)

The Brunauer, Emmett and Teller (BET) technique's gas adsorption analysis was used to measure the zeolite surface area, whereby nitrogen (N_2) was employed as the probe

molecule that would be adsorbed by the zeolite sample.[15] The following equation was used to compute the zeolite BET surface area.

$$\frac{P/P_0}{Va\,(1-P/P_0)} = \frac{P}{Va(P_0-P)} = \frac{1}{Vm\times C} + [\frac{C-1}{Vm\times C}] \times P/P_0 \qquad (12)$$

Where P is the vapour pressure; P_0 is the saturated pressure of the adsorbate; Va is the volume of gas adsorbed at the equilibrium adsorbate pressure and the temperature of adsorption (-196.15^{o}C for nitrogen); Vm is the volume of the adsorbed gas in the monolayer ($cm^3\ g^{-1}$); C is the BET constant, representing the interaction between the adsorbent (solid) and adsorbate (gas).

The Vm and C are calculated by plotting $\frac{P}{Va(P_0-P)}$ versus P/P_0, which gives a linear plot with a slope = $[\frac{C-1}{Vm\times C}]$ and an intercept = $\frac{1}{Vm\times C}$

The surface area (S) can be then be obtained using the following equation:

$$S = Vm \times N \times \sigma \qquad (13)$$

Where N is the Avogadro's number and; and σ is the average area occupied by every molecule in the entire monolayer ($16.2\times10^{-20}\ m^2$ for N_2).

While the adsorption isotherms for solid were broad, the majority were placed into five categories (I to V).[16] As there is a substantial filling of micropores at low partial pressure, and with the adsorption process essentially completed at P/P_0 = 0.5, the adsorption of microporous solids, e.g., zeolite materials, refers to Type I, II, and III isotherms.[17, 18]

A Micromeritics ASAP 2020 static low-pressure volumetric adsorption unit was used to measure the BET surface area. A 0.2 g zeolite sample was placed in a bulb-ended tube. Next, it was degassed at >200 °C for 3 h under a constant helium flow using a Micromeritics Flowprep 060 to ensure that all moisture and contaminants were removed. Subsequently, the sample was adsorbed at -196 °C (temperature of liquid nitrogen). Finally, the sample vials were weighed, and the empty vial mass was subtracted to obtain the purged sample mass. Figure 2-14 presents a typical zeolite USY graph from a BET experiment.

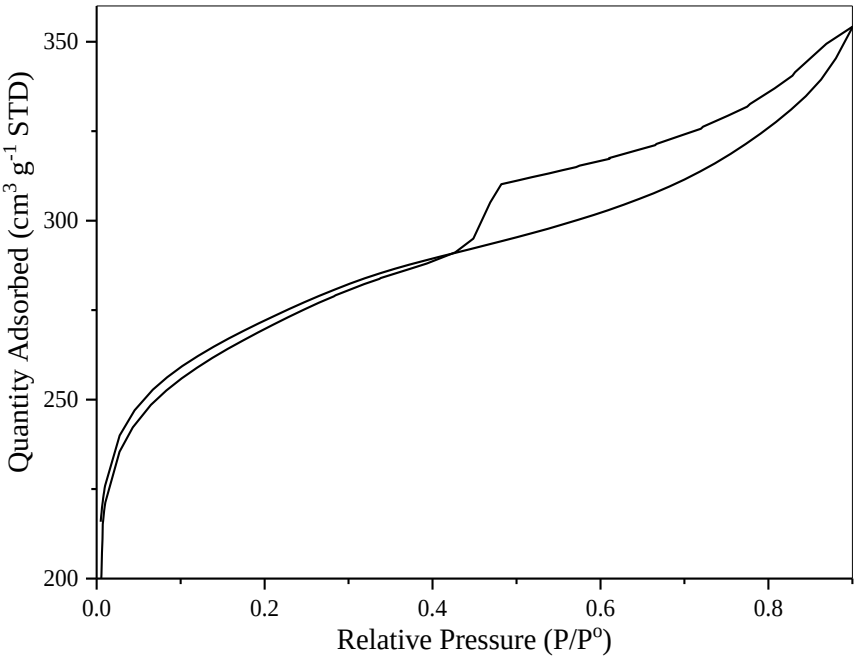

Figure 2-14 Typical N_2-BET graph of zeolite USY.

2.5.4 Thermogravimetric analysis (TGA)

Thermogravimetric analysis (TGA) is employed to determine a material's chemical and physical changes based on time or temperature within a controlled environment. Such measurements can show weight loss or gain due to dehydration, decomposition, or combustion.[19] A TA instruments Q5000-IR Thermogravimetric analyser, was used to investigate the zeolite powder samples before and after catalysis.

The zeolite sample (20–30 mg) was placed onto a ceramic pan and gently placed into the auto sampler. Once there, the sample was placed on the scale and the weight recorded. For the respective catalyst post-polymer conversion, the sample was heated from ambient temperature to 600 °C at a rate of 10 °C/min under a 50 ml/min nitrogen flow, and then isothermally held for 60 minutes. Subsequently, the nitrogen was replaced with air and the sample was left for a further 60 minutes to allow the coke and coke precursors to be oxidised fully to CO_2. Throughout the experiment, the catalyst weight change was observed and plotted against time (Figure 2-15).

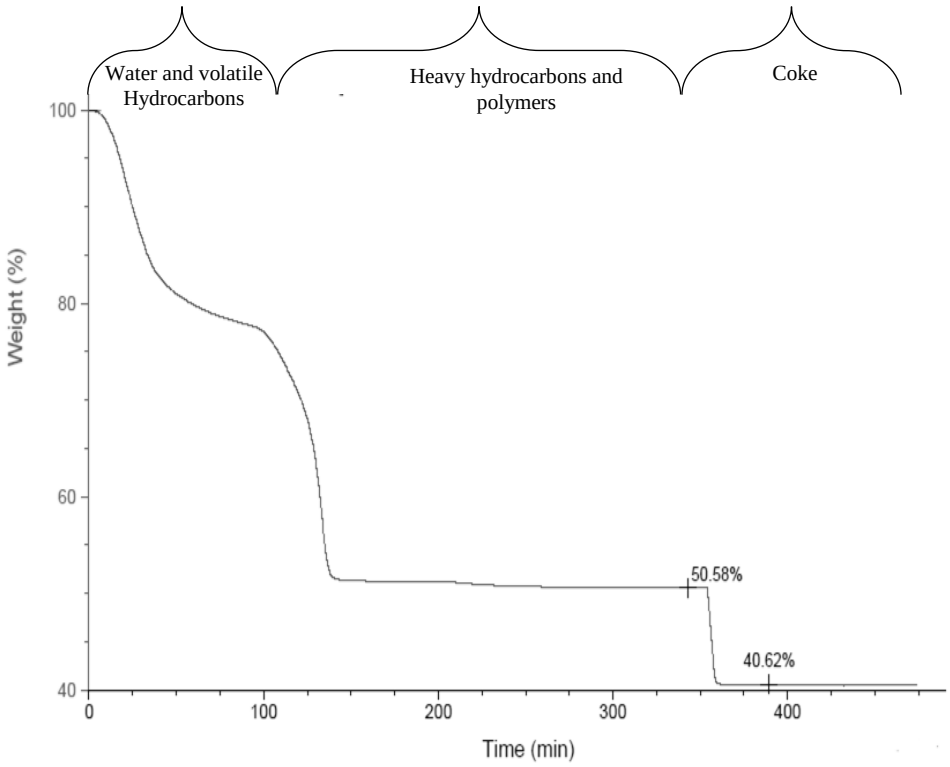

Figure 2-15 Typical example for the TGA analysis for the spent (coked) Beta catalyst with PS residue.

2.5.5 Temperature programmed desorption (TPD)

The temperature programmed desorption technique uses probe molecules which are adsorbed and then desorbed from the sample surface under study. TPD spectra are affected by the inert gas flow rate, particle size, catalyst pore size and catalyst bed depth. Since ammonia (NH_3) is basic in nature, it adsorbs onto the acidic sites on the

surface. The acidic sites allowing quantification in terms of the total ammonia molecules adsorbing onto the surface of catalysts in μmol/g. However, ammonia adsorption cannot distinguish between Brønsted or Lewis acid sites but can determines the total acidic sites as well as giving some indication of the strength from the temperature of desorption. The total area under the curve gives the capacity of the adsorption, and the multiple peak positions give the bond strength.[20-22] The acidity of the catalysts used in this thesis was quantified using the ammonia temperature programmed desorption of NH_3-TPD using an Quantachrome ChemBET Pulsar TPR/TPD analyser (Figure 2-16).

Figure 2-16 TPR/TPD analyser.

50 mg of modified zeolites with particle size of 300-500 μm first activated/reduced under a hydrogen flow of 40 cm^3/min at 480 °C for 3 h. Following that, the catalysts were cooled to ambient temperature, then exposed to 5% of NH_3 in an argon atmosphere (supplied by The Linde Group) and the temperature was ramped up to 800

°C. The signal for the NH_3 desorbed was recorded against the temperature (Figure 2-17) and integrated, giving the acidity profiles and concentrations.

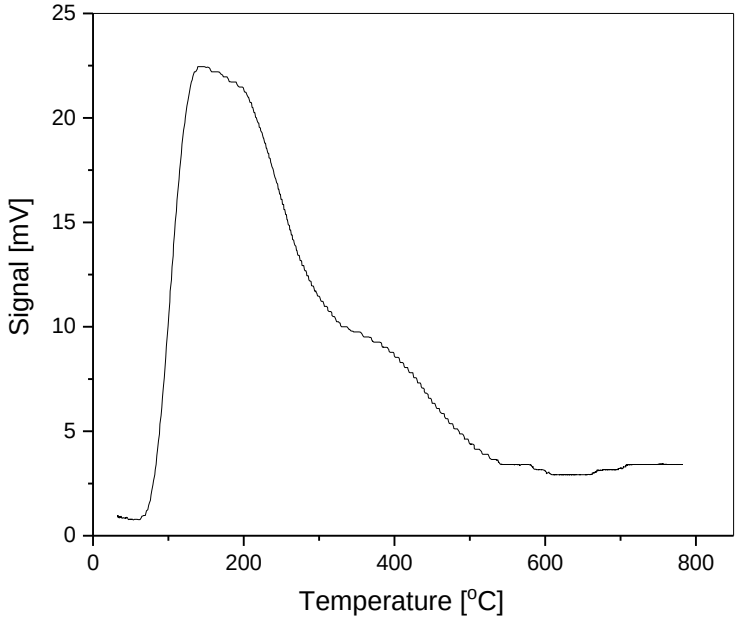

Figure 2-17 Typical TPD profile of ammonia adsorbed on USY.

2.5.6 X-ray fluorescence (XRF)

X-ray fluorescence refers to the characteristic or secondary X-rays emitted by a substance excited by high-energy electron or other X-ray or γ-ray photon bombardment. An incident particle with sufficient energy can knock an orbital electron out of its inner shell from the target atom. A higher-shell electron can then jump to the inner shell to replace the lost electron, thereby emitting a photon that has an energy that is equal to the difference in the two shells' binding energies of the two shells, as shown in Figure 2-18. X-ray fluorescence leads to an X-ray emission spectrum with discrete energies. The target element determines these emission spectral lines, which are, therefore, termed characteristic or fluorescent X-rays. A comparison of the peak's energy with the element's binding energy allows these spectra to be used to determine the elements.[23]

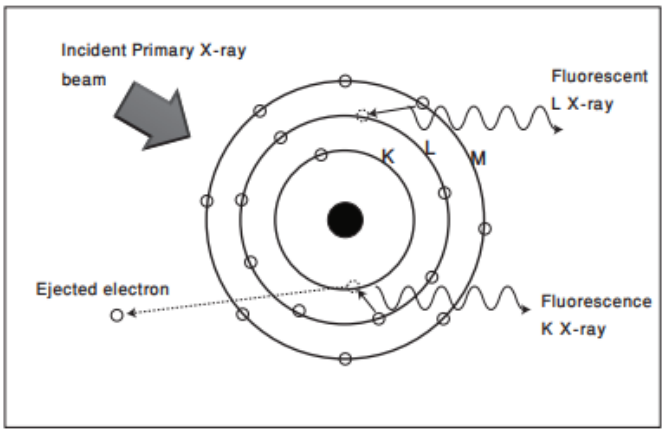

Figure 2-18 X-ray emission through fluorescence; reproduced from [23].

EDXRF spectrometers allow the relative abundances, regarding the intensities, of characteristic X-rays to be plotted against their energy. Therefore, the detector element is struck by the generated characteristic X-rays, causing an electron hole pair, which in turn, leads to a charge pulse that is proportional to the X-ray's energy. A charge-sensitive preamplifier then converts this charged pulse into a voltage pulse, which is then analysed and sorted based on voltage using a multi-channel analyser (MCA). A computer interface then depicts these data as the spectrum of the sample being irradiated by the X-ray; an example of an XRF spectrum is illustrated in Figure 2-19. Afterwards, the software processes the spectrum to determine the elements, and quantitative analysis is conducted to identify the sample's respective concentrations.[23]

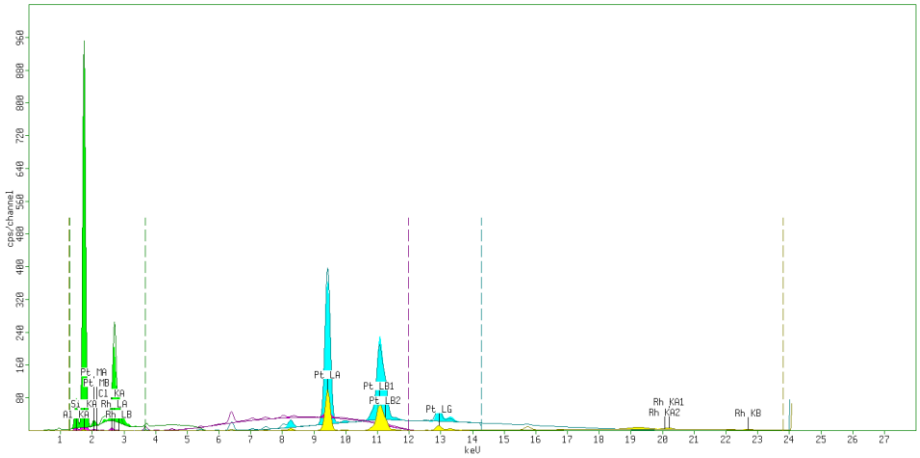

Figure 2-19 X-ray fluorescence spectrum of zeolite USY with 1%Pt.

2.6 References

1. Almulla, F. M.; Zholobenko, V. I.; Hill, P. I.; Chansai, S.; Garforth, A. A., Transalkylation of Toluene with 1, 2, 4-Trimethylbenzene over Large Pore Zeolites. *Industrial Engineering Chemistry Research* **2017,** *56* (35), 9799-9808.

2. McNair, H. M.; Miller, J. M.; Snow, N. H., *Basic gas chromatography*. 3rd ed.; John Wiley & Sons: 2019; p 266.

3. Jennings, W.; Mittlefehldt, E.; Stremple, P., *Analytical gas chromatography*. 2nd ed.; Academic Press: 1997; p 389.

4. De Hoffmann, E., Mass spectrometry. In *Encyclopedia of Chemical Technology*, 2000.

5. Hernandez-Martinez, J. Feedstock recycling of plastic waste by hydrocracking. The University of Manchester, United Kingdom, 2008.

6. Gross, J. H., *Mass spectrometry: a textbook*. 2nd ed.; Springer Science & Business Media: 2011; p 774.

7. Hull, A. W., A new method of chemical analysis. *Journal of the American Chemical Society* **1919,** *41* (8), 1168-1175.

8. Karge, H. G.; Robson, H., *Verified syntheses of zeolitic materials*. 2nd ed.; Elsevier: Amsterdam, The Netherlands, 2001; p 266.

9. Baerlocher, C. Database of zeolite structures. http://www.iza-structure.org/databases/ (accessed 20/03/2021).

10. Bartholomew, C.; Farrauto, R., *Fundamentals of industrial catalytic processes*. 2nd ed.; 2010; p 992.

11. Cullity, B. D., *Elements of X-ray diffraction. Reading*. 2nd ed.; Addison-Wesley: 1978; p 569.

12. Ojha, K.; Pradhan, N. C.; Samanta, A. N., Zeolite from fly ash: synthesis and characterization. *Bulletin of Materials Science* **2004,** *27* (6), 555-564.

13. Heath, J., *Energy dispersive spectroscopy*. 2nd ed.; John Wiley & Sons Ltd: UK, 2015; p 32.

14. Jentys, A.; Lercher, J. A., Techniques of zeolite characterization. *Studies in Surface Science and Catalysis* **2001,** *137*, 345-386.

15. Hanaor, D. A. H.; Ghadiri, M.; Chrzanowski, W.; Gan, Y., Scalable surface area characterization by electrokinetic analysis of complex anion adsorption. *Langmuir* **2014,** *30* (50), 15143-15152.

16. Prins, R.; Wang, A.; Li, X., *Introduction to Heterogeneous Catalysis*. World Scientific Publishing Company: 2016; Vol. 1, p 348.

17. Rouquerol, J.; Rouquerol, F.; Llewellyn, P.; Maurin, G.; Sing, K., *Adsorption by powders and porous solids: principles, methodology and applications*. second edition ed.; Academic Press: 2013; p 646.

18. Sing, K. S. W., Adsorption, Surface Area and Porosity. *Academic Press, London* **1982**.

19. Wieboldt, R. C.; Lowry, S. R.; Rosenthal, R. J., TGA/FT-IR: thermogravimetric analysis with fourier transform infrared detection of evolved gases. *Microchimica Acta* **1988,** *94* (1), 179-182.

20. Anderson, J. R.; Pratt, K. C., *Introduction to characterization and testing of catalysts*. Academic Press: 1985; p 457

21. Thomas, J. M.; Thomas, W. J., *Principles and practice of heterogeneous catalysis*. John Wiley & Sons: 2014; p 768.

22. Thomas, J.; Thomas, W., Heterogeneous catalysis. *Kapitel* **1997,** *2*, 67.

23. Khalid, A.; Khan, A. T.; Anwar, M. S., X-Ray Fluorescence (XRF) spectrometry for materials analysis and "discovering" the atomic number. *Journal of Physics* **1996,** *64*, 335-338.

3 Catalysing the Hydrocracking of Low Density Polyethylene

3.0 The relevance of the "Catalysing the Hydrocracking of Low Density Polyethylene" paper to the thesis context

The manuscript presented in this chapter has been submitted to the *Industrial & Engineering Chemistry Research*, published on October 21st 2019. The hydrocracking of polymer waste is the central theme of this thesis and for that to be accomplished, a greater understanding of the hydrocracking process and the catalysts utilised is required. Regarding the high complexity level of dealing with a mixed waste stream of polymers, the first step of this project was to hydrocrack the less viscous, model compound of squalane, which is a branched C_{30} hydrocarbon with a similar chemical framework to saturated polyolefins. The main objectives of this step were to test the catalytic reactor and solve any technical issues, as well as to study the performance of different catalysts under reaction conditions. Therefore, a better understanding of the fundamental properties of the hydrocracking process could be obtained for application to the polymer target materials in this study.

The second step was to convert a pure polymer, to reduce the complexity that comes from additives and colourants added to processed consumer polymers. The focus was initially on the hydrocracking of low-density polyethylene (LDPE) being the most produced polymer and subsequently the largest in the waste stream. In addition, LDPE is reported to be the most difficult polymer to be hydrocracked (Section 1.5.1.4), therefore, the hydrocracking conditions and catalysts proposed are very likely to successful convert the other types of polyolefin.

Catalysing the Hydrocracking of Low Density Polyethylene

Abdulrahman Bin Jumah,[1] Vanithasri Anbumuthu,[1] Aleksander A. Tedstone[1] and Arthur A. Garforth[1]*

**Corresponding Author: arthur.garforth@manchester.ac.uk*

1) School of Chemical Engineering and Analytical Science, University of Manchester, The Mill, Sackville Street, M1 3BB, United Kingdom

3.1 Abstract

The hydrocracking of squalane and low density polyethylene (LDPE) into low molecular weight hydrocarbons has been demonstrated with the use of bifunctional zeolite catalysts, Pt- impregnated USY and Beta, with selectivity towards isomers of C_4-C_6 alkanes. Quantification of liquid and gaseous products via GC-FID and GC-MS demonstrated that appropriate catalyst selection can yield >95% conversion of polymer to fluid products at mild reaction conditions of 330 °C, 20 bar H_2 and short reaction times of <15 min in a batch system. Zeolite Beta exhibits a marked selectivity towards C_4 hydrocarbons and its efficacy in this reaction is related to its acidic and structural properties, and the appropriate selection of reaction time, temperature and Pt-loading are discussed.

3.2 Introduction

Polypropylene and polyethylene represent 30-40% of plastic consumer waste in the UK, and can be separated from the ~2.3 Mtonnes per annum collected by local authorities, but is not readily recycled via mechanical reprocessing or biodegradable.[1, 2] On a global scale, this will become a greater problem as countries become more

developed and demand increases. Some condensation polymers can be readily depolymerised to monomer,[3-6] but addition polymers like polyolefins are generally more chemically stable.[7-9] They do, however, represent a highly refined hydrocarbon source in their life beyond single-use plastics, and if reprocessed chemically could become a viable alternative to extracted oil and gas sources for petrochemical feedstocks and fuels. The added environmental incentives are the avoidance of landfill and incineration, with their associated containment and emissions issues.[10, 11]

Pyrolysis of plastic waste has been extensively researched and can generate useful products,[12] and offers an alternative to other types of disposal, but still poses problems in terms of the efficiency of the process,[13] which catalysis may help to address. Previous efforts have identified metal-loaded zeolite catalysts as promising candidates for short reaction times under mild conditions in the hydrocracking of polymer feedstocks.[3, 14] Production of hydrocarbon fuels can be performed with this process, as well as platform chemicals for various industries, but without the associated efficiencies to make it a viable long term solution.[15]

Polyolefin materials represent a distinct challenge for heterogeneous catalysis; despite similarities in the nature of their chemical bonding to smaller hydrocarbons, the physical properties conferred by their high molecular weights cause a number of issues when attempting chemical transformations. Mass and heat transfer are inefficient (and often anisotropic) due to the high viscosity of most polymer melts,[16, 17] and long carbon chains hinder access to catalytic sites, notably the active site-containing micropores of zeolite catalysts that have proven effective in hydrocarbon transformations in industrial processes. Previous efforts to catalytically convert polyolefins into valuable hydrocarbon fractions have focused on production of fuels, and can produce

significant fractions of unsaturated hydrocarbons,[18] with efforts being made to direct the process to higher yields of paraffins.[19] Previous work has also indicated the possibility of re-use of fluid cracking catalysts for this process.[20]

Other attempts to catalyse the pyrolysis of polyolefins have been made; R. van Grieken et al. carried out thermal pyrolysis of LDPE at 420°C for 30 min resulting in 95 wt.% solid and 5 wt.% liquid yield.[21] To enhance the conversion, the reaction is catalysed by nano-H-ZSM-5 yielding 35% liquid and 65% gas at the reduced temperature of 380 °C.[21] Supporting the idea of catalytic pyrolysis, zeolite-Y[22, 23], mordenites[23, 24], and silica/alumina[23] converted HDPE[22, 23] and PP[22] to produce 70 to 81 wt.% oil in the gasoline range (C_6-C_{12}) at reaction times of 30 min at 450°C.[23] In the absence of catalyst, a heavier liquid product is produced, that solidifies during storage.[23] The liquid stream produced by catalytic pyrolysis is mainly formed of unsaturated hydrocarbons.[22, 23] There remains room to improve the process to yield more stable and desired hydrocarbon fractions, for example, isomerised alkanes for fuels.[25, 26]

Hydrocracking of PE progresses to full conversion at conditions of 270-800 °C, 55-71 bar H_2 and relatively short reaction time[14, 27-29] over bi-functional catalysts, such as Ni on activated carbon,[27] Pt-USY[14] and Co-Mo-modified natural zeolite[29], enhance the hydrocracking reaction, as the selected metals facilitate hydrogenation-dehydrogenation pathways. The product stream on hydrocracking of LDPE is predominately gases (C_1-C_4) and the liquid fraction is gasoline range oil.[29]

This study investigates the zeolite-catalysed hydrocracking of a branched long chain hydrocarbon, squalane (Figure 3-1A), as a model compound for depolymerised polyolefins, and the environmentally problematic polymer low density polyethylene (LDPE) (Figure 3-1B, C). The effects of metal-loading, reaction temperature and time

are studied, as well as mixing parameters that can influence the production of relatively small hydrocarbons in the ranges of gas, liquid petroleum gas (LPG), naphtha, gasoline and diesel. This approach to plastic waste supports a circular economy in the polymer industry, providing a route to recapture the value of this ubiquitous commodity. Zeolite USY, a dealuminated form of zeolite Y, and zeolite Beta, a partially disordered zeolite, are the focus of this study.

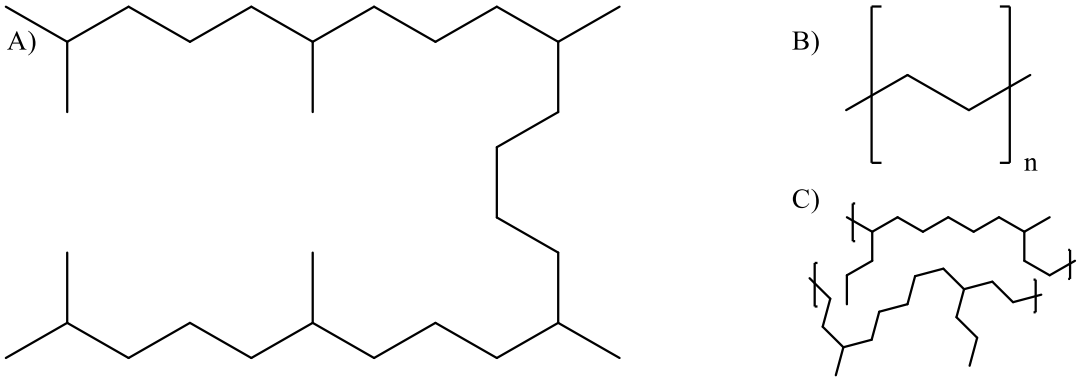

Figure 3-1 (A) Squalane (2,6,10,15,19,23-hexamethyltetracosane) (B) Polyethylene repeat unit (C) Schematic of the branched structure of LDPE, containing primary, secondary and tertiary carbons.

3.3 Experimental

Chemicals were obtained from Sigma Aldrich. Zeolite powders were obtained from Zeolyst International, and high purity Low Density Polyethylene (M_w ~ 150 000 g/mol) (LDPE) from Goodfellows were received in powder (< 400 μm) or pellet form and was used as a model polymer for the hydrocracking tests. The zeolite catalysts used in this study were acidic H-form Beta (Si/Al_{bulk} 12.5 and 175) and acidic H-form USY (Si/Al_{bulk} 6 and 15). All catalysts were used in pellet form in the size range 212 – 500 μm.

3.3.1 Platinum impregnation

Platinum loading of zeolite catalysts was performed with aqueous tetraamineplatinum (II) chloride ($Pt[NH_3]_4Cl_2$, 4.59 mmol/dm aq.) at solid/solution loadings of 0.01 g/mL.

Catalysts were calcined in a tubular reactor with a flow of air (50 mL/min) at 450 °C for 240 min to remove water and organic components. They were subsequently reduced with H_2 (50 mL/min) at 450 °C for 240 min slow heating and cooling ramps (2 °C/min) were used.

3.3.2 Catalyst characterisation

The catalysts used were characterised using SEM/EDX and performed with a Quanta 250 system equipped with an Oxford Instruments $XMax^N$ EDX detector. Imaging was performed at 5 kV and EDX at 10 kV to excite the Mα and Lα emissions at 2.05 and 9.44 keV respectively (Figure 3-8). The identity and crystallinity of the catalysts were obtained by X-ray diffraction (XRD) using a Bruker D2 Phaser (Figure 3-9). Pt-dispersion measurements of the catalysts were quantified by Temperature Program Desorption (TPD, Quantachrome ChemBET Pulsar TPR/TPD analyser. The Pt modified catalysts were first reduced under H_2 flow of 40 mL/min at 485 ^oC, and then exposed to pulses of 1 mol% of CO in helium at 850 ^oC to initiate desorption. The distribution and size of the platinum within Beta catalyst was, also, observed using high-angle annular dark-field (HAADF) imaging on a FEI F30 transmission electron microscope (TEM) operating at 300kV in STEM mode (Figure 3-10) Platinum particles were observed to be 1.0-1.5 nm and located on the external surfaces of the catalyst as the pore diameter (0.67 nm) would exclude the particles. The acidity of the catalysts quantified by Temperature Program Desorption (TPD, Quantachrome ChemBET Pulsar TPR/TPD analyser. The Pt modified catalysts were first reduced under H_2 flow of 40 mL/min at 485 ^oC, and then cooled to room temperature, then exposed to 5% of NH_3 in Ar and the temperature was ramped up to 800 ^oC. The signal of NH_3 desorbed was recorded against temperature, and integrated to yield weak acid

concentrations (150-300 °C) and strong acid site concentrations (300-800 °C) (Table 3-1, Figure 3-11). In addition, the coke formed on the catalysts during the reactions was quantified using thermogravimetric analysis (TGA, Q5000-IR TA instrument) at a heating rate of 10 °C/min in air to 600 °C, and held at this temperature for 1 hr. The ramping step was performed in nitrogen for the used catalyst post-LDPE conversion, and carbon content determined by mass loss above 300 °C after the removal of water (Table 3-2). Platinum concentrations determined by X-ray Fluorescence (XRF) with a PANalytical MiniPal 4 EDXRF (Table 3-1).

Table 3-1 Characteristics of zeolites used

Zeolite	Si/Al[a]	Weak acid concentration (µmol /g)	Strong acid concentration (µmol /g)	Surface area (m^2/g)	Platinum wt%[c]	Designation
USY	6.0	-	-	730[a] 571[b]	-	USY(6)
USY	15	-	-	780[a]	-	USY(15)
Beta	12.5	-	-	680[a] 485[b]	-	Beta(12.5)
Beta	175	-	-	620[a]	-	Beta(175)
Pt-USY	6.0	631	343	542[b]	1.07	1 wt% Pt-USY(6)
Pt-USY	15	453	182	-	0.92	1 wt% Pt-USY(15)
Pt-Beta	12.5	877	516	407[b]	1.08	1 wt% Pt-Beta (12.5)
Pt-Beta	12.5	-	-	-	0.69	0.75 wt% Pt-Beta (12.5)
Pt-Beta	12.5	-	-	-	0.46	0.5 wt% Pt-Beta (12.5)
Pt-Beta	175	324	85	-	0.96	1 wt% Pt-Beta (175)

[a] As quantified by manufacturer .[b] Values determined by N_2 BET. [c]Values determined by XRF

3.3.3 Reaction with squalane/polymer

Catalytic hydrocracking of squalane and polymer was performed at a feed:catalyst ratio of 10:1, in a 300 mL stainless steel Parr Reactor, agitated by an ‘anchor’ style stirrer, with a PTFE gasket seal. Squalane or polymer (20 g) and catalyst (2 g) mixtures were loaded into the reaction vessel, which was subsequently sealed and purged three times with hydrogen gas to a pressure of 5 bar, before filling with hydrogen at the

reaction pressure. The temperature of reaction was recorded via a K-type thermocouple (RS Instruments) inserted into the reaction vessel, and submerged in the molten polymer. External reactor temperature was maintained by an additional K-type thermocouple coupled to a Parr Instruments 4841 Temperature Controller. The reaction vessel was configured as shown in Figure 3-2, where ideally thermocouple TI is submerged in the heterogeneous reaction mixture.

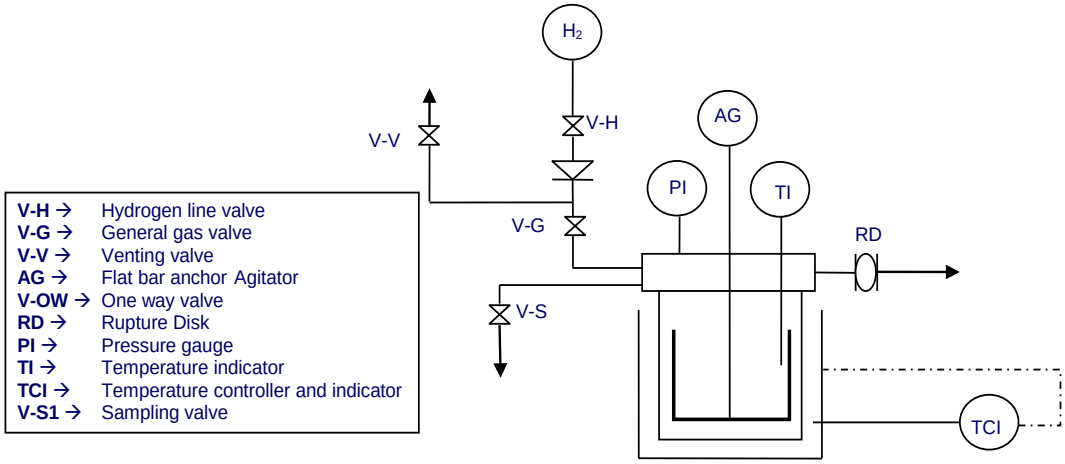

Figure 3-2 Reactor configuration with control over temperature, agitation type and speed, and pressure.

Reaction temperature is achieved within 40-50 min (heating time), and the reaction temperature and pressure was recorded at 1 minute intervals during the experiment. Figure 3-3 illustrates an example of temperature and pressure profile versus time. At a specified reaction time, the reactor is cooled down and products are collected at room temperature for GC analysis.

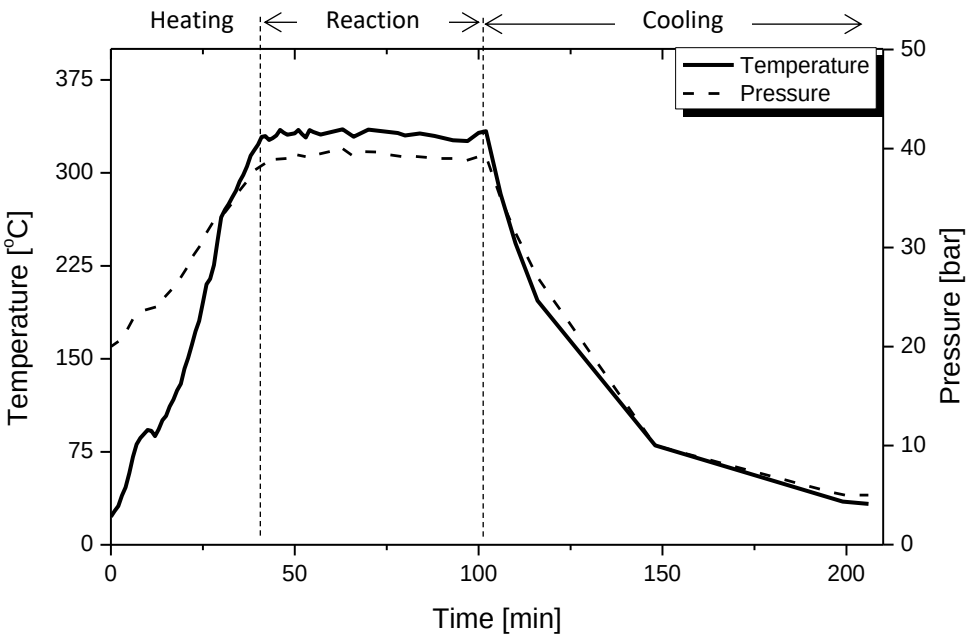

Figure 3-3 Typical temperature and pressure profile for LDPE with 1 wt% Pt Beta (12.5), plateau region is the stated reaction time of 60 min.

3.3.4 Product analysis

Liquid samples were analysed by Gas Chromatography-Mass Spectrometry (GC-MS) using Agilent Technologies 6890N Network GC fitted with a 100 m × 0.25 mm i.d. Pona CB column. For the gas samples, a Varian CP3800 GC-FID fitted with a 50 m × 0.32 mm i.d. PLOT Al_2O_3/KCl capillary column was used, and quantification was performed against a 1 mol% gas standard mixture (C_1-C_5).

3.4 Results and discussion

3.4.1 Squalane hydrocracking

In order to isolate the effects of the polymers physical properties (high viscosity, low hydrogen solubility) from its chemical properties with respect to hydrocracking, a model compound was chosen for initial experiments. Squalane (2,6,10,15,19,23-hexamethyltetracosane, $C_{30}H_{62}$) acts as a sufficiently long hydrocarbon to simulate polyethylene chains in the hydrocracking environment, being of sufficient size to be excluded from the catalyst pores, with no difference in chemical functionality. The

mass transfer and heat transfer limitations of polymeric melts are reduced, as squalane is liquid at room temperature and can therefore be intimately mixed with the catalyst prior to heating, and squalane has a boiling point of 176 °C.[15] Similar to low density polyethylene, a degree of branching due to methyl substituents on the main hydrocarbon backbone of squalane gives primary, secondary and tertiary carbon environments. Figure 3-1 demonstrates the molecular structure of squalane and its similarity to the moderately branched form of polyethylene used in this study. The additional benefit of squalane is that unreacted material will yield a single, well defined component during product analysis and will elute in gas chromatography for quantification of conversion.

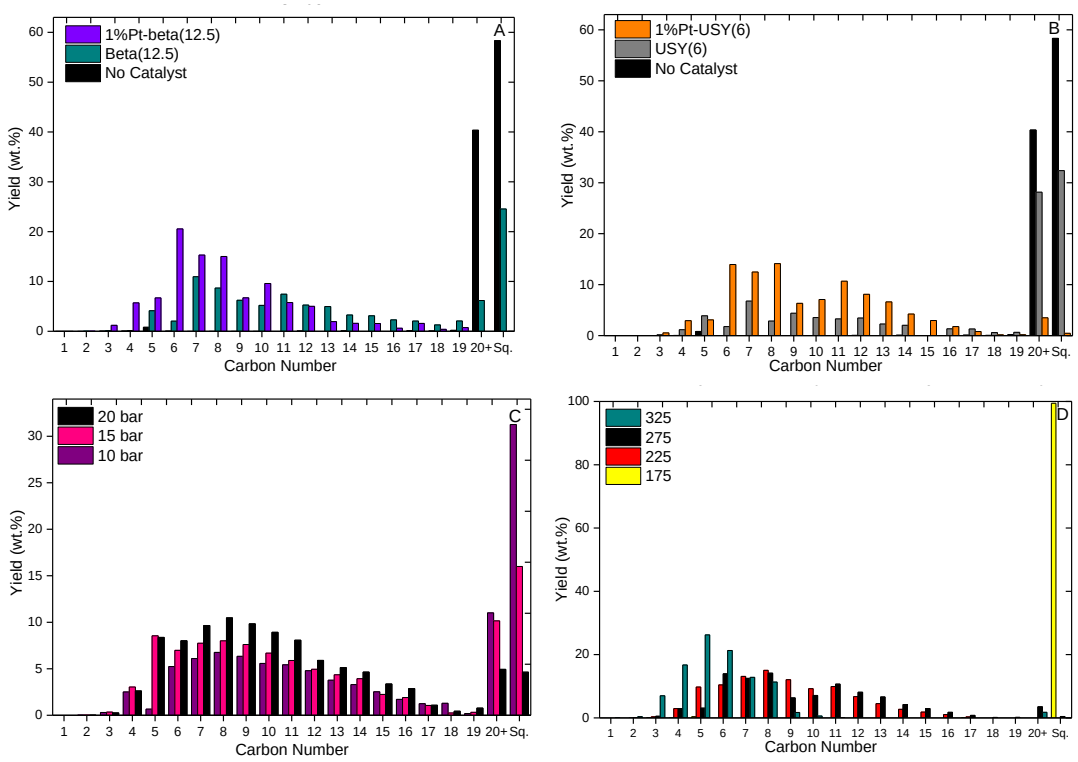

Figure 3-4 (A) Product distribution of zeolite beta-catalysed squalane hydrocracking at 275 °C and 20 bar. (B) Product distribution of zeolite USY-catalysed squalane hydrocracking at 275 °C and 20 bar (C) Effect of pressure on product distributions of Pt-USY (6) catalysed squalane hydrocracking reactions, performed at 275°C and with varying pressure of H_2 (D) Comparison of product distributions in the 1 wt% Pt-USY(6) catalysed hydrocracking of squalane with varying temperature at 20 bar.

The inclusion of a solid acid catalyst in the hydrocracking reaction of squalane drastically improves the yield of light hydrocarbons (Figure 3-4), with platinum

impregnation at 1.0 wt% provides an even greater increase in conversion to C_5-C_{10} hydrocarbons. Zeolite Beta (12.5) proved more effective at reducing the molecular weight of the products than USY (6), and as the Si/Al ratio of zeolite catalyst is well known to influence the concentration of Brønsted and Lewis acid sites,[30] this property was further investigated by variation of this ratio in the two different zeolite types.

Zeolite Beta (12.5) impregnated with 1 wt% Pt(0) was chosen to explore the parameters of degradation of low density polyethylene (LDPE). The irregularity in the crystalline structure of zeolite Beta arising from its alternating layer structure may have speculative benefits in mass transfer of the polymer due to the mesoporosity found within the layers. Limited tests of zeolite USY (6) impregnated with 1 wt% Pt(0) were also performed as it also demonstrated potential as a polymer hydrocracking catalyst. The platinum particles are 1.0-1.5 nm, and are located on the surface of the zeolite catalyst, as evidenced by HAADF-TEM (Figure 3-10), meaning hydrocarbons will be capable of interacting with the Pt(0) catalytic sites despite being size-excluded by the pore channel system of the zeolite itself.

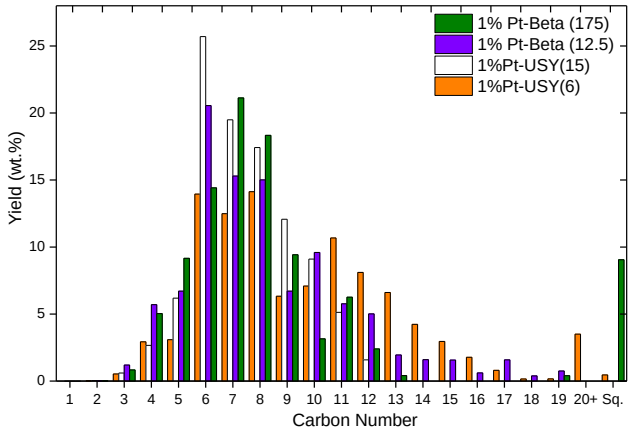

Figure 3-5 Product distributions of squalane hydrocracking with varying bifunctional catalysts at 275 °C, and an initial H_2 pressure of 20 bar.

The influence of zeolite acidity is presented in Figure 3-5, clearly demonstrating that in the case of zeolite Beta, extensive dealumination and hence a silica-rich structure

such as Beta (175) reduces the conversion of squalane to lighter products. Corroborated with the acidity measurements in Table 3-1, this is likely to be a result of the decrease in acid-site density. The USY catalyst does not suffer as dramatic a loss of activity upon increased Si/Al ratio, with a slightly increased selectivity towards C_6 hydrocarbons. This is a potential benefit of the more siliceous catalyst, however the lower ratio USY(6) was chosen to investigate LDPE hydrocracking due to its established position in industrial hydrocracking processes.[31, 32] The coke contents of the catalysts after reaction (summarised in Table 3-2) shown in Figure 3-5 correspond to their acidity – the highest coke level of 7.4 wt% at a reaction temperature of 275 °C is found on the more acidic form of USY(6), relative to 5.0 wt% on USY(15) at the same reaction conditions. An increased reaction temperature led to higher levels of carbon content on the USY(6) catalyst, but a greater preference for the production of C_5 hydrocarbons; this illustrates the importance of optimising the process parameters to avoid an excessive need to regenerate the catalyst.

3.4.2 Low density polyethylene hydrocracking

Low density polyethylene exhibited significantly greater resistance to hydrocracking relative to squalane, requiring a higher reaction temperature, but very similar product distributions were observed when appropriate conditions were selected to overcome its lower reactivity. The lower conversion, *X*, was attributed to the high viscosity of the molten polymer limiting the mass transfer to the catalyst particle surfaces and subsequently kinetically blocking entry into the zeolite pores once the products were of suitably low molecular weight to enter the micropores (7.35 Å and 5.95 Å for USY and Beta respectively) of the structure. Additionally, hydrogen solubility in the molten polymer is low and this will provide a further barrier to reaction in the early stages of

reaction. Sun et al. found that hydrogen solubility in polyethylene is limited to around 10^{-3} g [H_2]/g [PE] in molten polymer at 90 °C and 8 atm pressure, rising with both temperature and pressure.[33] It is clear therefore that effective mixing is very important for this reaction to proceed, not only between substrate and catalyst, but between the reagent gas and this mixture. The temperatures and pressures required also reflect the mass transfer limitations, but at a comparatively mild temperature relative to pyrolysis processes, that are typically performed at >400 °C.[12, 34]

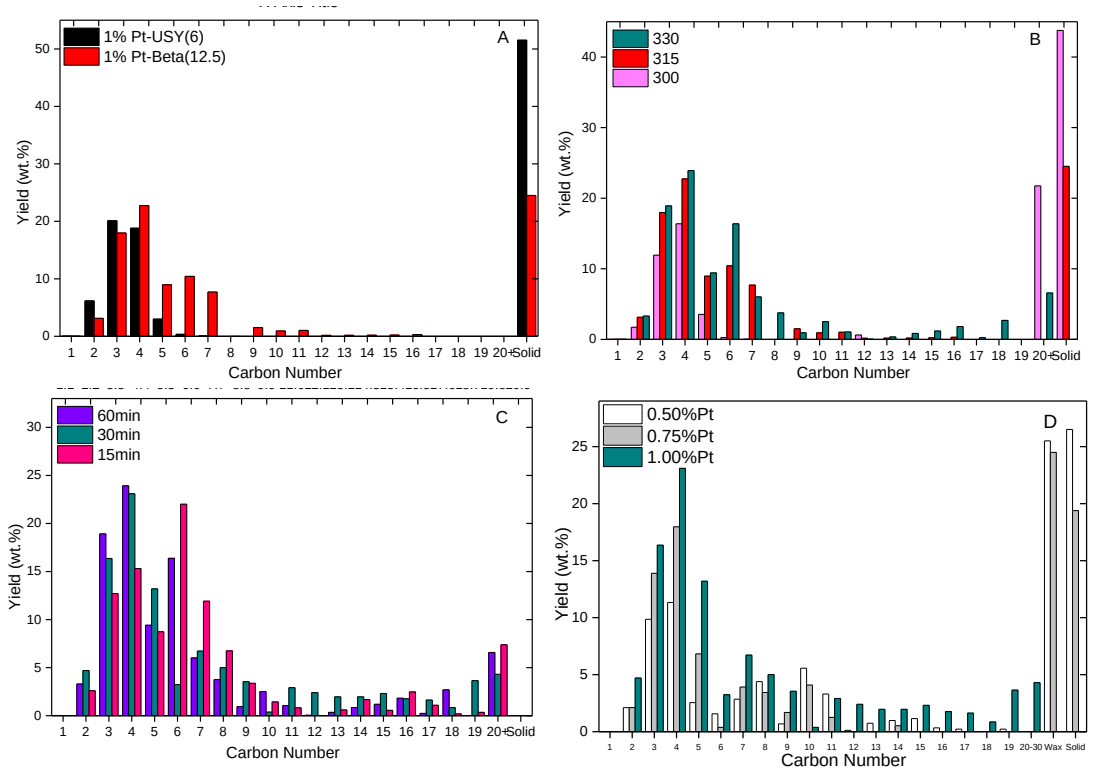

Figure 3-6 Product distributions of catalytic degradation products of LDPE. All reactions performed with an initial pressure of 20 bar H_2. (A) Comparison of the performance of 1 wt% Pt-impregnated USY(6) and Beta (12.5) at 315 °C for 60 mins. (B) The effect of varying reaction temperature at 60 min reaction time at 330 °C with 1 wt% Pt-Beta (12.5). (C) The effect of varying reaction time using 1 wt% Pt-Beta (12.5) at 330 °C. (D) The effect of platinum loading at 0.50 wt%, 0.75 wt% and 1.00 wt%, at 330 °C.

Figure 3-6A demonstrates the enhanced ability of zeolite Beta versus USY to reach higher conversion rates at 315 °C, under an initial hydrogen pressure of 20 bar in a 300 mL volume, at the expense of some loss of selectivity toward C_3 and C_4 hydrocarbons. The benefit of an increased reaction time was demonstrated in Figure 3-6C; the zeolite micropore selectively produces alkanes of a similar size to the

channels within the crystalline structure. Conversion is also highly dependent on temperature (Figure 3-6B); increasing the reaction temperature from 300 °C to 330 °C results in full conversion of the solid into fluid hydrocarbons ($X_{Solid\ to\ Fluid} = 1$). This may be attributable to the heat transfer and mass transfer issues associated with the polymer melt, as the product distribution is very similar at 300 °C, 315 °C and 330°C, but $X_{Solid\ to\ Fluid}$ increases from 0.562 to 0.755 to 1.00 at these temperatures respectively. Squalane did not exhibit this temperature dependent behaviour despite very similar chemical functionality of squalane and the polyethylene repeat unit; relatively few carbon chain scission reactions are required in the case of squalane before the products can enter the pores of the zeolite catalysts. In the case of polyethylene, it will be excluded from the pores until near-complete conversion, and catalyst is likely to remain in a fluid melt until very high conversion is achieved. Higher temperatures or extended reaction times are therefore critical in yielding $X_{Solid\ to\ Fluid} = 1$. The consequence of an extended reaction time is a higher coke content on the catalyst, rising from 8.4 wt% after 15 min of reaction to 9.9 wt% after 60 min of reaction (Table 3-2) for 1 wt% Pt-Beta(12.5).

Partial disorder in zeolite beta plays an important role in achieving high values of $X_{Solid\ to\ Fluid}$, as the structure places adsorbed molecules at the zeolite surface nearer to a pore opening and hence reactive sites for bond scission. The hydrodynamic volume of polymer molecules is typically 10 to 1000 the size of zeolite micropores (1-10 Å), demonstrated by the typical choice of stationary phase materials in gel permeation chromatography.[35] The majority of bond scission must therefore be occurring on surface sites of the zeolite particle, prior to the smaller hydrocarbons entering the pore system to introduce potential selectivity.

At the reaction temperatures and catalyst concentration in this study, the reaction proceeded quickly (within 15 min), with extended reaction times bringing the product distribution to lower carbon numbers. Relatively small amounts of methane (< 0.1%) and ethane (< 5%) are produced, consistent with other attempts to pyrolyse plastic both catalytically and non-catalytically at temperatures of 400-600 °C.[36, 37] Exceeding this temperature tended to produce greater quantities of methane irrespective of the catalyst.[38]

The mechanism of catalytic polyethylene reaction in an inert atmosphere has been proposed as proceeding *via* carbenium ions on the polymer chain that perform "back-biting" reactions.[39] The acidic zeolite donates a proton to this intermediate, and the balance of Brønsted acid sites and Lewis acid sites is therefore important in determining the number of active sites for catalysis. As tertiary carbon environments are most capable of stabilizing the positive charge, this frequently leads to the production of branched isomers.[40] Hydrogen plays a dual role in maintaining the activity of the catalyst (preventing both hard coke formation and maintaining a reductive environment for platinum) as well as hydrogenating the polymer and its cracking products; this has been extensively characterised in the case of zeolite hydrocracking reactions. Direct hydrogenolysis of hydrocarbons at the metal sites gives high yields of methane and ethane,[32, 41] and due to low quantities being observed in this study, it is evidently not the dominant reaction pathway. It is hypothesised that protonation at the acid sites within the zeolites and the hydrogenation/dehydrogenation function of the metal sites are responsible for the reactivity observed. Bifunctional metal-loaded zeolites are very active hydroisomerisation catalysts, and particular Pt-functionalised zeolite beta, as demonstrated by near-quantitative n-pentane conversion to isopentane at 230°C in a fixed-bed continuous flow reactor.[42] It is therefore difficult

to selectively produce linear alkanes with this approach. Figure 3-6D demonstrates the importance of sufficient Pt-loading for high $X_{Solid\ to\ Fluid}$, and is another factor to consider in the optimisation of this reaction.

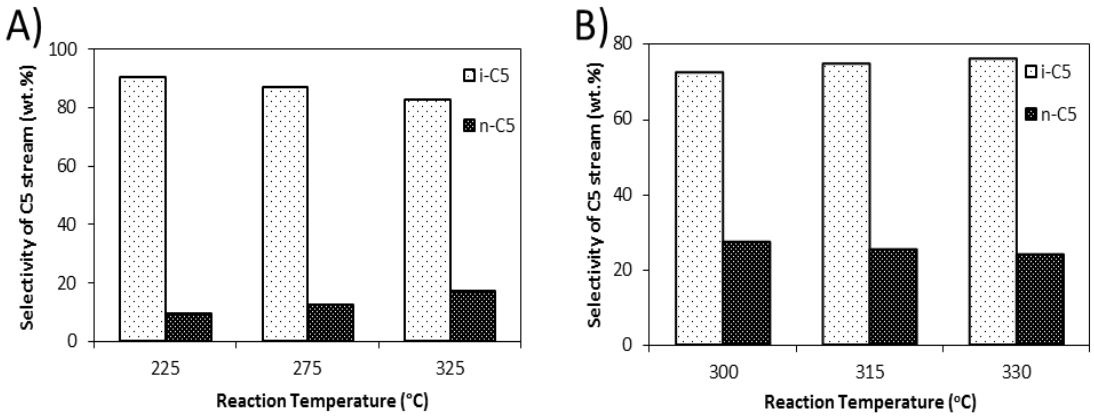

Figure 3-7 Ratio of i-pentane to n-pentane with increasing temperature in the hydrocracking of (A) squalane (B) LDPE with an initial H_2 pressure of 20 bar.

The high excess of iso-pentane relative to n-pentane is demonstrated in Figure 3-7 and is consistent with a mechanism proceeding via tertiary carbenium ions and back-biting reactions. The reduced selectivity (90.5% to 82.7%) towards iso-pentane with increasing temperature shown in Figure 3-7A may be a result of further hydro-isomerisation,[43, 44] which proceeds within zeolites and is highly dependent upon the micropore dimensions.[45, 46] In the case of LDPE, isopentane is not produced in as high an excess relative to n-pentane (72% to 75%), possibly attributable to varying amounts of tertiary carbons in the feedstock. The thermal stability of polyolefins is highly dependent on the amount of tertiary carbons[14, 47, 48] as well as on their tacticity;[49] more tertiary carbon content (ie. branching in the polymer) and steroisomeric randomness decreases their thermal stability.

As this process develops towards real waste streams with potential contaminants such as sulfur, the resistance to active site poisoning will require consideration, with bimetallic systems such as Pt-Pd H-Beta proving effective in this respect,[50] as well as

metal sulphide systems that can specifically perform hydrodesulfurization processes.[51, 52]

3.5 Conclusions

As our previous work and this study demonstrate, zeolitic catalysts have great potential to reduce the energy required for conversion of polyolefin plastic waste, with a degree of specificity toward alkanes of molecular weights defined by the pore size of the catalyst. Catalytic hydrocracking of low density polyethylene with bifunctional zeolite catalysts has been demonstrated to yield low molecular weight hydrocarbons that can be classified as naphtha, at mild conditions as 300-330 °C in a 5-20 bar hydrogen atmosphere. This product stream can easily be incorporated into widespread industrial petrochemical refining activities such as distillation and steam cracking.

Having established this catalytic approach to polymer hydrocracking as an alternative to pyrolysis, further development of the reaction system with optimised reactor geometries and conditions is now possible. Investigation of other plastic waste streams and the influence of contaminants will yield further insight into the applicability of catalysed approaches for waste reclamation, as industrialisation of this type of process offers an extra solution among many to counter the growing global problem of plastic waste.[9] Due to its partially disordered structure and high acidity, zeolite Beta with a 1wt% platinum impregnation is found to be particularly suitable for this application.

3.6 Acknowledgements

Abdulrahman Bin Jumah would like to acknowledge the support of King Saud University in Riyadh (KSA) for research funding. UK Catalysis Hub is kindly thanked

for resources and support provided via our membership of the UK Catalysis Hub Consortium and funded by EPSRC grant: EP/R027129/1.

3.7 Associated content

Supporting Information Available: Additional figures and tabulated information supporting the experimental work are available as supporting information Figure 3-8: Secondary electron images of selected catalysts. Figure 3-9: pXRD of selected catalysts. Figure 3-10: HAADF-TEM of representative catalyst particle. Figure 3-11: Ammonia TPD acidity profiles for selected catalysts. Table 3-2: Carbon content summary of catalysts used. Table 3-3: Carbon monoxide TPD metal adsorption data for Pt-impregnated catalysts.

3.8 References

1. Cui, H.; Sosic, S., Recycling common materials: effectiveness, optimal decisions, and coordination mechanisms. *European Journal of Operational Research* **2019,** *274* (3), 1055-1068.

2. Hopewell, J.; Dvorak, R.; Kosior, E., Plastics recycling: challenges and opportunities. *Philosophical Transactions of the Royal Society B: Biological Sciences* **2009,** *364* (1526), 2115-2126.

3. Garforth, A. A.; Ali, S.; Hernandez-Martinez, J.; Akah, A., Feedstock recycling of polymer wastes. *Current Opinion in Solid State and Materials Science* **2004,** *8* (6), 419-425.

4. Yang, Y.; Lu, Y.; Xiang, H.; Xu, Y.; Li, Y., Study on methanolytic depolymerization of PET with supercritical methanol for chemical recycling. *Polymer Degradation and Stability* **2002,** *75* (1), 185-191.

5. Chen, J. Y.; Ou, C. F.; Hu, Y. C.; Lin, C. C., Depolymerization of poly(ethylene terephthalate) resin under pressure. *Journal of Applied Polymer Science* **1991,** *42* (6), 1501-1507.

6. Siddiqui, M. N.; Achilias, D. S.; Redhwi, H. H.; Bikiaris, D. N.; Katsogiannis, K. A. G.; Karayannidis, G. P., Hydrolytic depolymerization of PET in a microwave reactor. *Macromolecular Materials and Engineering* **2010,** *295* (6), 575-584.

7. Gray, R. L., Accelerated testing methods for evaluating polyolefin stability geosynthetic testing for waste containment applications. ASTM International: West Conshohocken, PA, 1990; pp 57-74.

8. Sen, S. K.; Raut, S., Microbial degradation of low density polyethylene (LDPE): A review. *Journal of Environmental Chemical Engineering* **2015,** *3* (1), 462-473.

9. Barnes, D. K. A.; Galgani, F.; Thompson, R. C.; Barlaz, M., Accumulation and fragmentation of plastic debris in global environments. *Philosophical Transactions of the Royal Society B: Biological Sciences* **2009,** *364* (1526), 1985-1998.

10. Li, C.-T.; Zhuang, H.-K.; Hsieh, L.-T.; Lee, W.-J.; Tsao, M.-C., PAH emission from the incineration of three plastic wastes. *Environment International* **2001,** *27* (1), 61-67.

11. Eriksson, O.; Finnveden, G., Plastic waste as a fuel - CO_2-neutral or not? *Energy & Environmental Science* **2009,** *2* (9), 907-914.

12. Anuar Sharuddin, S. D.; Abnisa, F.; Wan Daud, W. M. A.; Aroua, M. K., A review on pyrolysis of plastic wastes. *Energy Conversion and Management* **2016,** *115*, 308-326.

13. Rollinson, A. N.; Oladejo, J. M., 'Patented blunderings', efficiency awareness, and self-sustainability claims in the pyrolysis energy from waste sector. *Resources, Conservation and Recycling* **2019,** *141*, 233-242.

14. Akah, A.; Hernandez-Martinez, J.; Rallan, C.; Garforth, A. A., Enhanced feedstock recycling of post-consumer plastic waste. *Chemcal Engineering Transactions* **2015,** *43*, 2395-2400.

15. Buekens, A. G.; Huang, H., Catalytic plastics cracking for recovery of gasoline-range hydrocarbons from municipal plastic wastes. *Resources, Conservation and Recycling* **1998,** *23* (3), 163-181.

16. Hassan, H.; Regnier, N.; Pujos, C.; Defaye, G., Effect of viscous dissipation on the temperature of the polymer during injection molding filling. *Polymer Engineering & Science* **2008,** *48* (6), 1199-1206.

17. Griskey, R. G.; Wiehe, I. A., Heat transfer to molten flowing polymers. *AIChE Journal* **1966,** *12* (2), 308-312.

18. Escola, J. M.; Aguado, J.; Serrano, D. P.; Briones, L.; Díaz de Tuesta, J. L.; Calvo, R.; Fernandez, E., Conversion of polyethylene into transportation fuels by the combination of thermal cracking and catalytic hydroreforming over Ni-Supported hierarchical beta zeolite. *Energy Fuels* **2012,** *26* (6), 3187-3195.

19. Arthur, G.; Yeuh-Hui, L.; Paul, S.; John, D., Catalytic polymer degradation for producing hydrocarbons over zeolites. In *Studies in Surface Science and Catalysis*, Hattori, H.; Otsuka, K., Eds. Elsevier: 1999; Vol. 121, pp 197-202.

20. Salmiaton, A.; Garforth, A. A., Multiple use of waste catalysts with and without regeneration for waste polymer cracking. *Waste Management* **2011,** *31* (6), 1139-1145.

21. Van Grieken, R.; Serrano, D. P.; Aguado, J.; Garcıa, R.; Rojo, C., Thermal and catalytic cracking of polyethylene under mild conditions. *Journal of Analytical and Applied Pyrolysis* **2001,** *58*, 127-142.

22. Santos, B. P. S.; Almeida, D. D.; Marques, M. d. F. V.; Henriques, C. A., Degradation of polypropylene and polyethylene wastes over HZSM-5 and USY zeolites. *Catalysis Letters* **2019,** *149* (3), 798-812.

23. Seo, Y.-H.; Lee, K.-H.; Shin, D.-H., Investigation of catalytic degradation of high-density polyethylene by hydrocarbon group type analysis. *Journal of Analytical and Applied Pyrolysis* **2003,** *70* (2), 383-398.

24. Aguado, J.; Serrano, D. P.; Escola, J. M.; Peral, A., Catalytic cracking of polyethylene over zeolite mordenite with enhanced textural properties. *Journal of Analytical and Applied Pyrolysis* **2009,** *85* (1-2), 352-358.

25. Ji, C.; Sarathy, M. S.; Veloo, P. S.; Westbrook, C. K.; Egolfopoulos, F. N., Effects of fuel branching on the propagation of octane isomers flames. *Combustion and Flame* **2012,** *159* (4), 1426-1436.

26. Chevalier, C.; Pitz, W. J.; Warnatz, J.; Westbrook, C. K.; Melenk, H., Hydrocarbon ignition: Automatic generation of reaction mechanisms and applications to modeling of engine knock. *In Symposium (International) on Combustion* **1992,** *24* (1), 93-101.

27. Karagöz, S.; Yanik, J.; Uçar, S.; Song, C., Catalytic coprocessing of low-density polyethylene with VGO using metal supported on activated carbon. *Energy Fuels* **2002,** *16* (5), 1301-1308.

28. Yasuda, H.; Yamada, O.; Zhang, A.; Nakano, K.; Kaiho, M., Hydrogasification of coal and polyethylene mixture. *Fuel* **2004,** *83* (17-18), 2251-2254.

29. Sriningsih, W.; Saerodji, M. G.; Trisunaryanti, W.; Armunanto, R.; Falah, I. I., Fuel production from LDPE plastic waste over natural zeolite supported Ni, Ni-Mo, Co and Co-Mo metals. *Procedia Environmental Sciences* **2014,** *20*, 215-224.

30. Leite, L.; Benazzi, E.; Marchal-George, N., Hydrocracking of phenanthrene over bifunctional Pt catalysts. *Catalysis Today* **2001,** *65* (2-4), 241-247.

31. Degnan, T., Recent progress in the development of zeolitic catalysts for the petroleum refining and petrochemical manufacturing industries. In *Studies in Surface Science and Catalysis*, Xu, R.; Gao, Z.; Chen, J.; Yan, W., Eds. Elsevier: 2007; Vol. 170, pp 54-65.

32. Blomsma, E.; Martens, J. A.; Jacobs, P. A., Isomerization and hydrocracking of heptane over bimetallic bifunctional PtPd/H-Beta and PtPd/USY zeolite catalysts. *Journal of Catalysis* **1997,** *165* (2), 241-248.

33. Sun, J.; Wang, H.; Chen, M.; Ye, J.; Jiang, B.; Wang, J.; Yang, Y.; Ren, C., Solubility measurement of hydrogen, ethylene, and 1-hexene in polyethylene films through an intelligent gravimetric analyzer. *Journal of Applied Polymer Science* **2017,** *134* (8).

34. Demirbas, A., Pyrolysis of municipal plastic wastes for recovery of gasoline-range hydrocarbons. *Journal of Analytical and Applied Pyrolysis* **2004,** *72* (1), 97-102.

35. Moore, J. C., Gel permeation chromatography. I. A new method for molecular weight distribution of high polymers. *Journal of Polymer Science Part A: General Papers* **1964,** *2* (2), 835-843.

36. Ding, W.; Liang, J.; Anderson, L. L., Hydrocracking and Hydroisomerization of High-Density Polyethylene and Waste Plastic over Zeolite and Silica−Alumina-Supported Ni and Ni−Mo Sulfides. *Energy Fuels* **1997,** *11* (6), 1219-1224.

37. Aguado, J.; Serrano, D. P.; Escola, J. M., Fuels from waste plastics by thermal and catalytic processes: a review. *Industrial & Engineering Chemistry Research* **2008,** *47* (21), 7982-7992.

38. Scott, D. S.; Czernik, S. R.; Piskorz, J.; Radlein, D. S. A. G., Fast pyrolysis of plastic wastes. *Energy Fuels* **1990,** *4* (4), 407-411.

39. Ishihara, Y.; Nanbu, H.; Saido, K.; Ikemura, T.; Takesue, T., Back biting reactions during the catalytic decomposition of polyethylene. *Bulletin of the Chemical Society of Japan* **1991,** *64* (12), 3585-3592.

40. Mordi, R.; Fields, R.; Dwyer, J., Thermolysis of low density polyethylene catalysed by zeolites. *Journal of analytical and applied pyrolysis* **1994,** *29* (1), 45-55.

41. Zheng, J.; Dong, J.-L.; Xu, Q.-H.; Liu, Y.; Yan, A.-Z., Comparison between β and L zeolites supported platinum for n-hexane aromatization. *Applied Catalysis A: General* **1995,** *126* (1), 141-152.

42. Chao, K.-j.; Wu, H.-c.; Leu, L.-j., Hydroisomerization of light normal paraffins over series of platinum-loaded mordenite and beta catalysts. *Applied Catalysis A: General* **1996,** *143* (2), 223-243.

43. Chica, A.; Corma, A., Hydroisomerization of pentane, hexane, and heptane for improving the octane number of gasoline. *Journal of catalysis* **1999,** *187* (1), 167-176.

44. Corma, A.; Juan-Rajadell, M. I.; López-Nieto, J. M.; Martinez, A.; Martínez, C., A comparative study of O_4^{2-}/ZrO_2 and zeolite beta as catalysts for the

isomerization of n-butane and the alkylation of isobutane with 2-butene. *Applied Catalysis A: General* **1994,** *111* (2), 175-189.

45. Park, K.-C.; Ihm, S.-K., Comparison of Pt/zeolite catalysts for n-hexadecane hydroisomerization. *Applied Catalysis A: General* **2000,** *203* (2), 201-209.

46. Lugstein, A.; Jentys, A.; Vinek, H., Hydroisomerization and cracking of n-octane and C8 isomers on Ni-containing zeolites. *Applied Catalysis A: General* **1999,** *176* (1), 119-128.

47. Martinez-Romo, A.; Gonzalez-Mota, R.; Soto-Bernal, J. J.; Rosales-Candelas, I., Investigating the degradability of HDPE, LDPE, PE-BIO, and PE-OXO films under UV-B radiation. *Journal of Spectroscopy* **2015,** *2015* (586514), 1-6.

48. Çit, İ.; Sınağ, A.; Yumak, T.; Uçar, S.; Mısırlıoğlu, Z.; Canel, M., Comparative pyrolysis of polyolefins (PP and LDPE) and PET. *Polymer bulletin* **2010,** *64* (8), 817-834.

49. Terano, M.; Liu, B.; Nakatani, H., New approaches for the development of highly stable polypropylene. *Macromolecular Symposia* **2004,** *214* (1), 299-306.

50. Lee, J.-K.; Rhee, H.-K., Sulfur tolerance of zeolite beta-supported Pd−Pt catalysts for the isomerization of n-hexane. *Journal of Catalysis* **1998,** *177* (2), 208-216.

51. Topsøe, H.; Clausen, B. S., Importance of Co-Mo-S type structures in hydrodesulfurization. *Catalysis Reviews Science and Engineering* **1984,** *26* (3-4), 395-420.

52. Lecrenay, E.; Sakanishi, K.; Nagamatsu, T.; Mochida, I.; Suzuka, T., Hydrodesulfurization activity of CoMo and NiMo supported on Al_2O_3–TiO_2 for some model compounds and gas oils. *Applied Catalysis B: Environmental* **1998,** *18* (3), 325-330.

3.9 Supporting Information: Catalysing the Hydrocracking of Low Density Polyethylene

3.9.1 Scanning Electron Microscopy (SEM) of post reaction catalysts

SEM images are included to evidence catalyst post-reaction where Figure 3-8C and Figure 3-8D clearly show the difference post-reaction of squalane compared to LDPE, and to verify that catalyst particle size is not affected by the agitation process in the batch reactor system.

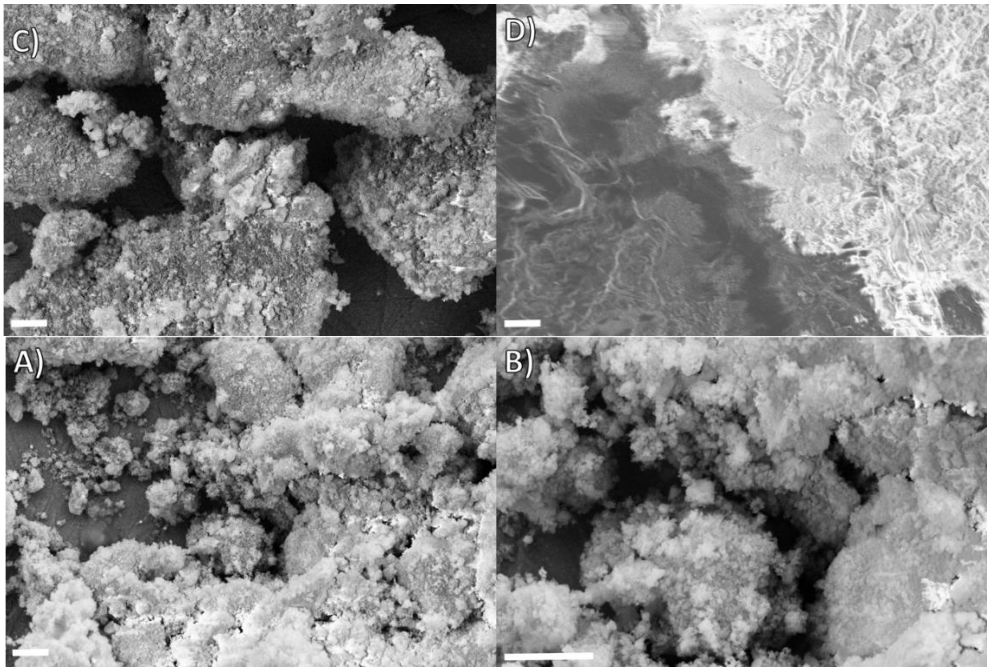

Figure 3-8 Scanning Electron Microscopy images recorded at 5 kV, all scale bars 2 µm A) 1 wt% Pt-Beta B) 1 wt% Pt-Beta C) 1 wt% Pt-Beta post-reaction with squalane D) 1 wt% Pt-Beta post-reaction with LDPE.

3.9.2 Coke content determined on selected catalyst

Table 3-2 Carbon content summary for hydrocracking reaction of squalane and LDPE over 20 H_2 bar and 370 rpm

	Squalane hydrocracking			LDPE hydrocracking		
Reaction temperature (°C)	225	275	325	330	330	330
Reaction time (min)	15	15	15	60	30	15
	Carbon content (wt.%)					
1%Pt-USY(6)	5.1	7.4	8.9			
1%Pt-USY(15)		5.0				
1%Pt-beta(12.5)		5.9		9.9	8.8	8.4
1%Pt-beta(175)		2.8				

3.9.3 Crystallinity of catalysts post catalysis

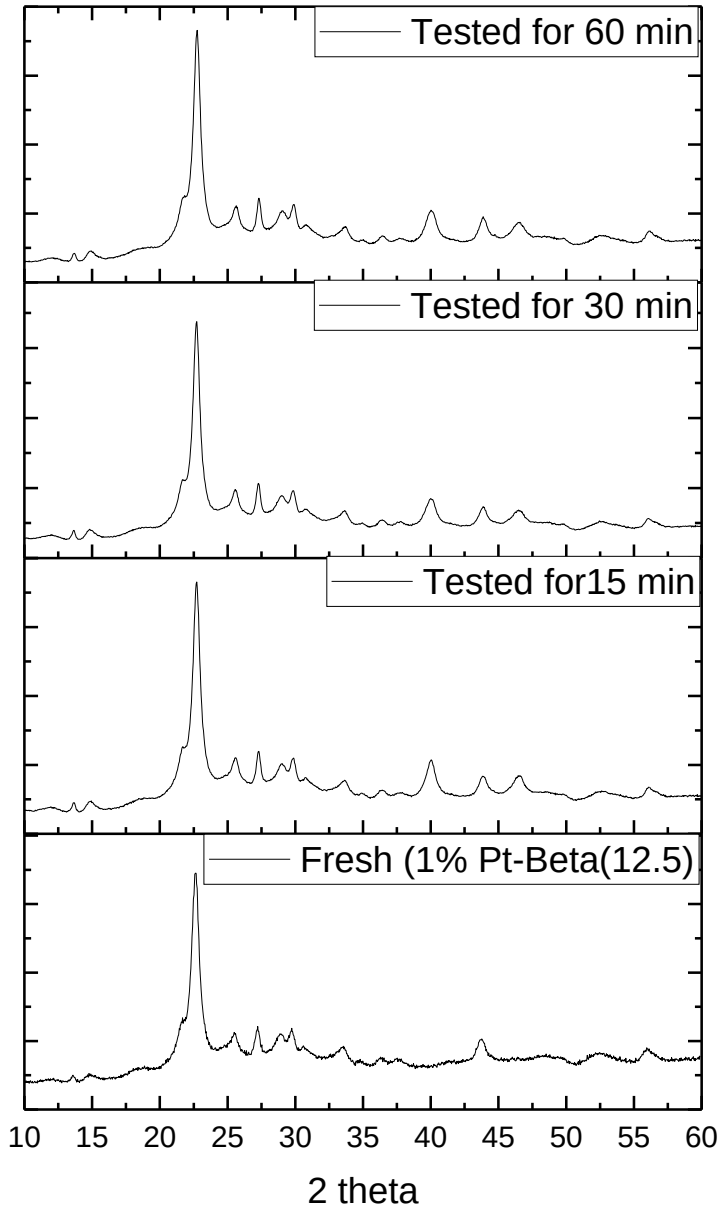

Figure 3-9 pXRD of selected catalysts demonstrating the preservation of the beta crystal structure after 15, 30 and 60 min reaction time.

3.9.4 High resolution microscopy of Pt dispersed on zeolite Beta

The distribution and size of the platinum within Beta catalyst was observed using high-angle annular dark-field (HAADF) imaging on a FEI F30 transmission electron microscope (TEM) operating at 300 kV in STEM mode. Platinum particles were

observed to be 1.0-1.5 nm and located on the external surfaces of the catalyst as the pore diameter (0.67 nm) would exclude the particles (Figure 3-10).

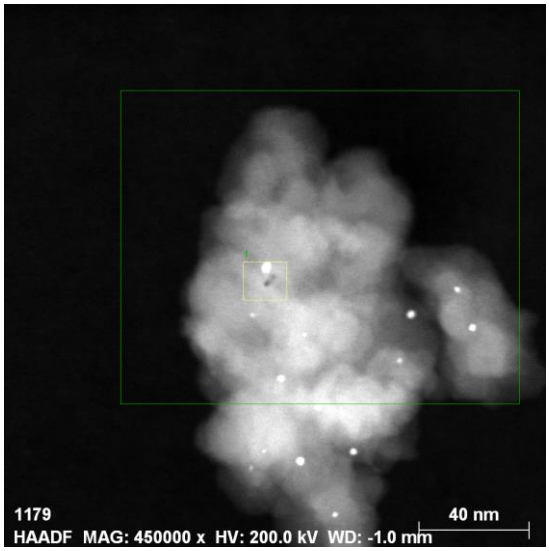

Figure 3-10 Distribution and size of the platinum within Beta catalyst

3.9.5 Temperature programmed desorption of CO

All catalysts loaded with Pt were studied using CO adsorption carried out on 50 mg of pelleted catalyst (300-500 μm)

Table 3-3. TPD results for the pulsed chemisorption of CO onto platinum sites in the zeolite catalysts and the derived quantities metallic dispersion and average particle size

Catalyst	Metallic surface area (m^2/g)	Metallic dispersion (%)	Average Pt particle size (nm)
1%Pt-USY(6)	1.399	56.6	1.8
1%Pt-USY(15)	0.570	23.1	4.3
1%Pt-Beta(12.5)	0.761	30.8	3.2
1%Pt-Beta(175)	0.730	29.6	3.4
0.75%Pt-Beta(12.5)	1.349	72.8	1.4

3.9.6 Ammonia TPD of selected catalysts

The acidity of the catalysts quantified by Temperature Program Desorption TPD, Quantachrome ChemBET Pulsar TPR/TPD analyser. The Pt modified catalysts were first reduced under H_2 flow of 40 mL/min at 485 ^oC, and then cooled to room temperature, then exposed to 5% of NH_3 in Ar and the temperature was ramped up to

800 °C. The signal of NH_3 desorbed was recorded against temperature, and integrated to yield weak acid concentrations (150-300 °C) and strong acid site concentrations (300-800 °C). The NH_3-TPD are summarised in Figure 3-11 and Table 3-1.

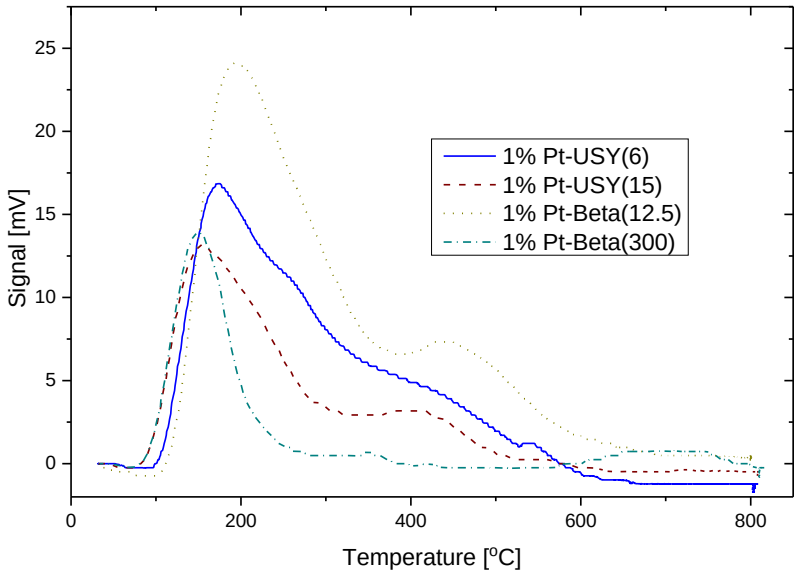

Figure 3-11. Ammonia TPD profiles for selected catalysts.

4 Kinetic Modelling of Low Density Polyethylene Hydrocracking in a Batch Reactor

4.0 The relevance of the "Kinetic Modelling of Low Density Polyethylene Hydrocracking in a Batch Reactor" paper submitted to the thesis context

The manuscript presented here has been submitted to the *ACS Sustainable Chemistry & Engineering*. As discussed in Chapter Three, the hydrocracking of LDPE obtained promising results over a Pt-Beta(12.5) catalyst with high selectivity toward light hydrocarbons. However, to compare the hydrocracking outcome with other types of cracking, thermal and catalytic, a study of the kinetics is required to be undertaken to examine the effects of the catalyst and the hydrogen pressure on the recycling process.

This manuscript reports on a kinetic study using a lumping model that describes the hydrocracking of LDPE in a batch reactor. In developing the kinetic model, mass transfer was taken into consideration. The slight changes in the experimental operation procedure between this study and previous work, included starting the rotation of the agitator at the reaction temperature only and the use of ice to quench the reactor at the desired reaction time. These two steps were taken to control the reaction to be within the reaction time and obtaining realistic kinetic results.

Kinetic parameters and mass transfer coefficients were determined using a nonlinear regression model of the experimental results via MATLAB software. The proposed reaction network used to describe the hydrocracking system was obtained after series of modelling trials, starting from the network represented in Figure 4-1, in order to achieve the best fitting of the experimental data.

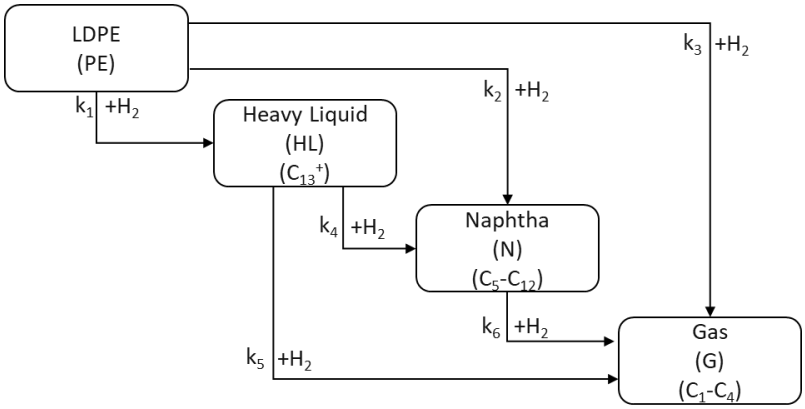

Figure 4-1 First attempt of four-lump model to describe the hydrocracking of LDPE.

However, more experimental data points and a deeper study of all parameters that affect the kinetics of the reaction should be incorporated in order to increase the level of accuracy of the lumping model. This is highlighted by the poor fitting at 300 °C, shown in Figure 4-11, it is reasonable to assume that a different lump model might be suitable for higher temperatures (>300 °C) as thermal cracking is likely participant.

Kinetic Modelling of Low Density Polyethylene Hydrocracking in a Batch Reactor

*Abdulrahman bin Jumah[1,2], Maryam Malekshahian[1], Aleksander A. Tedstone[1], Arthur A. Garforth[1]**

**Corresponding Author: arthur.garforth@manchester.ac.uk*

1) Department of Chemical Engineering and Analytical Science, University of Manchester, The Mill, Sackville Street, M1 3BB, United Kingdom

2) College of Engineering, King Saud University, P.O. Box 800 Riyadh 11421, Saudi Arabia

4.1 Abstract

Hydrocracking offers potential for the selective recovery of useful chemical fractions from polyolefin waste at relatively moderate reaction conditions with the possibility of heteroatom- and contaminant-tolerance. This study develops a kinetic model for low density polyethylene (LDPE) hydrocracking over a bifunctional zeolite namely, 1%Pt-Beta using a lumping model that describes the kinetics in a batch process. In developing the kinetic model, mass transfer limitations and vapour-liquid equilibrium were taken into consideration. Kinetic parameters were estimated from experimental results obtained at a hydrogen pressure of 20 bar and different reaction temperatures (250-300 °C) as well as different batch reaction times (0-40 min). Kinetic parameters, mass transfer coefficients and effectiveness factors were determined using a nonlinear regression model of the experimental results via MATLAB software. The physical properties of the product streams as well as vapour-liquid equilibrium data of the system were estimated using the flash unit in Aspen HYSYS software. The product

stream was dominated by the naphtha fraction, decreasing with longer batch times. The results of the model indicate mild gas-liquid mass transfer limitation and unavoidable diffusion limitations of the macro molecules of molten LDPE and heavy liquid through the catalyst pores, especially at high reaction temperature.

4.2 Introduction

Generation of polymer waste has raised a global environmental concern since landfilling is the traditional method of waste management. In EU countries alone, 27.1 Mt of polymers waste collected annually by local authorities and only 31.1% of which was recycled in 2016.[1] Polyolefins, including low density polyethylene (LDPE), are addition type polymers that are chemically stable and cannot be depolymerised to their original monomers as in the case of condensation polymers.[2-5] Recovery of valuable hydrocarbon feedstock materials by cracking is a supplementary technology to mechanical recycling for management of polymer wastes. There are also the added environmental incentives of avoiding containment failure, and emissions issues associated with landfilling and incinerators.[6, 7]

With the increasing concerns of polymer accumulation and adverse effect to the environment, the most widespread approach to recycling the polymer chemically is pyrolysis (or cracking). Thermal cracking of polymer waste has been extensively studied but still has limitations in terms of the efficiency and high temperature demands.[8-10] Catalysis, however, may help to address the issue by lowering the required temperature and also enhancing the product distribution.[11] Previous studies have proven the high activity of bifunctional zeolite as promising catalysts for hydrocracking of polymers under mild conditions.[2, 12] A full conversion of polyethylene to fluid products has been reported in the literature in the temperature

range of 270-800 °C, and 55-71 bar of H_2 pressure and relatively short reaction time over metals such as Ni, Pt, Co and Mo impregnated on acidic support.[12-15] The product stream of LDPE hydrocracking is dominated by gases (C_1-C_4) and gasoline fractions.[14]

The main challenges for heterogeneous catalysts in the hydrocracking of polyolefin materials could be summarised by the high molecular weight and the high viscosity of the polymer melt causing mass and heat transfer issues.[16, 17] The long carbon chains of the polymers limit diffusion to catalytic sites of the microporous zeolite catalysts. There is recent experimental evidence that mesopores can allow these macromolecules to enter heterogeneous catalysts and confer selectivity,[18] but the sub- to few-nanometre scale of zeolite pores will exclude large species.

A limited amount of research in the literature concerns kinetic studies the hydrocracking of polymer. Ramdoss and Tarrer carried out a kinetic study of plastic waste liquefaction in the absence of catalysts at different temperatures and reaction times based on a five-lump model, considering the yields of unconverted polymer, heavy oil, light oil, gas and coke.[19] The results of the study showed the highest activation energy of 121.7 kJ/mol obtained over the hydrocracking of light liquids to gaseous products, and the lowest energy of 11.8 kJ/mol over the conversion of heavy liquid to light liquid. In comparison, Schubert et al. obtained higher activation energies in the range between 147 and 313 kJ/mol by studying the kinetics of continues pyrolysis of LDPE and a heavy petroleum fraction mixture based on four-lumps model.[20] Edwin et al. studied the role of mass transfer in the hydrocracking of PS dissolved in decahydronaphthalene over a bifunctional Pt/H-Beta catalyst.[11] The authors concluded that the gas−liquid and liquid−solid mass transfer steps could be minimized by optimising the operation conditions, but that diffusion could be the

limiting step of the hydrocracking reaction of polymer due to the structure of the catalyst.

This present paper introduces a kinetic study of hydrocracking the environmentally problematic polymer, LDPE, over 1% platinum impregnated zeolite Beta in a batch reactor with consideration of the mass transfer and the internal diffusion limitations. The proposed model used lumping techniques of the product stream to estimate the kinetic constants and mass transfer coefficients, as well as the activation energies. The findings could be utilised for the benefits of reactor design, simulation and optimisation of LDPE hydrocracking.

4.3 Experimental section

4.3.1 Materials

The zeolite catalyst (Zeolyst international, code no. CP814C*) used in this study was acidic NH_4^+-form Beta (Si/Al_{bulk}=12.5). Tetraammineplatinum(II) chloride hydrate was used as a platinum source and supplied by Sigma Aldrich with a purity of 99%. The catalyst used was pelleted into varying average particle sizes between 175–550 μm. Virgin polymers of high purity LDPE (Mw ~ 150,000 g/mol, code no. ET316031) was received from Goodfellows in powder form (< 400 μm).

4.3.2 Catalyst preparation

Pt-beta zeolite was prepared following an impregnation method, by diluting the metal salt ($Pt(NH_3)_4Cl_2.H_2O$) in deionized water in a solution concentration of 2.17 g/L, then mixing with zeolite beta in a ratio of 1 g:10 mL zeolite: solution, for 24 h. Following that, the catalyst was dried and pelleted to the required size based on the purpose of

the experiment. Then, the prepared catalyst was activated/reduced ex situ at 480 ^{o}C for 16 h under hydrogen flow of 50 ml/min in a tubular reactor.

4.3.3 Catalyst characterisation

4.3.3.1 XRF elemental analysis and BET

The Si/Al ratio as well as the added Pt level on the catalysts were determined using energy-dispersive X-ray fluorescence (EDXRF). The total surface area of the studied catalyst was measured using BET (Micromeritics ASAP 2020 static low-pressure volumetric adsorption unit). The characterisation results of the prepared catalyst are summarised in Table 4-1.

Table 4-1 Characteristics of the Pt-Beta catalyst

Channel dimension	1D
Pore entrance (T atoms)	12
Channel diameter (nm)	0.65 x 0.67, 0.65 x 0.56
BET surface area[a] (m^2/g)	406
Pore volume[a] (cm^3/g)	0.11
Si/Al[b]	15.1
Pt (wt. %)[b]	0.97

[a] As quantified by BET analysis, [b] As quantified by XRF analysis

4.3.3.2 X-Ray Absorption Spectroscopy

Transmission Pt L3-edge X-ray absorption spectra were collected at the B19 beamline at the Diamond Light Source. Spectra were recorded between 200 eV before the L3-edge to 1000 eV after the L3-edge, with a step size of 0.27 eV; energy calibration was performed with a Pt foil reference sample. Data processing was carried out in the Demeter open-source software package (version 0.9.26) with XAS spectra processing (normalisation and background subtractions) and linear combination fitting conducted within the Athena programmes. A K-Weight of 2 was applied to the during EXAFS

processing. All Pt-Beta and PtO_2 samples were diluted in boron nitride for spectrum collection.

4.3.4 Hydrocracking of LDPE

The activity of the prepared catalyst was tested using a 300 mL stainless steel Parr Reactor, agitated by an 'anchor' style stirrer, reactor configuration is shown in Figure 4-22. A feed of virgin LDPE (typically 20 g) was mixed with the prepared/activated catalyst in a polymer:catalyst ratio of 10 g:1 g. After the feed of polymer and catalyst was loaded into the reactor, it was subsequently sealed and purged with hydrogen then pressured to the reaction pressure (typically 20 bar H_2). The reactor was then heated to the desired reaction temperature, which was recorded via a thermocouple inserted into the reaction vessel, and submerged in the molten polymer.

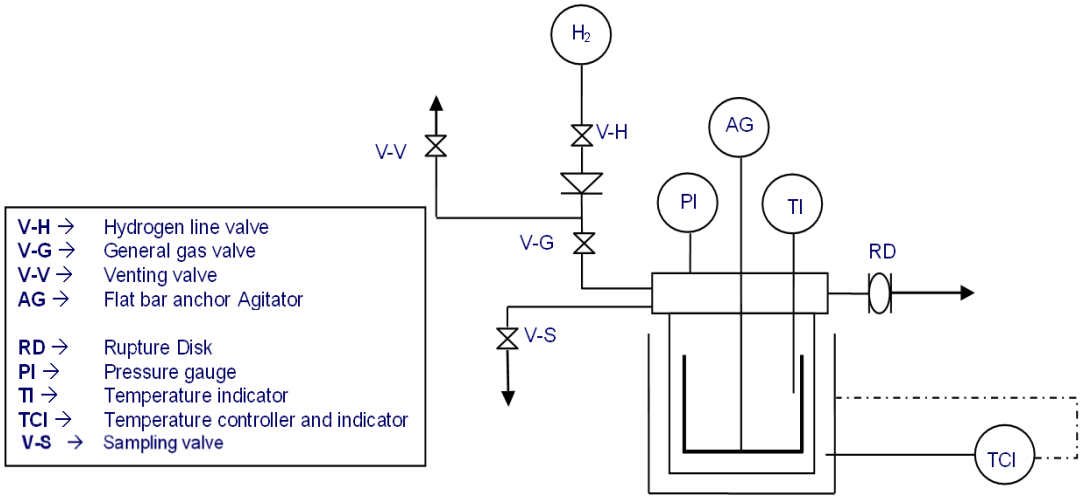

Figure 4-2 Reactor configuration with control over temperature, agitation type and speed, and pressure.

Reaction temperature (typically, 250-300 °C) was reached within 40-50 min. Agitation (typically, 200-800 rpm) was commenced at the target reaction temperature and the temperature was held constant during the reaction time (typically, 0-40 min). When the reaction time was over, ice was used to quench the reactor to reach ambient temperature within 10 minutes, and the products were collected for GC analysis. The

typical temperature and pressure profile are exemplified in Figure 4-3. The overall conversion was calculated using Equation 1 where the conversion was considered as solid to fluid at the studied temperatures (250, 275, 300 °C), and the solid remain in the reactor after the experiment considered to be unconverted LDPE.

$$X_{(wt.\%)} = \frac{Solid_{out} - Polymer_{in} - Catalyst_{in}}{Polymer_{in}} \times 100 \quad (1)$$

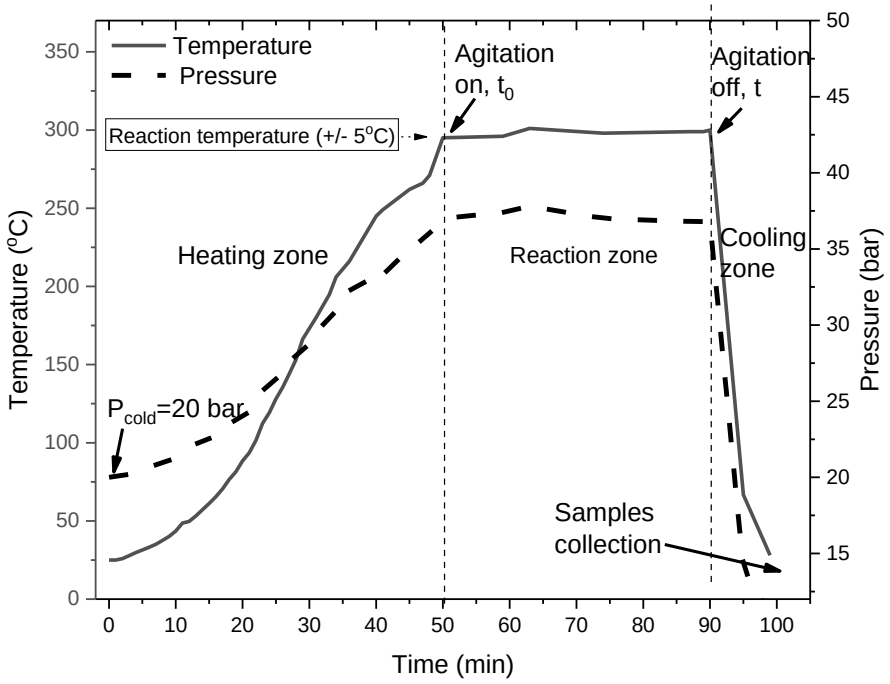

Figure 4-3 Typical temperature and pressure profile for LDPE hydrocracking over 1 wt.% Pt-Beta (12.5), plateau region is the stated reaction time of 40 min.

4.3.5 Product analysis

Liquid samples were analysed by Gas Chromatography-Mass Spectrometry (GC-MS) using Agilent Technologies 6890N Network GC fitted with a 100m × 0.25mm i.d. PONA CB column. For the gas samples, a Varian CP3800 GC-FID fitted with a 50m × 0.32mm i.d. PLOT Al_2O_3/KCl capillary column was used, and quantification was performed against a 1 mol.% gas standard mixture (C_1-C_5). The average mass balance for each run was ~90 wt.%, with loss occurring due to evaporation and unavoidable retention of liquids and solids by the stirrer and the reactor wall.

4.4 Results and discussion

4.4.1 Model description

The product stream of LDPE hydrocracking consists of an expansive range of hydrocarbon molecules. Considering each intermediate and product molecule involved in the reaction would require impractical data-collection. The similarity between heavy petroleum and polymers cracking allows use of similar lumped models of reaction pathways. They are commonly employed to describe all types of cracking reactions including thermal[20-22], catalytic[23-25] and hydrocracking[19, 26, 27]. Usually, the lumping process is based on the boiling cuts or the components bond-types such as paraffins, olefins, naphthenes and aromatics.[20] For this study, lumping the product is employed based on the carbon numbers to simplify the complexity of the mixture, and yet able to describe the hydrocracking reaction properly to meet the objective of implementing a kinetic model.

The hydrocarbon fraction is divided into four lumps for the purpose of this model, namely, gas (G, C_1-C_4), naphtha (N, C_5-C_{12}), heavy liquid (HL, C_{13}^+), and LDPE (PE), and each lump was considered as a singular chemical component. The preference is to obtain a product stream rich in naphtha, relating to its high value in the petrochemical industry, where it can be handled easily in comparison to gas. It also has direct application as a feedstock to a steam cracker unit, for the production of olefins and hydrogen.[28] For chemical recycling of polymers to become a viable part of a circular economy, it must produce a well-defined feedstock that can have value added and be compatible with existing processing.

The hydrocracking reaction considered here consists of three phases: solid (catalyst and coke decomposition products), liquid (the molten polymer and the cracked liquid products) and gas (H_2 and the gaseous products).

Figure 4-4 illustrates the theoretical steps of three phase hydrogenation reaction of LDPE. In our previous study of LDPE hydrocracking, performed with a small particle size catalyst at 330 °C,[29] we found that the amount of coke formed was very low, less than 1 wt.% of the total yield. This was accounted for suggesting that the highly active hydrogenation function of the catalyst hydrogenated any coke formed, and thus, the coke is not considered in this model. The oxidation state of the metallic platinum component of the bifunctional catalyst remains Pt0 through the reaction at this set of reaction parameters, as revealed by X-ray Absorption Spectroscopy (XAS, Figure 4-5). The absorption spectra for 1 wt% Pt-Beta correspond to a metallic Pt0 foil standard, with the reductive H_2 atmosphere maintains the metallic oxidation state of the zeolite-supported platinum, which has a pivotal role in hydrogenation-dehydrogenation reactions within the system, as well as minimising the formation of coke. We therefore build this model upon the premise that Pt remains active in both of these roles throughout the reactions studied experimentally herein.

Catalyst particles are assumed to be distributed homogeneously in the well-mixed liquid phase and the liquid-solid mass transfer limitation was minimised and assumed neglected based on the small particle size of catalyst used (175 μm) and effective stirring of the reactants (600 rpm). Gas and liquid volume are assumed to be constant during the reaction time. The gas produced occupies the contained volume, and replaces consumed hydrogen; however the reaction is not isobaric.

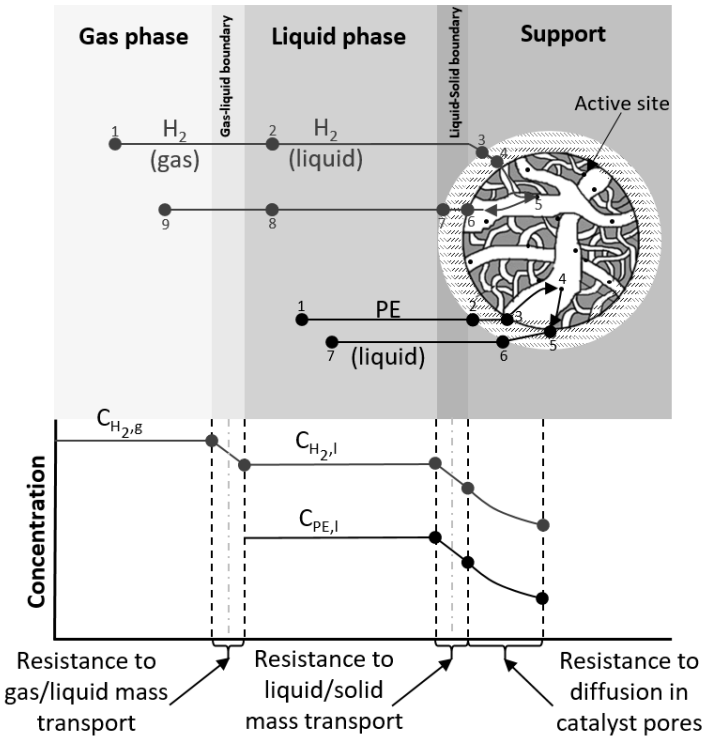

Figure 4-4 Steps of three phase hydrogenation reaction of LDPE.

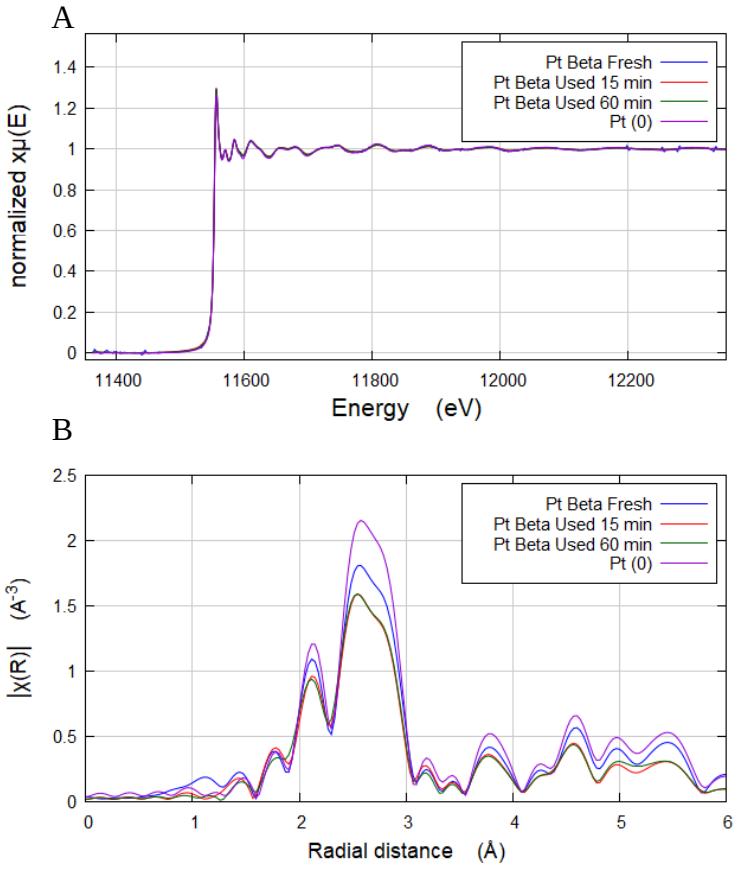

Figure 4-5 (A) XAS Spectra of 1 wt% Pt-Beta before use, after 15 minutes of reaction, and after 60 minutes of reaction, and a Pt(0) foil reference. (B) The EXAFS demonstrates.

4.4.2 Kinetic modelling

The reaction network proposed in this study was adopted from the pyrolysis of polymer and rubber, as well as the hydrocracking of heavy petroleum fractions, [11, 30-32] and it assumed four irreversible reactions (Figure 4-6). The proposed network was structured with two parallel hydrocracking reactions of polyethylene (PE) to heavy liquid (HL) and naphtha (N), and subsequent reactions of HL to N then gas (G). This reaction pathway was proposed using the assumption that large molecules crack gradually to smaller molecules, therefore reactions of PE and HL directly into gas were insignificant based on the kinetic results obtained. This reaction network shown in Figure 4-6 was used to describe quantitatively the experimental kinetic data on the hydrocracking of LDPE.

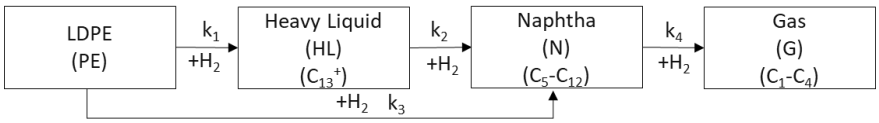

Figure 4-6 Four-lump model to describe the hydrocracking of LDPE via heavy liquid (HL) and naphtha (N), with the ultimate reaction product being C_1-C_4 gases (G)..

The excess of H_2 in the hydrocracking process contributes in rapid equilibrium achievement between gas and liquid phase and maintains a constant H_2 concentration in the liquid phase.[33] In this study, the hydrogen concentration in the output gas stream was measured at greater than 82% of the total gas, and therefore, zero order reaction is assumed with respect to hydrogen. However, monomolecular, irreversible, first-order reactions are assumed with respect to the hydrocarbon lumps of the hydrocracking reactions.

By assuming constant volumes for both gas and liquid phase, the kinetic model was developed based on the mass balance around the liquid phase. Reactions only occur in liquid phase, as demonstrated in Figure 4-7. Based on the analysis of gas and liquid

product samples, the only lumps exchanged between liquid and vapour phases are gas and naphtha lumps. Because of the existence of external mass transfer and internal diffusion limitations, the mass transfer coefficient ($k_L a$) and effectiveness factor (η), which indicate the diffusion, are introduced in the model for a reasonable description of the process kinetics.

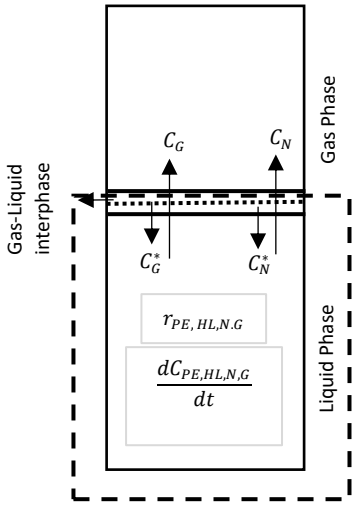

Figure 4-7 Schematic drawing for the batch stirred reactor.

The overall material balance for liquid phase can be determine by the following equation:

$$\frac{dC_i}{dt} - N_{exchange}\frac{S_{exchange}}{V_L} = r_{v,i}.\eta_i \qquad (2)$$

Where C_i is the mass concentration of lump i in liquid phase; t is the reaction time; $N_{exchange}$and $S_{exchange}$ are, respectively, the exchange flux and the exchange surface area between the vapour and liquid phases; V_L is the liquid volume; $r_{v,i}$ is the intrinsic production rate of lump i; and η_i is the effectiveness factor of lump i.

For the lumps that are not exchanging with the gas phase (PE and HL), the mass balance can be written as:

$$\eta_i . r_{v,i} = \frac{dC_i}{dt} \quad (3)$$

For lumps that exchange with the gas phase (N, and G)

$$\frac{dC_i}{dt} - k_L a(C_i^* - C_i) = r_{v,i} . \eta_i \quad (4)$$

Where $k_L a$ is the volumetric mass transfer coefficient and the same mass transfer coefficient for all lumps are assumed; and C_i^* is the mass concentration of lump i in liquid phase in equilibrium with lump i in vapour phase.

For each reaction, a kinetic expression was formulated as a function of product mass concentration in the liquid phase (C_i) and the equilibrium interphase (C_i^*), kinetic constant (k_j), mass transfer coefficient ($k_L a$) and effectiveness factor (η). On this basis, and the assumptions of a first order reaction with respect to hydrocarbon lumps and zero order reaction with respect to hydrogen, the following kinetic expressions for each lump were obtained:

PE: $$(-k_1 C_{PE} - k_3 C_{PE})\eta_{PE} = \frac{dC_{PE}}{dt} \quad (5)$$

HL: $$(k_1 C_{PE} - k_2 C_{HL})\eta_{HL} = \frac{dC_{HL}}{dt} \quad (6)$$

N: $$(k_2 C_{HL} + k_3 C_{PE} - k_4 C_N)\eta_N = \frac{dC_N}{dt} - k_L a(C_N^* - C_N) \quad (7)$$

G: $$(k_4 C_N)\eta_G = \frac{dC_G}{dt} - k_L a(C_G^* - C_G) \quad (8)$$

By developing these kinetics equations, understanding of the hydrocracking mechanism of LDPE will enable rational design and scaling-up of the process. It is critical that the desired fraction can be produced from this process regardless of scale,

and various parameters can be controlled to this end, including temperature, pressure, agitation rate, catalyst particle size and reaction time.

4.4.3 Mass transfer limitation

The mass transfer limitation steps shown in Figure 4-4 were investigated by two sets of experiments – varying particle size and varying agitation speed, in order to minimize the mass transfer limitations by selecting the right experimental variable. The external mass transfer and the internal diffusion through the catalyst pores were examined by varying the average catalyst particle size in the range of 175-550 μm, Figure 4-8, under reaction condition of 300 °C, 20 bar and agitation speed of 400rpm. The results show that the LDPE conversion increased from 36 to 48 wt.%, as expected, by decreasing the average particles size from 550 to 175 μm due to the reduction of the area of liquid-solid mass transport resistance as well as shortening the diffusion distance. The reduction in particle size affected the product distribution by increasing the selectivity to heavier product, possibly by allowing heavier molecules to exit the catalyst pores quicker in the smaller particles, Figure 4-8B. The results presented in Figure 4-8 indicate the existence of internal mass transfer diffusion limitation and it is vital to consider this in the kinetic model and that is expressed by the effectiveness factor (η) in the model.

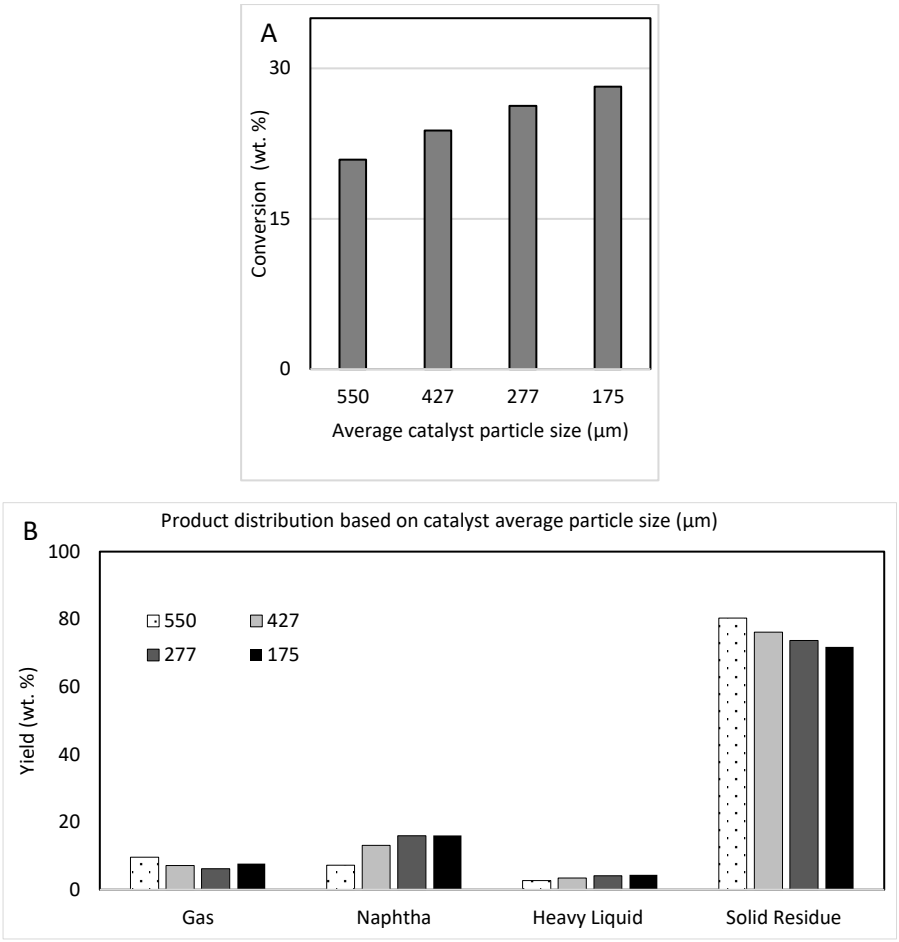

Figure 4-8 (A)Conversion and (B) product distribution of zeolite beta-catalysed LDPE hydrocracking at 300 °C, 5 min, 400 rpm, and 20 bar over different average catalyst particle size.

Another experimental study was carried out to check the influence of varying the rotation speed from 200 to 800 rpm on LDPE hydrocracking (at 300 °C and 20 bar over 1%Pt-beta) with an average particle size of 175µm, Figure 4-9. The conversion of LDPE is observed to be enhanced with better mixing, where the conversion of 22% at rotation speed of 200 rpm was increased to 33% at 600 rpm. This is attributable to the reduction of external mass transfer limitation between the phases. However, minor conversion enhancement increments occurred with further increasing in stirring rate from 600 to 800 rpm under the studied conditions. Moreover, the product distribution shows an increase in the yield of gaseous products by maximising the agitation speed, as shown in Figure 4-9B.

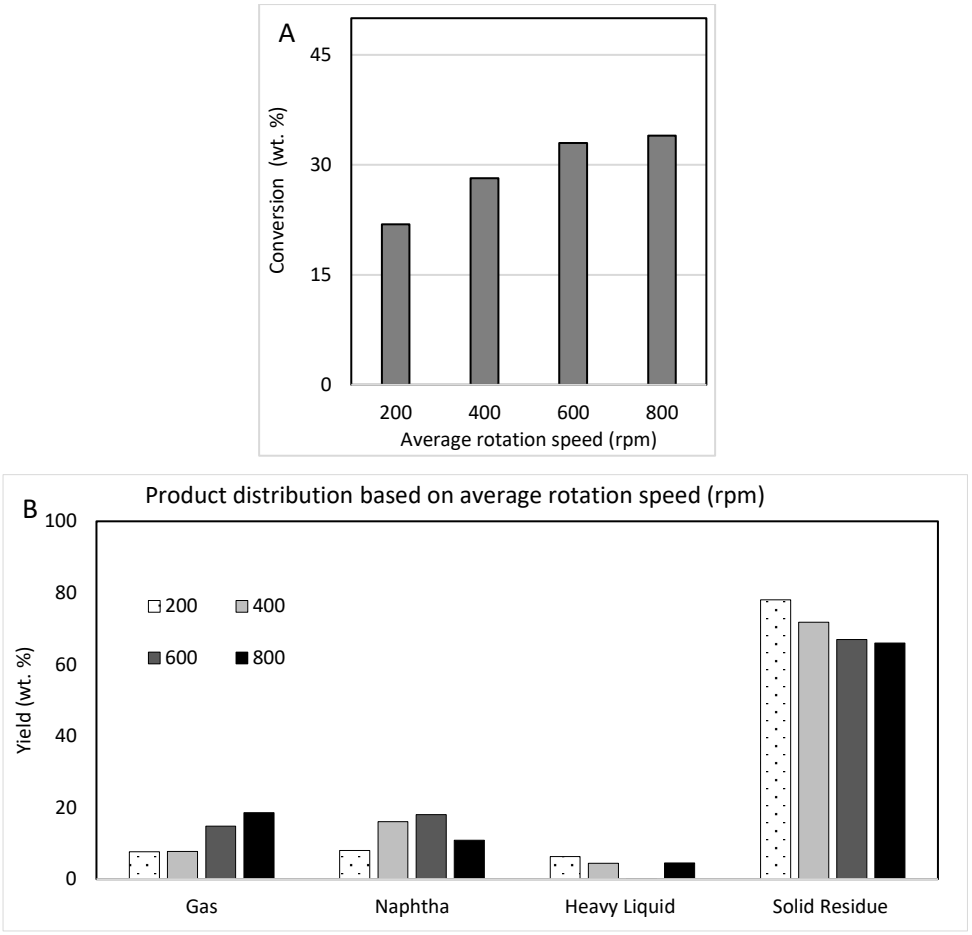

Figure 4-9 (A) Conversion and (B) product distribution of zeolite beta-catalysed LDPE hydrocracking at 300 °C, 5 min, 175 μm of average catalyst particle size, and 20 bar over different rotation stirring speed.

From the optimisation of conditions given here, all the kinetic experiments were carried out over 175μm of average catalyst particle size and at 600 rpm of rotation speed, to minimise the effects of diffusion of reactants and products within the catalyst. Figure 4-10 demonstrates the conversion of LDPE (solid to fluid, equation 1) in the kinetic experiments at three sets of temperatures (250, 275 and 300 °C) and four batch times (0, 5, 20 and 40 min). Conversion was highly dependent on temperature; increasing the reaction temperature from 250 °C to 300 °C resulted in increasing the conversion by ~25 wt.%.

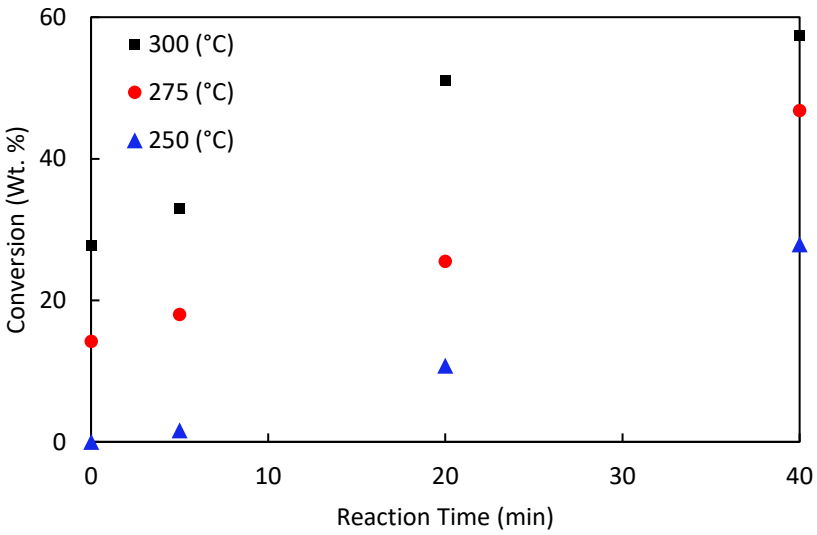

Figure 4-10 Conversion of zeolite beta-catalysed LDPE hydrocracking at three different temperatures, four reaction times, 175 μm of average catalyst particle size, 20 bar of H_2 pressure and 600 rpm of rotation stirring speed.

4.4.4 Estimation of parameters

The concentration of the four lumps in the liquid phase have been obtained at different temperatures and reaction times, with an average error of ± 5%. The mass concentration was calculated by dividing the mass of each lump in the liquid phase by the total liquid volume (45 mL). The equilibrium data in the gas-liquid interphase of lumps N and G were determined using the flash separator in Aspen HYSYS. Since the Aspen HYSYS databank does not contain any polymers as a pure component, LDPE was added as a hypothetical component.[34] To achieve this, ethylene was chosen as the chemical species model, and the properties of density, molecular weight and normal boiling point were added based on the data sheet of the polymer supplier as following: density (923 kg/m^3), molecular weight (150,000 g/mol), and normal boiling point (248°C, assumed). Other hydrocarbons involved in the system were added to the simulation as pure paraffin components in proportion determined from to the experimental results derived from GC-MS analysis, with an assumption of iso/normal paraffin ratio of 4:1, based on previous findings.[29] The Peng-Robinson (PR) property

package was used as the equation of state in the simulation as it widely used for hydrocarbon mixtures.[35]

The estimation of the kinetic parameters, along with the mass transfer coefficient and effectiveness factors, was done by minimizing the objective function, based on the sum of square errors between the experimental and predicted mass concentrations from the model output. The objective function was solved by using least-squares criterion with a nonlinear regression procedure using MATLAB software.

4.4.5 Kinetic model parameter estimation

Each isothermal experiment has been modelled alone and a set of kinetic constants were estimated for each lump. The results of the model output are reported in Figure 4-11. The proposed model is adequate for the hydroprocessing of LDPE based on the satisfactorily fitting obtained of the experimental data with minimum average nonlinear regression least-squares coefficient (R^2) of 0.83. From the experimental results, the selectivity towards naphtha fraction is much higher than that of heavy liquid and gas over the reaction conditions studied. The selectivity towards gas and heavy liquid fractions increased with increasing temperature and reaction time, especially at the temperature of 300 °C. This behaviour of could be accounted for the involvement of thermal cracking at high temperature, which contributes to production of more gaseous products and heavy hydrocarbons.

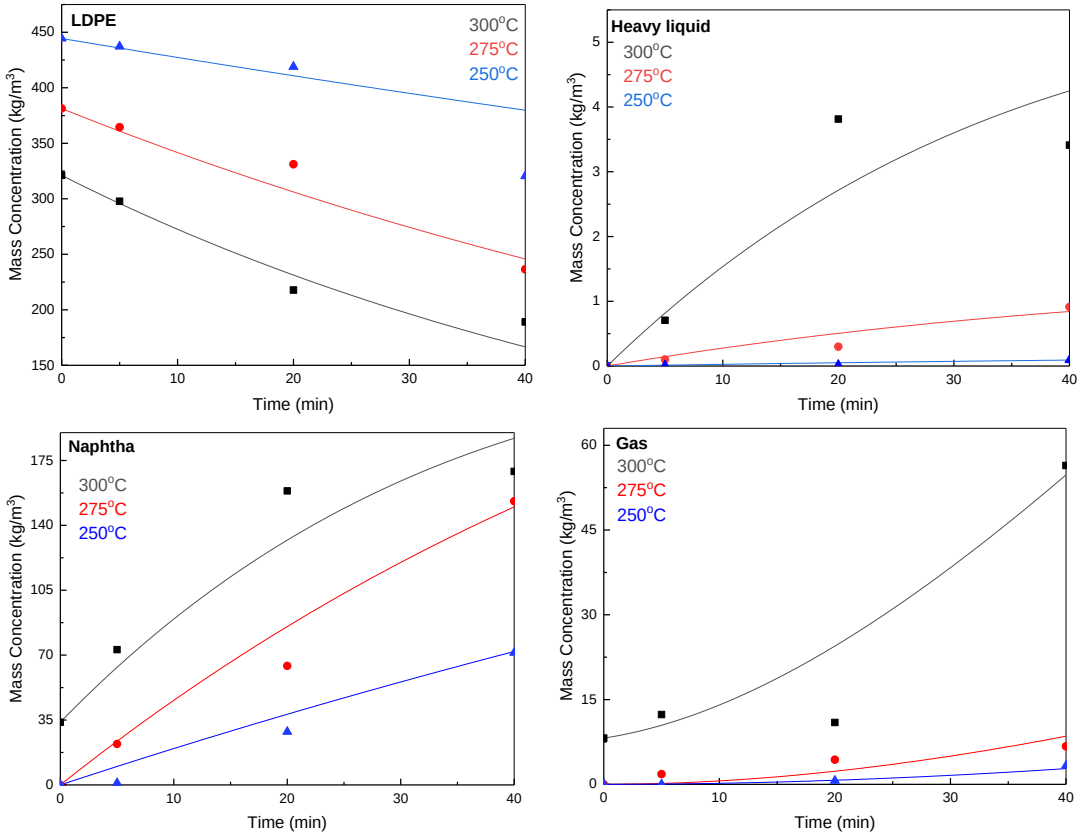

Figure 4-11 The mass concentrations yields of the lumps used in the model as a function of time at different reaction temperatures for the hydrocracking of LDPE over 1wt.%Pt-Beta, the points are for the experimental and the lines are for the predicted data by the model.

A comparison between experimental and predicted mass concentrations by the model of lumps LDPE, HL, N and G are shown in Figure 4-12, along with the average nonlinear regression coefficients (R^2). The nonlinear regression coefficients (R^2) for the model outputs were obtained at each temperature using the following equations:

$$R^2 = 1 - \frac{S_{res}}{S_{tot}} \tag{9}$$

$$S_{tot} = \sum(y_i - \bar{y})^2 \tag{10}$$

$$S_{res} = \sum(y_i - f_i)^2 \tag{11}$$

Where the S_{tot} is the total of the squares; S_{res} is sum squares of residuals; y_i experimental data; $\bar{y}$ the mean of the experimental data; and f_i is the predicted data by the model.

A relatively good correlation was achieved between the concentrations of the experimental and predicted ones.

In addition, to validate the accuracy of the proposed model of describing the outcome of hydrocracking process of LDPE in the modelled range, a series of experiments have been carried out at different reaction temperatures at a reaction time of 10 minutes. The results of the validation experiments indicated good agreement between obtained and modelled mass concentrations, where the average errors for each lumps was less than ±15% and less than ±2% for polyethylene. The proposed model can describe obtainable product mass concentrations independently of reactor design and catalyst used in the investigated range.

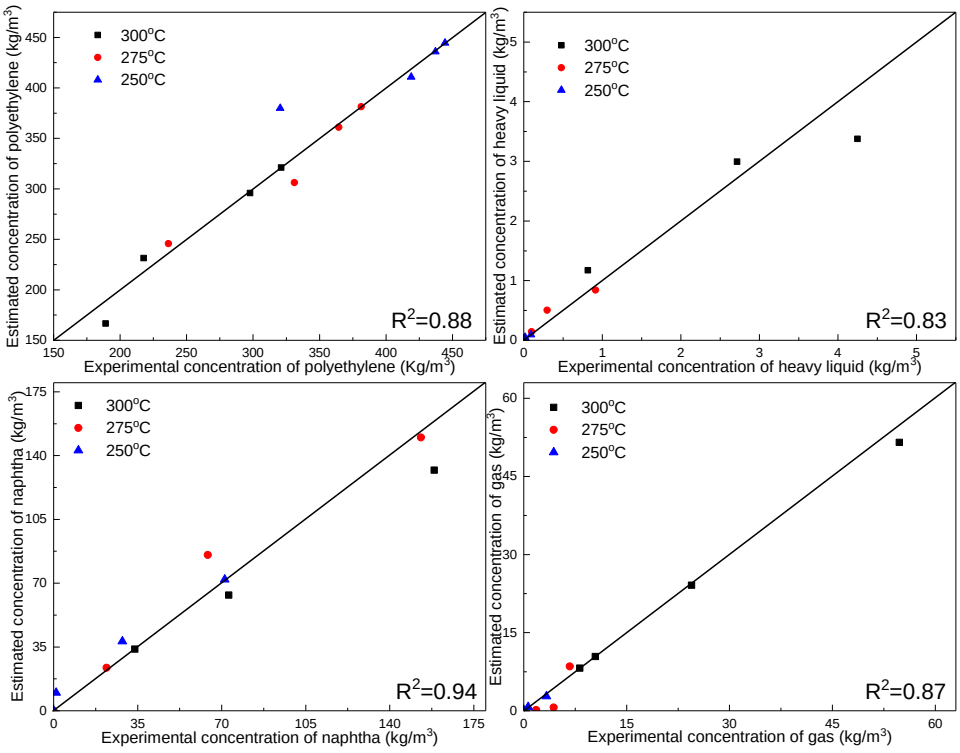

Figure 4-12 Comparison of predicted and experimental mass concentrations from the proposed lumps used in the model as a function of time at different reaction temperatures for the hydrocracking of LDPE over 1wt.%Pt-Beta.

The kinetic constant values as well as the mass transfer coefficients are summarized in Table 4-2. With comparison to the literature, the rate constants vary based on the

reaction temperature and the cracking type. Schubret, T et al.[20] obtained the rate constants values for co-pyrolysis of LDPE and a heavy petroleum fraction at 450 ˚C in the range of 10^{-9}-10^{-4} s^{-1} for different lumps. Prakash, K et al.[19] estimated the kinetic values in the range between 10^{-6} -10^{-3} s^{-1} for high-temperature liquefaction of waste plastics at 475 ºC and approximately 8 bar of cold pressure. In this study, the values of the rate constants are in the range of 10^{-7} -10^{-4} s^{-1} which are broadly in the range found in literature of similar processes of polymer and heavy petroleum fractions hydrocracking.[27, 32, 36]

From the rate constants summarised in Table 4-2, generally, it can be seen that the kinetic rate constants increased by increasing reaction temperature where the maximum kinetic constants values obtained at 300 ºC. The formation reactions of naphtha from PE and heavy liquids play a dominant role since they have the maximum rate constants. The hydrocracking reaction supplying heavy liquid via PE seems to be negligible at low temperature of 250 °C, but becomes more significant at higher temperatures. Increasing reaction temperature in the tested range primarily causes a rise in gas and naphtha formation but more remarkable effects among the formation of heavy liquid. Since naphtha consumption resulted in the formation of gas, and the naphtha formed from the hydrocracking of PE and heavy liquid, it can be deduced that the amount of naphtha decreases much less than PE and heavy liquid at increasing temperatures.

Table 4-2 Kinetic parameters and mass transfer coefficient

T (ºC)	k_1 (s^{-1})	k_2 (s^{-1})	k_3 (s^{-1})	k_4 (s^{-1})	$k_L a$ (s^{-1})
300	1.22 x 10^{-5}	1.91 x 10^{-4}	4.11 x 10^{-4}	1.62 x 10^{-4}	2.12 x 10^{-6}
275	1.57 x 10^{-6}	1.43 x 10^{-4}	2.41 x 10^{-4}	4.47 x 10^{-5}	1.58 x 10^{-6}
250	1.19 x 10^{-7}	1.09 x 10^{-4}	8.02 x 10^{-5}	3.16 x 10^{-5}	1.08 x 10^{-6}

The mass transfer coefficient was also determined at three temperatures (Table 4-2) and showed a remarkable sensitivity with temperature increase and significance at higher temperature. In general, the effect on the kinetics was low even at the highest value obtained at 300 °C. The estimated values increase with the temperature, since the external mass transfer coefficients typically are linearly proportional to temperature. Theoretically, the mass transfer coefficient in a batch system is dependent not only on the temperature and the pressure but also on the agitation speed, and the stirrer type,[37, 38] as it is essential to physically mix the components without relying on diffusion alone. The stirrer used in this study was of the 'anchor' type to maximise the physical mixing of the reaction mixture that can otherwise stagnate at the vessel edges. The stirring speed was 600 rpm corresponding to the highest conversion obtained in the mass transfer experiments reported earlier in Figure 4-9. The k_La values obtained are in an agreement with a similar study (Nguyen, T et al.[32]), that obtained a mass transfer coefficient of 4×10^{-5} and 5.6×10^{-5} s^{-1} at the temperatures of 420 and 430 $^{\circ}$C, respectively, for the same type of reactor. Even though the feed nature is different, where the referenced study hydrocracked atmospheric residue, it could be comparable in terms of the similarity of the product streams and the process setup.

The effectiveness factors estimated for each operating condition studied are reported in Table 4-3 and approach almost unity ($\eta = 1$) with decreasing temperature from 300 to 250 °C for the lighter lumps of naphtha and gas. It also can be observed that the effectiveness factor values are lower for the heavier lumps in all cases studied. As might be expected, the effectiveness factor is an indicator for diffusion limitation into the catalyst pellet, which is directly related to the viscosity of the reactants. The finding in this study is in agreement with a kinetic study for hydrocracking of heavy oil by

Martínez, J and Ancheyta, J.[27] They found that the effectiveness factor decreased with temperature and attributed this to the dominance of diffusion limitation rather than intrinsic reaction rate at higher temperature. A significantly larger pellet size will generally reduce the effectiveness factor as the path length that molecules need to travel during diffusion in and out of the pellet is increased so it is critical that this factor is considered when designing larger reaction systems.

Table 4-3 Effectiveness factors of the four lumps studied

Temperature (°C)	PE	HL	N	G
300	0.65	0.74	0.83	0.97
275	0.75	0.85	0.88	0.97
250	0.82	0.88	0.94	0.98

Activation energies for each reaction were calculated by employing the linearized Arrhenius equation:

$$\ln k_j = \ln A_j - {}^{E_j}/_{RT} \tag{10}$$

Where A_j and E_j are the frequency factor and activation energy, respectively, for each reaction j; R is the gas constant; and T is the reaction temperature in Kelvin.

The activation energies values for the proposed kinetic model are summarised in Table 4-4 and the Arrhenius plots for the kinetic constants are reported in Figure 4-13.

The values obtained are within the range of those reported by similar studies in the literature discussing the hydrocracking of heavy petroleum fractions (38-261 kJ/mol).[27, 33] with respect to other types of chemical recycling of polymers, it has been shown that hydrocracking reduce the activation energy significantly , where the activation energy range in catalytic cracking was reported to be from 157 to 257 kJ/mol,[25] and 109-386 kJ/mol in thermal cracking [39].

Table 4-4 Activation energies of the studied hydrocracking reactions

Reaction	E_{aj} (kJ/mol)
$LDPE + H_2 \longrightarrow HL$	231
$HL + H_2 \longrightarrow N$	28
$LDPE + H_2 \longrightarrow N$	82
$N + H_2 \longrightarrow G$	81

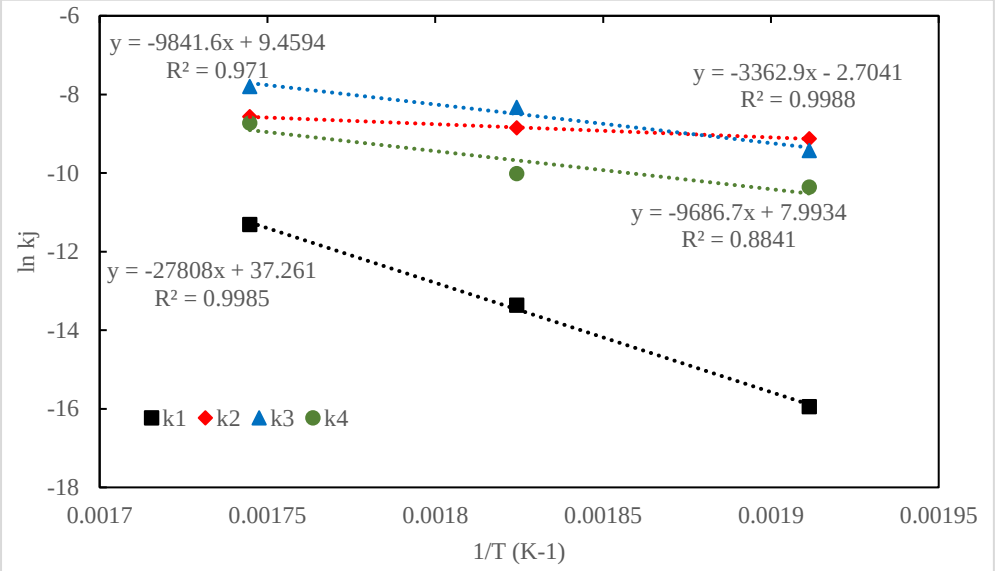

Figure 4-13 Arrhenius plot for the rate constants of LDPE hydrocracking

4.5 Conclusions

The kinetics of pure LDPE hydrocracking has been developed with consideration of the mass transfer coefficient and effectiveness factors. Overall, the obtained results demonstrate the ability of the proposed lumping model to simulate the hydrocracking of LDPE over 1%Pt-Beta, and indicate that the most significant rate-limiting step is the hydrocracking of LDPE into heavy liquid. Bifunctional catalysts of Pt-Beta(12.5) showed great potential to hydrocrack LDPE and yield a rich naphtha stream. The results indicate mild external mass transfer and significant internal diffusion control which cannot be neglected, especially at high temperature due to the high viscosity and the large size of the molten reactant of LDPE. The unknown parameters of the model were estimated by achieving good fittings of the experimental data using nonlinear optimisation model with at least 0.83 of the nonlinear regression coefficients

obtained (R^2). However, more experimental data points and deeper study of all parameters that could affect the kinetics of the reaction should be incorporated in order to increase the level of accuracy of the lumping model. Hydrocracking technology without doubt would contribute to lowering the energy requirement of polyolefin cracking compared to thermal and catalytic cracking, as proven by the lower activation energy obtained in this study comparing to the literature.

4.6 Acknowledgements

The authors would like to acknowledge the support of King Saud University in Riyadh (KSU) for research funding. In addition, the UK Catalysis Hub is kindly thanked for resources and support for Dr Tedstone via our membership of the UK Catalysis Hub Consortium and funding through EPSRC grant EP/R027129/1. The authors, also, wish to acknowledge the Diamond Light Source for provision of beamtime via B18BAG#4_4 on the EPSRC grant EP/R026939/1, and the assistance of Dr. Nitya Ramanan in collection of data. Finally, the authors would like to acknowledge Dr Mohamed Aljamri for technical assistance with using MATLAB.

4.7 References

1. PlasticsEurope Plastics –the facts 2017 An analysis of European plastics production, demand and waste data. https://www.plasticseurope.org/application/files/5715/1717/4180/Plastics_the_facts_2017_FINAL_for_website_one_page.pdf (accessed 10/02/2021).

2. Garforth, A. A.; Ali, S.; Hernandez-Martinez, J.; Akah, A., Feedstock recycling of polymer wastes. *Current Opinion in Solid State and Materials Science* **2004,** *8* (6), 419-425.

3. Yang, Y.; Lu, Y.; Xiang, H.; Xu, Y.; Li, Y., Study on methanolytic depolymerization of PET with supercritical methanol for chemical recycling. *Polymer Degradation and Stability* **2002,** *75* (1), 185-191.

4. Siddiqui, M. N.; Achilias, D. S.; Redhwi, H. H.; Bikiaris, D. N.; Katsogiannis, K. A. G.; Karayannidis, G. P., Hydrolytic depolymerization of PET in a microwave reactor. *Macromolecular Materials and Engineering* **2010,** *295* (6), 575-584.

5. Gray, R. L., Accelerated testing methods for evaluating polyolefin stability geosynthetic testing for waste containment applications. ASTM International: West Conshohocken, PA, 1990; pp 57-74.

6. Li, C.-T.; Zhuang, H.-K.; Hsieh, L.-T.; Lee, W.-J.; Tsao, M.-C., PAH emission from the incineration of three plastic wastes. *Environment International* **2001,** *27* (1), 61-67.

7. Eriksson, O.; Finnveden, G., Plastic waste as a fuel - CO_2-neutral or not? *Energy & Environmental Science* **2009,** *2* (9), 907-914.

8. Rollinson, A. N.; Oladejo, J. M., 'Patented blunderings', efficiency awareness, and self-sustainability claims in the pyrolysis energy from waste sector. *Resources, Conservation and Recycling* **2019,** *141*, 233-242.

9. Anuar Sharuddin, S. D.; Abnisa, F.; Wan Daud, W. M. A.; Aroua, M. K., A review on pyrolysis of plastic wastes. *Energy Conversion and Management* **2016,** *115*, 308-326.

10. Szekely, T.; Varhegyi, G.; Till, F.; Szabo, P.; Jakab, E., The effects of heat and mass transport on the results of thermal decomposition studies: Part 1. The three reactions of calcium oxalate monohydrate. *Journal of Analytical Applied Pyrolysis* **1987,** *11*, 71-81.

11. Fuentes-Ordóñez, E. G.; Salbidegoitia, J. A.; González-Marcos, M. a. P.; González-Velasco, J. R., Transport phenomena in catalytic hydrocracking of polystyrene in solution. *Industrial Engineering Chemistry Research* **2013,** *52* (42), 14798-14807.

12. Akah, A.; Hernandez-Martinez, J.; Rallan, C.; Garforth, A. A., Enhanced feedstock recycling of post-consumer plastic waste. *Chemcal Engineering Transactions* **2015,** *43*, 2395-2400.

13. Karagöz, S.; Yanik, J.; Uçar, S.; Song, C., Catalytic coprocessing of low-density polyethylene with VGO using metal supported on activated carbon. *Energy Fuels* **2002,** *16* (5), 1301-1308.

14. Sriningsih, W.; Saerodji, M. G.; Trisunaryanti, W.; Armunanto, R.; Falah, I. I., Fuel production from LDPE plastic waste over natural zeolite supported Ni, Ni-Mo, Co and Co-Mo metals. *Procedia Environmental Sciences* **2014,** *20*, 215-224.

15. Yasuda, H.; Yamada, O.; Zhang, A.; Nakano, K.; Kaiho, M., Hydrogasification of coal and polyethylene mixture. *Fuel* **2004,** *83* (17-18), 2251-2254.

16. Hassan, H.; Regnier, N.; Pujos, C.; Defaye, G., Effect of viscous dissipation on the temperature of the polymer during injection molding filling. *Polymer Engineering & Science* **2008,** *48* (6), 1199-1206.

17. Griskey, R. G.; Wiehe, I. A., Heat transfer to molten flowing polymers. *AIChE Journal* **1966,** *12* (2), 308-312.

18. Tennakoon, A.; Wu, X.; Paterson, A. L.; Patnaik, S.; Pei, Y.; LaPointe, A. M.; Ammal, S. C.; Hackler, R. A.; Heyden, A.; Slowing, I. I.; Coates, G. W.; Delferro, M.; Peters, B.; Huang, W.; Sadow, A. D.; Perras, F. A., Catalytic upcycling of high-density polyethylene via a processive mechanism. *Nature Catalysis* **2020,** *3* (11), 893-901.

19. Ramdoss, P. K.; Tarrer, A. R., High-temperature liquefaction of waste plastics. *Fuel* **1998,** *77* (4), 293-299.

20. Schubert, T.; Lechleitner, A.; Lehner, M.; Hofer, W., 4-Lump kinetic model of the co-pyrolysis of LDPE and a heavy petroleum fraction. *Fuel* **2020,** *262*, 116597.

21. Singh, J.; Kumar, S.; Garg, M., Kinetic modelling of thermal cracking of petroleum residues: A critique. *Fuel processing technology* **2012,** *94* (1), 131-144.

22. Del Bianco, A.; Panariti, N.; Anelli, M.; Beltrame, P.; Carniti, P., Thermal cracking of petroleum residues: 1. Kinetic analysis of the reaction. *Fuel* **1993,** *72* (1), 75-80.

23. Ancheyta-Juárez, J.; López-Isunza, F.; Aguilar-Rodríguez, E., 5-Lump kinetic model for gas oil catalytic cracking. *Applied Catalysis A: General* **1999,** *177* (2), 227-235.

24. Zhang, R.; Li, L.; Liu, Z.; Meng, X., Nine-lump kinetic study of catalytic pyrolysis of gas oils derived from Canadian synthetic crude oil. *International Journal of Chemical Engineering* **2016,** *2016*.

25. Cardona, S. C.; Corma, A., Kinetic study of the catalytic cracking of polypropylene in a semibatch stirred reactor. *Catalysis Today* **2002,** *75* (1-4), 239-246.

26. Sánchez, S.; Ancheyta, J., Effect of pressure on the kinetics of moderate hydrocracking of Maya crude oil. *Energy Fuels* **2007,** *21* (2), 653-661.

27. Martínez, J.; Ancheyta, J., Kinetic model for hydrocracking of heavy oil in a CSTR involving short term catalyst deactivation. *Fuel* **2012,** *100*, 193-199.

28. Keyvanloo, K.; Towfighi, J.; Sadrameli, S.; Mohamadalizadeh, A., Investigating the effect of key factors, their interactions and optimization of naphtha steam cracking by statistical design of experiments. *Journal of AnalyticalApplied Pyrolysis* **2010,** *87* (2), 224-230.

29. Bin Jumah, A.; Anbumuthu, V.; Tedstone, A. A.; Garforth, A., Catalyzing the Hydrocracking of Low Density Polyethylene. *Industrial & Engineering Chemistry Research* **2019,** *58* (45), 20601-20609.

30. Miranda, M.; Cabrita, I.; Pinto, F.; Gulyurtlu, I., Mixtures of rubber tyre and plastic wastes pyrolysis: a kinetic study. *Energy* **2013,** *58*, 270-282.

31. Quitian, A.; Ancheyta, J., Experimental methods for developing kinetic models for hydrocracking reactions with slurry-phase catalyst using batch reactors. *Energy Fuels* **2016,** *30* (6), 4419-4437.

32. Nguyen, T. S.; Tayakout-Fayolle, M.; Ropars, M.; Geantet, C., Hydroconversion of an atmospheric residue with a dispersed catalyst in a batch reactor: Kinetic modeling including vapor–liquid equilibrium. *Chemical Engineering Science* **2013,** *94*, 214-223.

33. Loria, H.; Trujillo-Ferrer, G.; Sosa-Stull, C.; Pereira-Almao, P., Kinetic modeling of bitumen hydroprocessing at in-reservoir conditions employing ultradispersed catalysts. *Energy & Fuels* **2011,** *25* (4), 1364-1372.

34. Adeniyi, A. G.; Eletta, O. A. A.; Ighalo, J. O., Computer aided modelling of low density polyethylene pyrolysis to produce synthetic fuels. *Nigerian Journal of Technology* **2018,** *37* (4), 945-949.

35. Wu, J.; Prausnitz, J. M., Phase equilibria for systems containing hydrocarbons, water, and salt: An extended Peng− Robinson equation of state. *Industrial Engineering Chemistry Research* **1998,** *37* (5), 1634-1643.

36. Fukuyama, H.; Terai, S., Kinetic study on the hydrocracking reaction of vacuum residue using a lumping model. *Petroleum Science Technology* **2007,** *25* (1-2), 277-287.

37. Meille, V.; Pestre, N.; Fongarland, P.; de Bellefon, C., Gas/liquid mass transfer in small laboratory batch reactors: comparison of methods. *Industrial Engineering Chemistry Research* **2004,** *43* (4), 924-927.

38. Oyevaar, M.; Westerterp, K., Mass transfer phenomena and hydrodynamics in agitated gas—liquid reactors and bubble columns at elevated pressures: State of the art. *Chemical Engineering Processing: Process Intensification* **1989,** *25* (2), 85-98.

39. Aguado, R.; Olazar, M.; Gaisán, B.; Prieto, R.; Bilbao, J., Kinetic study of polyolefin pyrolysis in a conical spouted bed reactor. *Industrial Engineering Chemistry Research* **2002,** *41* (18), 4559-4566.

4.8 Supporting information: Kinetic Modelling of Low Density Polyethylene Hydrocracking in a Batch Reactor

4.8.1 Model validation data

Table 4-5 Model validation data for the proposed model of LDPE hydrocracking at three different temperatures, 10 min, 175 μm of average catalyst particle size, 20 bar of H_2 pressure and 600 rpm of rotation stirring speed

	Concentration in liquid phase (kg/m3)			
Temperature (°C)	PE	HL	N	G
300	218	3.8	157	11
275	331	0.3	64	4

4.8.2 MATLAB secripts for the kinatic Model

4.8.2.1 Regression part

```
clear;
clc;
A = [];
b = [];
Aeq = [];
beq = [];
nvars=9;
options.PopulationSize = 200;
options.MaxGenerations = 100;
options.FunctionTolerance = 1e-20;
options.PlotFcn = {@ga,'PlotFunction';
options = optimoptions(@ga,'Display','iter');
[kk,fval,exitflag,output] =
ga(@Full_LDPE_Obj_ga_fun,nvars,A,b,Aeq,beq,[],[],[],options);
tm = [0 5 20 40];
 % define objective function (scaled sum of squared errors)
function objective = Full_LDPE_Obj_ga_fun(kk,tm,~)
% data for regression
tm = [0 5 20 40];
% % 300oC
PEl = [321.1111111; 297.7777778; 217.7777778; 189.1111111];
HLl = [0;0.706142721;3.813826686;3.41188885];
Nl = [33.8262708;72.93995523;158.5753529;169.0582836];
Gl = [8.173729195;12.35390205;10.94415378;56.41871649];
x=[PEl, HLl, Nl, Gl];
PE = x(1);
HL = x(2);
N = x(3);
G = x(4);
% initial parameter guess
%%300oC
x0 = [321.1111111; 0; 33.8262708; 8.173729195];
tspan = [0:0.5:40];
opts = odeset('RelTol',1e-7,'AbsTol',1e-7,'NonNegative',1:4);
[t,xp] = ode15s(@(t,x)Full_LDPE_ODE_Sys_ga(tm,x,kk),tspan, x0, opts);
xP = [];
xP(1) = xp(1);
xP(2) = xp(12);
xP(3) = xp(42);
xP(4) = xp(82);
objective = sum(sqrt(((xP - x)/x).^2), 'all');
end
% define prediction function
function dxdt = Full_LDPE_ODE_Sys_ga(t,x,kk)
dxdt=zeros(size(x));
```

```
PEl = x(1);
HLl = x(2);
Nl = x(3);
Gl = x(4);
dxdt(1) = (-kk(1)*x(1) - kk(3)*x(1))*kk(6);
dxdt(2) = (kk(1)*x(1) - kk(2)*x(2))*kk(7);
dxdt(3) = ((kk(3)*x(1) + kk(2)*x(2) - kk(4)*x(3))*kk(8)) + kk(5)*(0.02104591 - x(3));
dxdt(4) = ((kk(4)*x(3))*kk(9)) + kk(5)*(0.243791604 - x(4));
dxdt = [dxdt(1); dxdt(2); dxdt(3); dxdt(4)];
end
```

4.8.2.2 Testing the output of the regression part

```
clear all
clc
tm=[0 5 20 40];
% % 300oC
% PEl = [321.1111111; 297.7777778; 217.7777778; 189.1111111];
% HLl = [0;0.706142721;3.813826686;3.41188885];
% Nl = [33.8262708;72.93995523;158.5753529;169.0582836];
% Gl = [8.173729195;12.35390205;10.94415378;56.41871649];
x = [PEl, HLl, Nl, Gl];
%%300oC
x0 = [321.11; 0; 33.828; 8.1735];
tspan = [0:.5:40];
opts = odeset('RelTol',1e-5,'AbsTol',1e-5,'NonNegative',1:4);
[t,xp] = ode15s(@Full_LDPE_ODE_test,tspan, x0, opts);
PEp=xp(:,1);
HLp=xp(:,2);
Np=xp(:,3);
Gp=xp(:,4);
xp=[PEp, HLp, Np, Gp];
plot(t,PEp,'b',tm,PEl,'b*',t,HLp,'r',tm,HLl,'r*',t,Gp,'k',tm,Gl,'k*',t,Np,'g',tm,Nl,'
g*');
hold on
legend('PEp','PE','HLp','HL','Gp','G','Np','N')
% plot(t,HLp,'r',tm,HLl,'r*',t,Gp,'k',tm,Gl,'k*');
% hold on
% legend('HLp','HL','Gp','G')
function  dxdt = Full_LDPE_ODE_test(t,x)
dxdt=zeros(size(x));
PEl = x(1);
HLl = x(2);
Nl = x(3);
Gl = x(4);
% % 300C
kk = [7.3427e-04,0.0114314,0.024654852,0.0096976,1.2789e-
04,0.6494019,0.7305759,0.8951098,0.96518272];
dxdt(1) = (-kk(1)*x(1) - kk(3)*x(1))*kk(6);
dxdt(2) = (kk(1)*x(1) - kk(2)*x(2))*kk(7);
dxdt(3) = ((kk(3)*x(1) + kk(2)*x(2) - kk(4)*x(3))*kk(8)) + kk(5)*(0.02104591 - x(3));
dxdt(4) = ((kk(4)*x(3))*kk(9)) + kk(5)*(0.243791604 - x(4));
dxdt = [dxdt(1); dxdt(2); dxdt(3); dxdt(4)];
end
```

5 Hydrocracking of Virgin and Post-Consumer Polymer

5.0 The relevance of the "Hydrocracking of Virgin and Post-Consumer Polymer" paper to the thesis context

The manuscript presented here is reformatted from the manuscript submitted to the *Microporous and Mesoporous Materials*, published February 2021. Having established that hydrocracking is more resource- and energy-efficient than competitors such as waste-to-energy or uncatalysed pyrolysis (4), the next experimental stage was to undergo the complexity of varying the feedstock to the hydrocracking unit by using single and mixed streams of pure and post-consumer polymers. This step would meet the ultimate target of the project which is proving the viability of hydrocracking over meso/microporous bifunctional zeolite as a sustainable recycling technology and rests on it being able to cope with mixed post-consumer polymer.

Mild reaction conditions of 330 °C, 20 bar H_2 and 30 minutes of reaction time, obtained from Chapter 3, were used to convert four different types of polyolefins, namely low and high density polyethylene (LDPE, HDPE), polypropylene (PP) and polystyrene (PS) into valuable petroleum cuts of LPG and naphtha. The hydrocracking of PE and PP streams gave a similar mix yield of rich light, highly branched paraffins, while PS was converted into aromatic products exemplified by benzene and ethylbenzene. Zeolite Beta impregnated with 1% Pt has demonstrated high conversion of the all tested polymers streams. Dealuminated USY with 1% Pt, however, was more selective towards liquid products (C_5-C_{20}) based on the more open structure.

Hydrocracking of Virgin and Post-Consumer Polymer

*Abdulrahman bin Jumah[1,2], Aleksander A. Tedstone[1], Arthur A. Garforth[1]**

**Corresponding Author: arthur.garforth@manchester.ac.uk*

1) Department of Chemical Engineering and Analytical Science, University of Manchester, The Mill, Sackville Street, M1 3BB, United Kingdom

2) College of Engineering, King Saud University, P.O. Box 800 Riyadh 11421, Saudi Arabia

5.1 Abstract

With the growing concern around polymer waste sent to landfill and its environmental release, one effective route for polymer recycling is hydrocracking over bifunctional zeolites. Zeolite Beta impregnated with 1% Pt has demonstrated high conversion of single and mixed streams of virgin and post-consumer polymers, LDPE, HDPE, PP and PS under mild reaction conditions of 330 °C, 20 bar H_2 and a 30 minute reaction time. The PE and PP streams giving a similar mix of low molecular weight hydrocarbons with higher selectivity toward gases (typically, C_3-C_4) and also, obtaining high iso- to normal paraffin ratio. PS was readily converted into an aromatic-rich product under these mild conditions and demonstrated the ability to be a source of benzene and ethylbenzene for use as raw materials in further polymer production. Dealuminated zeolite USY with 1% Pt increased the selectivity toward liquid products and resulting in more naphtha (C_5-C_{12}) and heavier liquids (C_{13}-C_{20}).

5.2 Introduction

Polymers are crucial elements in our modern life on which we are dependent, justified by their key features of light weight, versatility and relatively low production cost.[1] From the market point of view, polymer use is dominated by polyolefins, such as, polyethylene (PE), polypropylene (PP), and polystyrene (PS).[2] The growing global demand of these materials has risen on average of 5% per annum since 1990, with production reaching 359 million tonnes in 2018.[2-4] Increased demand has led to increased waste with more than 29 Mte generated in Europe (2018), of which only 43% was recycled properly without harming the environment with gas emissions.[4] Some condensation polymers can be depolymerised to their monomers,[5-8] but addition polymers including polyolefins are more chemically stable.[9-11] However, those polymers can be chemically recycled (cracked) into highly refined hydrocarbons to avoid the use of fossil fuel. To further emphasise, the sustainability of recycling these type of materials and the avoidance of their single use can be summarised in better containment and reduced emissions compared to landfill and incinerators, and improved circularity.[12, 13]

Chemical recycling of polymers by hydrocracking, a catalytic refining process, offers the potential for the selective recovery of useful chemical fractions of a desired, relatively lower boiling range at relatively modest reaction conditions. Hydrogen pressure is used to remove sulphur and chlorine impurities to yield products in the range of heavy diesel to light naphtha,[14] with high iso-paraffin and low olefin content.[15-17]. Hydrocracking requires a bifunctional catalyst with the acidic function enhancing the cracking typically provided by a high surface area support, such as a zeolite.[18-20] The hydrogenation/dehydrogenation function is provided by noble metals,

such as Pt or Pd, and in a milder form of hydrocracking, known as hydrotreating, by transition metals using an alumina support loaded with Mo, Co, W or Ni.[21] One of the main challenges facing the hydrocracking of polymers is their physical properties with molten viscous polymer creating mass and heat transfer limitations which are then exacerbated by diffusion issues created by the use of a microporous zeolite.[22, 23] Conventional catalysts, such as, microporous zeolites have proven to be effective catalysts in the hydrocracking of polymers, producing a significant fraction of saturated, branched paraffins.[24-26] Higher gas yields in the product stream can result because of hindered diffusion of large hydrocarbons through the narrow micropores of the catalyst. Introducing larger mesopores (2-50 nm) enhances the diffusivity of molten polymer as well as heavy molecular weight molecules and increases the selectivity towards liquid product (for example, C_5-C_{12}).[16, 27, 28] The preference for producing highly isomerised saturated naphtha is based on its high value in the petrochemical industry where it can be handled easily in comparison to gas and it has direct application as a feedstock to a steam cracker unit, for the production of olefins and hydrogen.

This study converts post-consumer and laboratory polymers of low and high density polyethylene (LDPE, HDPE), polypropylene (PP) and polystyrene (PS), into LPG (C_3-C_4) and naphtha products predominantly. The effect of catalyst morphology (Pt-loaded zeolite Beta and USY) and varying the feed stream are investigated by reacting each polymer type individually and mixture streams of virgin and post-consumer polymers. The key performance indicators are polymer conversion from solid to fluids phase, product yield, selectivity to naphtha, and H_2 consumption. Polymer waste recycling studied here will enhance the circular economy in the hydrocarbon industries, suggesting a method of recapturing the value of this ubiquitous commodity.

5.3 Experimental procedure

5.3.1 Materials

The zeolite catalysts (Zeolyst international, code no.s CP814C* and CBV720 respectively) used in this study were NH_4^+-form Beta (Si/Al_{bulk} 12.5) and acidic H-form USY (Si/Al_{bulk} 15). Tetraammineplatinum(II) chloride hydrate was used as a platinum source and supplied by Sigma Aldrich with a purity of 99%. All catalysts were used in pellet form in the size range 212–500 μm. Virgin polymers of high purity were received from Goodfellows in powder (< 400 μm) or pellet form, namely, low density polyethylene (M_w ~ 150,000 g/mol, code no. ET316031) (LDPE), polypropylene (M_w ~ 300,000 g/mol, code no. PP306312) (PP) and polystyrene (code no. ST316003) (PS). The post-consumer polymers were laboratory solvent wash bottles (LDPE) and centrifuge tubes (PP), and household milk bottles (HDPE, 1L, typical of retailers) and clear drinking cups (PS).

5.3.2 Feed preparation

The post-consumer samples were shredded to a size of 1-10 mm prior to being loaded into the reactor. The mixed polymer samples were prepared proportionally to their typical proportions in landfill of LDPE, HDPE, PP, and PS with proportions of 34%, 24%, 33% and 10% respectively.[2]

5.3.3 Catalyst preparation

Zeolite in NH_4^+ form was converted to its protonated form by calcining from ambient to 500 °C, at rate of 1.5 °C min^{-1}. Pt-zeolites were prepared following an impregnation method, in a solution of tetraammineplatinum(II) chloride hydrate in deionized water and then mixing the required concentration of solution for 24 h with the zeolite (10

cm^3: 1 g). Following that drying and then activating of the prepared catalysts was carried out in a tubular reactor by heating at 1.5 °C min^{-1} from ambient to 480 °C for 16 h under a hydrogen flow of 50 cm^3 min^{-1}.

5.3.4 Catalyst characterisation

The identity and crystallinity of the catalysts were determined using X-ray diffraction (XRD, Philips X'pert Pro PW3719). The Si/Al ratio as well as the added Pt level on the catalysts were determined using energy-dispersive X-ray fluorescence (EDXRF). The total surface area of the used catalysts was measured using BET (Micromeritics ASAP 2020 static low-pressure volumetric adsorption unit). The metal reduction temperature was obtained using temperature program reduction (TPR, Quantachrome ChemBET Pulsar TPR/TPD analyser). The acidity of the catalysts were quantified using ammonia temperature programmed desorption (NH_3-TPD, Quantachrome ChemBET Pulsar TPR/TPD analyser). The modified zeolites were first activated/reduced under hydrogen flow of 40 cm^3/min at 480 °C for 3 hours. Following that, the catalysts were cooled to ambient temperature, then exposed to 5% of NH_3 in Ar and the temperature was ramped up to 800 °C. The signal for the NH_3 desorbed recorded against temperature and integrated to give acidity profiles and concentrations.

5.3.5 Hydrocracking reaction

The hydrocracking activity of the prepared catalysts for different types of polymers was tested using a 300 mL stainless steel Parr Reactor, agitated by an 'anchor' style stirrer. Shredded polymer (20 g) was mixed with activated catalyst in a polymer: catalyst ratio of 10 g: 1 g. The polymer catalyst mixture was loaded into the reactor, subsequently sealed and purged with hydrogen before being charged to the reaction

pressure (typically 20 bar H_2). The reaction temperature of 330 °C ± 5 °C was reached within 45-55 min, and then kept isothermally for 30 min with an agitation speed of 400 rpm ± 25 rpm. After the reaction was completed, the reactor was air cooled quickly to ambient temperature and the products were collected for analysis. The overall conversion was calculated using equation 1 where the conversion was considered as solid to fluid.

$$X_{(wt.\%)} = \frac{Polymer_{in} - Soild_{out} - Catalyst_{in}}{Polymer_{in}} \times 100 \quad (1)$$

5.3.6 Product analysis

The analysis of the gas samples was performed using a Varian CP 3800 GC fitted with a 50 m X 0.32 mm i.d. PLOT Al_2O_3/KCl capillary column and a FID detector. The H_2 concentration in the gas stream was measured using a mass spectrometer (Hiden Analytical). The liquid samples were analysed by GC-MS system using an Agilent Technologies 6890N Network GC fitted with a 100 m X 0.25 mm i.d. PONA CB column.

5.4 Result and analysis

5.4.1 Characterisation results

5.4.1.1 XRF elemental analysis and BET

The elemental analysis of the modified used catalysts is listed in Table 5-1. The Si/Al ratios were in rough agreement with the ratios reported by the manufacturer which were 12.5 and 15 for zeolite Beta and USY, respectively. Platinum levels were within ± 8% error of the targeted amount of 1 wt.%, as quantified using EDXRF analysis.

Table 5-1 Characterisation results of the catalysts used in the study

Catalyst	Si/Al[a]	Metal loaded	Target metal loading (wt. %)	Metal level (wt. %)	BET surface area[b] (m^2/g)	Total acid concentration[c] ($\mu mol_{NH3}.g^{-1}$)	Designation
Beta	15.1	Pt	1	1.08	405	1393	BPt1
USY	18.6	Pt	1	0.92	738	636	YPt1

[a] As quantified by EDXRF, [b] As measured by BET, [c] As measured by NH_3-TPD

The N_2 adsorption/desorption isotherm for zeolite Beta and USY showed a steep increase in the isotherm at low relative pressure indicating micropores for both zeolites (Beta and USY, Figure 5-1). However, with USY the hysteresis loop at a relative pressure of about 0.4 highlighted the presence of mesopores generated by the dealumination process of acid leaching.[29, 30]

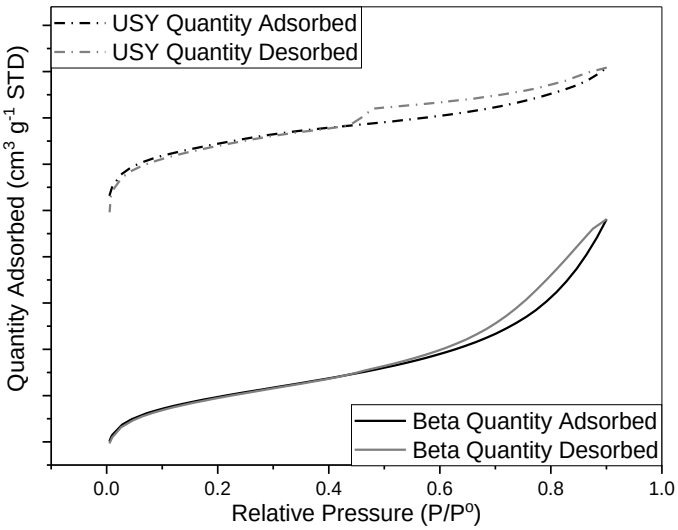

Figure 5-1 BET: N_2 Adsorption-desorption graph of zeolite Beta and USY.

5.4.1.2 H_2-Temperature programmed reduction

The H_2-TPR profiles of the two catalysts under test (Figure 5-2) indicated that platinum can be reduced/activated at the temperature of 480 °C. The Pt supported zeolite showed three H_2 reduction peaks at temperatures of ~ 280, 470 and 580 °C indicating the strong interaction between Pt and the zeolites.[31]

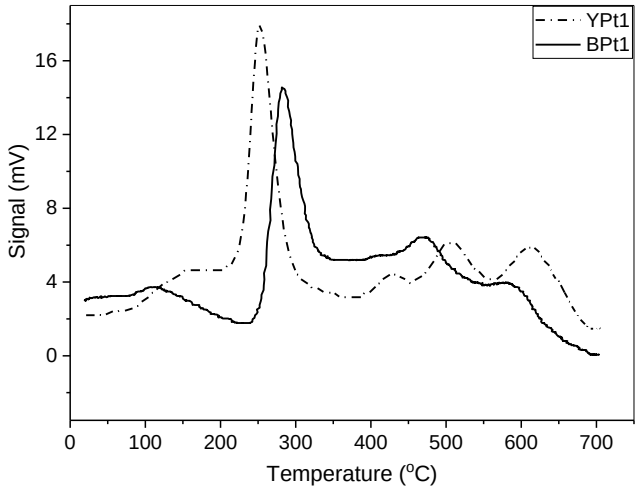

Figure 5-2 H_2-TPR profiles depicting H_2 consumed in arbitrary units as a function of temperature for BPt1 and YPt1.

Platinum reduction occurs at the more accessible surface PtO_x sites at 100-200 °C and bulk PtO_x at 250-300 °C.[32] Higher temperature reduction >400 °C is attributed to interactions of PtO_x with the zeolite support, accounting for the differences between USY and Beta zeolites in this region. Highly dealuminated zeolites such as USY have a greater concentration of silanol groups (Si-O-H) present that allow the formation of Si-O-Pt species,[33] with a correspondingly higher reduction potential than the PtO_x phase. H_2-TPR otherwise demonstrates that similar Pt species are present in both catalyst preparations, and will be activated at the reduction conditions described in section 2.3 to obtain metallic Pt(0) and hence catalytic activity.

5.4.1.3 NH_3 - Temperature programmed desorption

The strength and concentration of the acid sites of the catalysts tested were determined using NH_3 temperature program desorption (Figure 5-3). Zeolite Beta was more acidic catalyst compared to USY and both showed weak acid sites represented by the peak from 100-300 °C and strong acid sites represented by the peak from 300-800 °C.

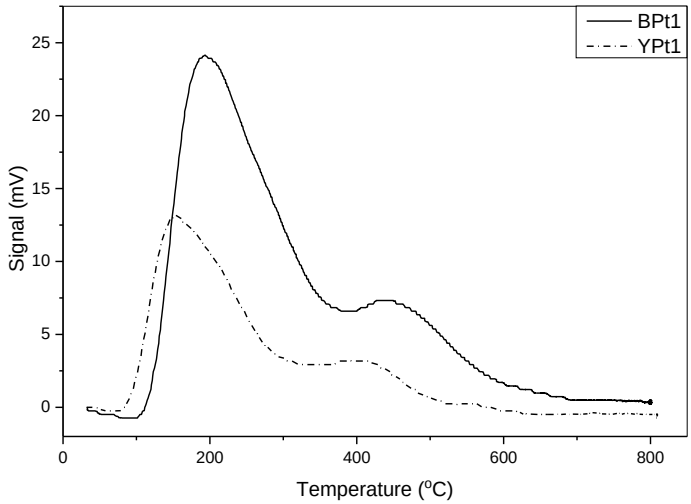

Figure 5-3 NH_3-TPD profile of zeolite Beta and USY both impregnated with 1% of Pt.

The acidity of the platinum impregnated catalysts is likely to be decreased, relative to platinum free zeolites, by the impregnation of metals due to the possibility of minor damage of the catalyst structure (Table 5-2) as well as partial blockage of the pores, preventing the adsorption of ammonia. Moreover, the impregnation could result in dealumination of the zeolite samples and a reduction of the Si-OH-Al group concentration. Also, the modification process may replace the H^+ in the Si-OH-Al as well as Si-OH and that leads to lowering the concentration of the hydroxyl groups.[34]

5.4.1.4 X-ray diffraction

The crystallinity of the modified used zeolites was examined against their parents by comparing the peaks areas for the 2θ range of 5-50°. As it can be seen from Figure 5-4 none of the modified catalysts suffered serious structural damage and the relative crystallinity of each catalyst was calculated using Equation 2. The lowest relative crystallinity of 80% was obtained by the impregnation of Pt on USY zeolite (Table 5-2).

$$Relative\ crystallinity\ (\%) = \frac{\sum_{i=1}^{n} Peak\ area\ of\ the\ modified\ sample}{\sum_{i=1}^{n} Peak\ area\ of\ the\ parent\ sample} \qquad (2)$$

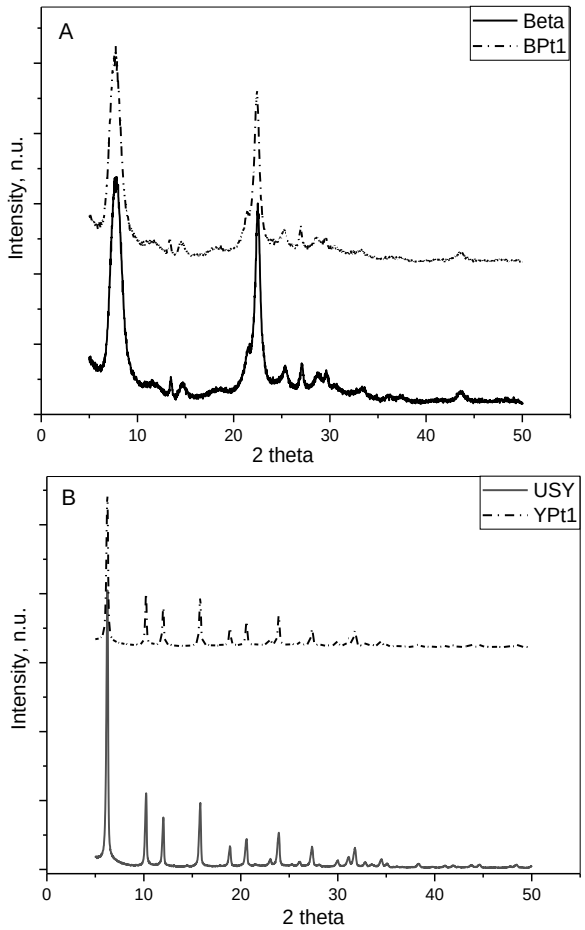

Figure 5-4 XRD patterns for zeolite (A) Beta and (B) USY both impregnated with 1% of Pt.

As expected there was slight damage to the framework by impregnation (Table 5-2, relative crystallinity) that could influence the catalyst properties, such as surface acidity.[35] Also noteworthy was no diffraction corresponding to the added metal of Pt shown in the XRD patterns which could be indicative of low concentration of the Pt impregnated or more likely, a high dispersion of the metal on the surface of the supported zeolites.

Table 5-2 Relative crystallinity of the modified catalysts based on parent samples

Catalyst	Relative crystallinity (%)	Catalyst	Relative crystallinity (%)
Beta	100	USY	100
BPt1	96	YPt1	80

5.4.2 Hydrocracking results

5.4.2.1 Hydrocracking of different types of post-consumer polymer

Generally, the tested virgin polyolefins were fully converted to hydrocarbon liquids while the post-consumers samples exhibited >95% conversion with the exception of LDPE (Figure 5-5). The hydrocracking of post-consumer samples are more complex than the virgin ones where during manufacturing trace amounts of metals (e.g. Mg, TiO_2 and Al) are added as well as colouring and inks.[36] Based on manufacturer specifications, post-consumer LDPE could contain variety of elements namely: Hg, Be, As, Cd, Pb, Sb, Se, Ag, Co, Cr, Cu, Mn, Th, V, Ba, Ni, Zn, Mg, Al, Ca, Fe, K and Na.[37] These contaminant elements affect negatively on the performance of the catalyst and resulting in poisoning and deactivating of the catalyst.

The hydrocracking of LDPE proceeds slower than in the case of HDPE for the same reaction conditions. That difference is a likely consequence of their framework, where LDPE has long and short side chain branching unlike the linear macromolecules of HDPE.[38] Therefore, more mass transfer and diffusion limitations are involved in the case of LDPE hydrocracking. By contrast, the high reactivity of PP comparing to PE can be explained by the presence of multiple tertiary carbons in the structure of the polymeric chain, helping to stabilise carbocations during reaction in the pores of the zeolite at the active sites. The maximum effective cross-sectional diameter of PP oligomer is 0.64 nm compared to the pore dimension of the zeolite Beta being 0.66 × 0.67 nm for the straight channel.[39, 40] Thus, tertiary carbenium ions can be formed rapidly on the highly acidic Beta catalyst.[41] Finally, PS was the easiest to be degraded with the highest selectivity towards liquid products achieved, followed by PP and PE.[42] Again, its ability to stabilise carbenium ions is key in its high reactivity, as shown

in Figure 5-6 Proposed pathway of (1) initiation, (2) propagation of PS hydrocracking, and (3) hydrogenation of styrene to produce ethylbenzene.

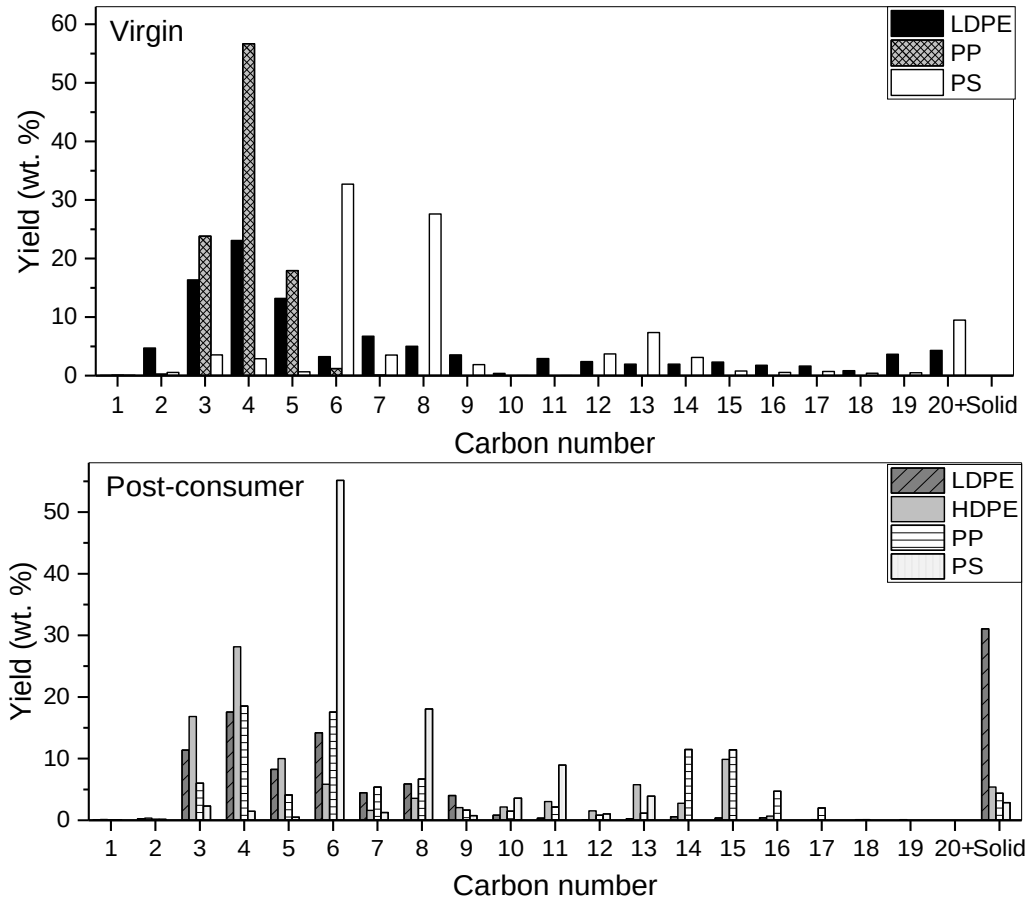

Figure 5-5 Product distribution of zeolite Beta with 1%Pt catalysed different type of virgin and post-consumer polyolefins at 330 °C and 20 bar.

The product distributions were different depending on the type of the polymer (Figure 5-5 and Figure 5-7A), for the LDPE and HDPE the product stream was dominated by gases predominantly C_3 and C_4 of ~36-56 wt.%, whilst in post-consumer PP the highest fraction was for branched alkanes in the liquid product.[20] PS gave mainly aromatics dominated by 60-80 wt.% of benzene and ethylbenzene (Figure 5-7B) with a small amount of gases (~5%). PS cracking is initiated by breaking the polymeric chain into two smaller chains mediated by the acid sites. Further cracking occurs as well as the hydrogenation of the olefins formed due to the presence of Pt in the catalyst. The next step is propagation, where intermediate chains with carbenium ions are further cracked yielding lower molecular weight chains or hydrocarbons, such as

oligomers and monomers. The formation of styrene and toluene are examples of the propagation step. Even though the styrene is not detected in the product liquid stream, the related compound ethylbenzene is identified where the ethylene branch in the benzene ring is hydrogenated. The reaction pathway in Figure 5-6 accounts for this product as the acidic functionality of the zeolite is capable of a carbenium-ion mediated scission mechanism, whilst the hydrogenation function of the platinum is responsible for the saturation of some parts of the product molecules.[43] The relatively mild reaction conditions with limited hydrogen pressure are insufficient to hydrogenate the aromatic rings resulting in the highest surplus of H_2 in the gas product stream in the case of polystyrene (Figure 5-7D).

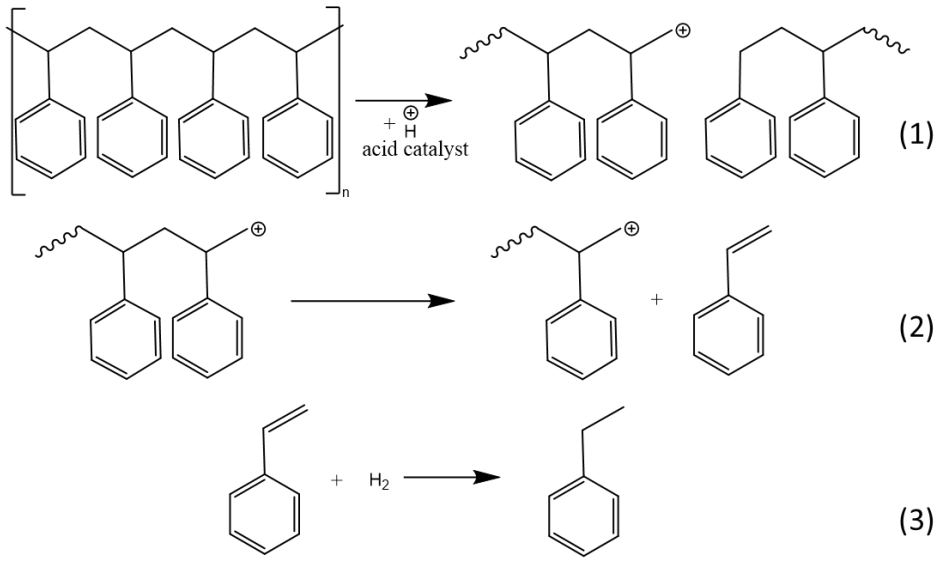

Figure 5-6 Proposed pathway of (1) initiation, (2) propagation of PS hydrocracking, and (3) hydrogenation of styrene to produce ethylbenzene.

The absence of olefins in the product stream of polymer hydrocracking proved the effectiveness of Pt in providing the appropriate amount of hydrogen transfer. As expected, hydroisomerisation resulted in a high ratio of i-C_4/n-C_4 typically in the range of 4:1 for all polymer types tested (Figure 5-7C).[44, 45]

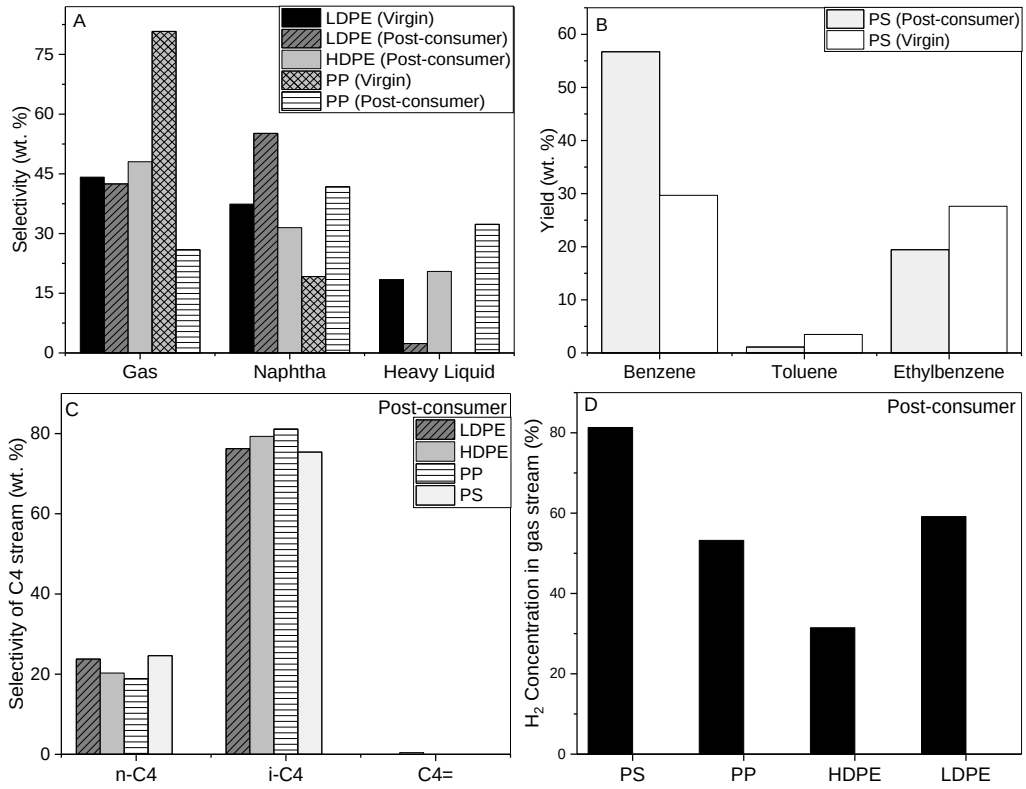

Figure 5-7 (A) Selectivity of gas, naphtha and heavy liquid in the product stream, (B) yield of benzene, toluene and Ethylbenzene, (C) Selectivity of normal, iso- paraffins and olefins in the C_4 stream, and (D) H_2 concentration in the final gas products in the hydrocracking of different type of polyolefins at 330 °C and 20 bar.

Hydrogen maintains the activity of platinum, as well as the activity of the acid catalyst, by hydrogenating the unsaturated products that are yielded in the earlier stages, thus reducing coke precursors and preventing pore blockage (Figure 5-7C).[46] In a previous study of the same catalyst, the coke formed during the hydrocracking reactions of LDPE was quantified in the range of (8-10 wt.%) using thermogravimetric analysis (TGA).[46] The surplus hydrogen in the gas stream of at least 30% (Figure 5-7) could be separated by a pressure swing adsorption unit and recycled to the process.[47] Even though there was a surplus of hydrogen in the gas stream, 20 bar H_2 was required to obtain high conversion of polymers in terms of enhancing the mass transport and the hydrogen solubility in the molten polymer, as it was reported in an earlier study.[46]

5.4.2.2 Hydrocracking of mixed polymers

Unfortunately, polymer waste contains more than just individual single polymer types. It is more complex with multi-layered laminates and co-extruded polymers consisting of several polymer types. In addition, there are additives such as titanium dioxide and talc, as well as composites including paper and metals, such as aluminium.[48] Therefore, a study of this complexity of the waste polymer stream dependent on use and user is crucial to the study of the viability of chemical recycling. With this in mind, a model mixture (LDPE 34%, HDPE 24%, PP 33%, and PS 10%) representing typical UK municipal waste was used.[2] The mixture of virgin polymers exhibited higher hydrocracking conversion of 72 wt.% (Figure 5-8A) compared to the mixture of post-consumer, where the highest conversion was 66 wt.% over BPt1 catalyst (Figure 5-8A). The complexity of decomposing the post-consumer polymer, as mentioned earlier in section 3.2.1, was due to the presence of additives such as heteroatoms and traces of metals as well as colouring matter that harnessed and deactivated the catalysts.[49] Moreover, the reaction was mass transport and diffusion limited, especially by the internal diffusion of large molecule polyolefins within the meso/microporous catalyst under the mild reaction conditions used in this study, which slowed down the reaction and limited the conversion rate.[50] However, the hydrocracking of both mixtures over BPt1 was selective more towards gaseous products, mainly C_3-C_4, reflecting the high proportion of polyethylene in the feed stream.

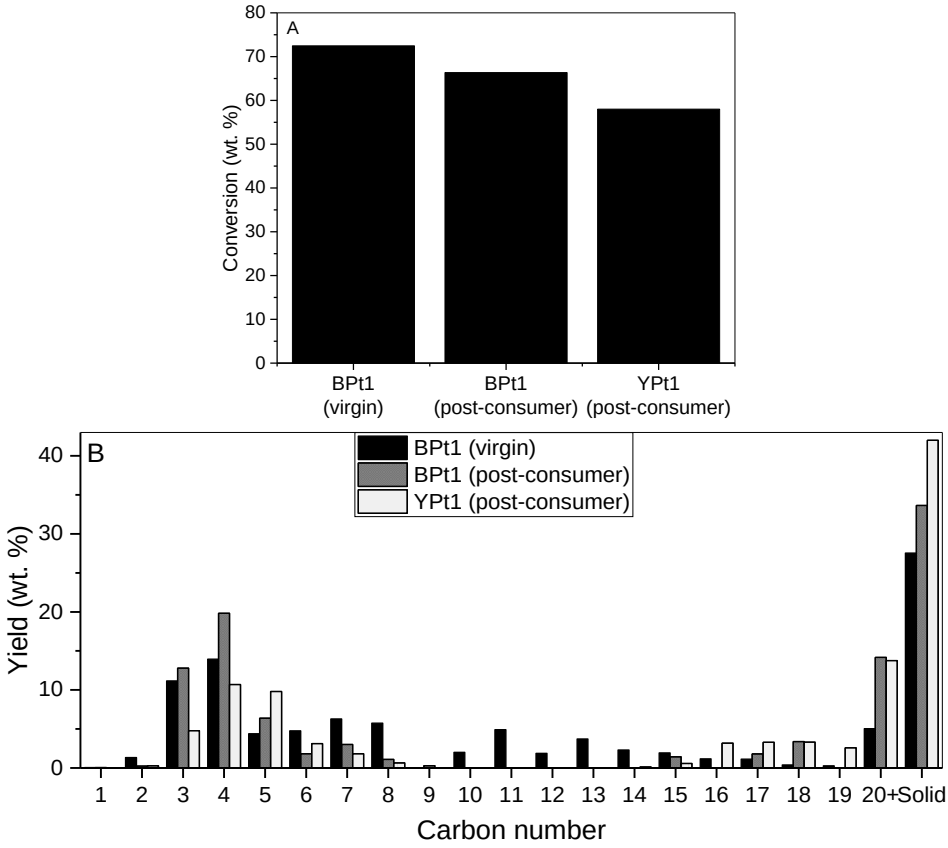

Figure 5-8 (A) Conversion and (B) product distribution of hydrocracking mixed virgin and post-consumer polymers over zeolite Beta and USY with 1%Pt at 330°C and 20 bar.

The higher activity of BPt1 compared to YPt1 on converting the post-consumer polymers was the result of higher acidity of the catalyst. In addition, the large alpha cage in zeolite USY allows the formation of bulky molecules which can cause pore blockage and, therefore, faster deactivation. After reaction, the coke levels were found to be 4.75% for BPt1 (post-consumer) and 11.76% for YPt1 (post-consumer), consistent with a greater amount of pore blockage and coke formation in the larger-pore USY zeolite, relative to Beta.

Zeolite USY was more selective towards liquid products typically naphtha and heavier fractions due to its open structure (Figure 5-8 and Figure 5-9A). The channel diameter for USY 074 × 0.74 nm and for Beta 0.65 × 0.67 and 0.56×0.56 nm. In the hydrogenation reaction, Pt dissociates the hydrogen molecule on the active site,

increasing its reactivity towards carbocation intermediates, and allowing formation of hydrogenated species from the polymer.[51]

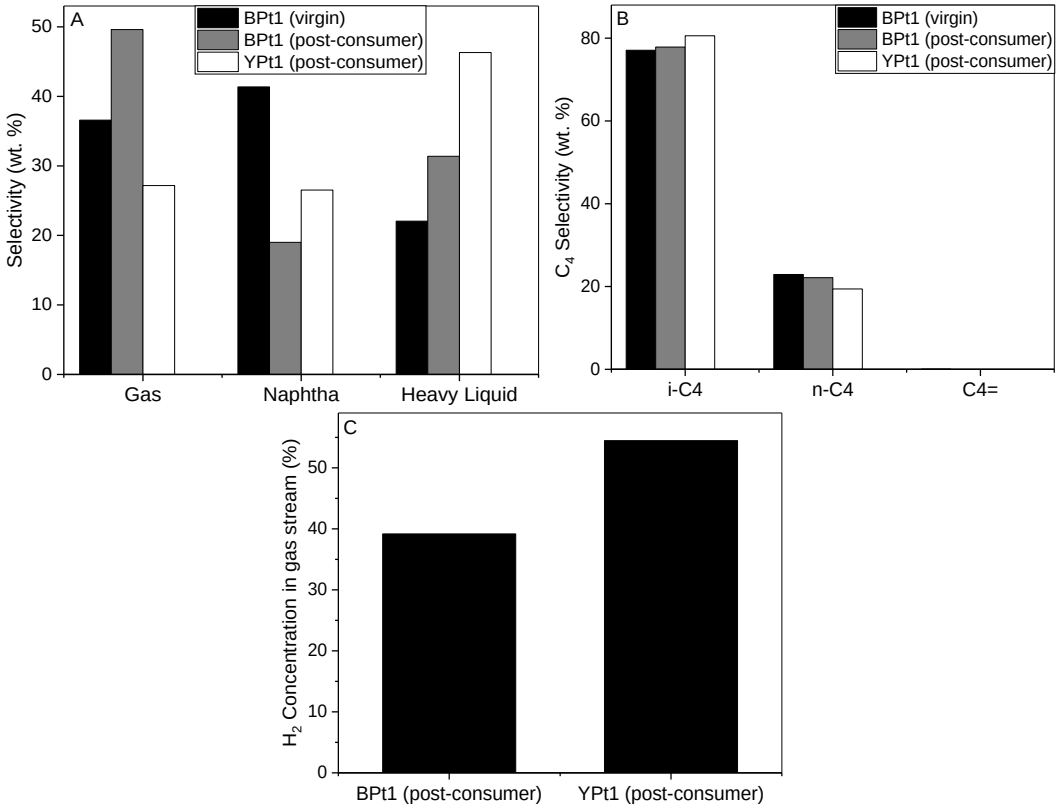

Figure 5-9 Selectivity of (A) gas, naphtha and heavy liquid in the overall product stream (B) normal, iso-paraffins and olefins in the C_4 stream, and (C) H_2 concentration in the gas stream of hydrocracking mixed virgin and post-consumer polymers over zeolite Beta and USY impregnating with 1% Pt at 330 °C and 20 bar.

As stated earlier, the hydrocracking of post-consumer polymer showed zeolite USY produced more liquid products whereas BPt1 more gases (Figure 5-9A). The ratio of iso/normal alkanes was high in both catalysts used, indicating a potentially high octane number of the liquid yielded (Figure 5-9B). The H_2 concentration post reaction was in line with the rate of catalyst deactivation as USY was likely to deactivate more quickly than Beta and hence produce more liquid. Beta being more acid would be more reactive and hence less H_2 remaining in the gas stream (Figure 5-9C).

5.5 Conclusions

The hydrocracking of pure and waste streams of single and mixed type of polymers was studied. The complexity of the feed to be degraded increased when the polymer

is post modified by the addition of additives. Bifunctional catalysts of Pt-Beta(12.5) and USY(15) showed high performance and great potential to yield rich light, highly branched paraffinic streams from virgin and waste polymer under mild reaction conditions (330 °C, 20 bar H_2 and 30 min). Based on the wider pore structure, dealuminated USY was more selective towards liquid products (C_5-C_{20}). Zeolite Beta, however, was more tolerant to degrading large and branched molecules of polyolefins and obtained higher overall conversion. The impregnation of Pt enhanced the overall activity and the hydrogenation of unsaturated products.

Hydrocracking using both real single polymers from daily use and a simulated "real" mixed feed is a major step towards the management of polymer waste by chemical recycling. Understanding the process variables needed to convert real waste, such as hydrogen pressure and energy for example will aid plant design. A recent survey by BASF has highlighted the sustainability of mechanical and chemical recycling to be matched in greenhouse emissions and much better than the incineration or waste for energy route.[52] Hydrocracking technology without doubt would contribute to lowering the energy requirement compared to thermal and catalytic cracking, lead to fewer landfill areas needed and less pollutants released to the atmosphere. Further developments are needed in terms of studying the kinetics of the reaction as well as reactor design to scale up the process to be commercialised.

5.6 Acknowledgements

The authors would like to acknowledge the support of King Saud University in Riyadh (KSU) for research funding. In addition, the UK Catalysis Hub is kindly thanked for resources and support for Dr Tedstone via our membership of the UK Catalysis Hub Consortium and funding through EPSRC grant EP/R027129/1. Finally the authors

would like to thank Dr Iain Ferguson (The Co-op), Adrian Whyle (Plastics Europe) for their continued support, the UKRI PRIF funding (EP/S025200/1: RE3 - Rethinking Resources and Recycling) and Dr Sarayute Chansai for technical assistance.

5.7 References

1. Al-Salem, S.; Antelava, A.; Constantinou, A.; Manos, G.; Dutta, A., A review on thermal and catalytic pyrolysis of plastic solid waste (PSW). *Journal of Environmental Management* **2017,** *197*, 177-198.

2. PlasticsEurope Plastics –the facts 2017 An analysis of European plastics production, demand and waste data. https://www.plasticseurope.org/application/files/5715/1717/4180/Plastics_the_facts_2017_FINAL_for_website_one_page.pdf (accessed 10/02/2021).

3. Chandrasekaran, S. R.; Sharma, B. K., Fuel properties associated with catalytic conversion of plastics. In *Plastics to Energy*, Elsevier: 2019; pp 173-220.

4. PlasticsEurope Plastics – the Facts 2019, An analysis of European plastics production, demand and waste data. https://www.plasticseurope.org/application/files/9715/7129/9584/FINAL_web_version_Plastics_the_facts2019_14102019.pdf (accessed 19/11/2020).

5. Garforth, A. A.; Ali, S.; Hernandez-Martinez, J.; Akah, A., Feedstock recycling of polymer wastes. *Current Opinion in Solid State and Materials Science* **2004,** *8* (6), 419-425.

6. Yang, Y.; Lu, Y.; Xiang, H.; Xu, Y.; Li, Y., Study on methanolytic depolymerization of PET with supercritical methanol for chemical recycling. *Polymer Degradation and Stability* **2002,** *75* (1), 185-191.

7. Chen, J. Y.; Ou, C. F.; Hu, Y. C.; Lin, C. C., Depolymerization of poly(ethylene terephthalate) resin under pressure. *Journal of Applied Polymer Science* **1991,** *42* (6), 1501-1507.

8. Siddiqui, M. N.; Achilias, D. S.; Redhwi, H. H.; Bikiaris, D. N.; Katsogiannis, K. A. G.; Karayannidis, G. P., Hydrolytic depolymerization of PET in a microwave reactor. *Macromolecular Materials and Engineering* **2010,** *295* (6), 575-584.

9. Gray, R. L., Accelerated testing methods for evaluating polyolefin stability geosynthetic testing for waste containment applications. ASTM International: West Conshohocken, PA, 1990; pp 57-74.

10. Sen, S. K.; Raut, S., Microbial degradation of low density polyethylene (LDPE): A review. *Journal of Environmental Chemical Engineering* **2015,** *3* (1), 462-473.

11. Barnes, D. K. A.; Galgani, F.; Thompson, R. C.; Barlaz, M., Accumulation and fragmentation of plastic debris in global environments. *Philosophical Transactions of the Royal Society B: Biological Sciences* **2009,** *364* (1526), 1985-1998.

12. Li, C.-T.; Zhuang, H.-K.; Hsieh, L.-T.; Lee, W.-J.; Tsao, M.-C., PAH emission from the incineration of three plastic wastes. *Environment International* **2001,** *27* (1), 61-67.

13. Eriksson, O.; Finnveden, G., Plastic waste as a fuel - CO_2-neutral or not? *Energy & Environmental Science* **2009,** *2* (9), 907-914.

14. Gruia, A., Hydrotreating. In *Handbook of petroleum processing*, Jones, D. S. J. S.; Pujadó, P. R., Eds. Springer Netherlands: Dordrecht, 2006; pp 321-354.

15. Garforth, A. A.; Ali, S.; Hernández-Martínez, J.; Akah, A., Feedstock recycling of polymer wastes. *Current Opinion in Solid State and Materials Science* **2004,** *8* (6), 419-425.

16. Munir, D.; Irfan, M. F.; Usman, M. R., Hydrocracking of virgin and waste plastics: a detailed review. *Renewable Sustainable Energy Reviews* **2018,** *90*, 490-515.

17. Brems, A.; Baeyens, J.; Dewil, R., Recycling and recovery of post-consumer plastic solid waste in a European context. *Thermal Science* **2012,** *16* (3), 669-685.

18. Escola, J.; Aguado, J.; Serrano, D. P.; Briones, L., Transportation fuel production by combination of LDPE thermal cracking and catalytic hydroreforming. *Waste Management* **2014,** *34* (11), 2176-2184.

19. Hesse, N. D.; White, R. L., Polyethylene catalytic hydrocracking by PtHZSM-5, PtHY, and PtHMCM-41. *Journal of Applied Polymer Science* **2004,** *92* (2), 1293-1301.

20. Akah, A.; Hernandez-Martinez, J.; Rallan, C.; Garforth, A. A., Enhanced feedstock recycling of post-consumer plastic waste. *Chemcal Engineering Transsactions* **2015,** *43*, 2395-2400.

21. Ochoa, R.; Van Woert, H.; Lee, W.; Subramanian, R.; Kugler, E.; Eklund, P., Catalytic degradation of medium density polyethylene over silica-alumina supports. *Fuel Processing Technology* **1996,** *49* (1-3), 119-136.

22. Hassan, H.; Regnier, N.; Pujos, C.; Defaye, G., Effect of viscous dissipation on the temperature of the polymer during injection molding filling. *Polymer Engineering & Science* **2008,** *48* (6), 1199-1206.

23. Griskey, R. G.; Wiehe, I. A., Heat transfer to molten flowing polymers. *AIChE Journal* **1966,** *12* (2), 308-312.

24. Escola, J. M.; Aguado, J.; Serrano, D. P.; Briones, L.; Díaz de Tuesta, J. L.; Calvo, R.; Fernandez, E., Conversion of polyethylene into transportation fuels by

the combination of thermal cracking and catalytic hydroreforming over Ni-Supported hierarchical beta zeolite. *Energy Fuels* **2012,** *26* (6), 3187-3195.

25. Garforth, A. A.; Lin, Y.-H.; Sharratt, P.; Dwyer, J., Catalytic polymer degradation for producing hydrocarbons over zeolites. In *Studies in Surface Science and Catalysis*, Hattori, H.; Otsuka, K., Eds. Elsevier: 1999; Vol. 121, pp 197-202.

26. Salmiaton, A.; Garforth, A. A., Multiple use of waste catalysts with and without regeneration for waste polymer cracking. *Waste Management* **2011,** *31* (6), 1139-1145.

27. Munir, D.; Usman, M. R. In *Synthesis and characterization of mesoporous hydrocracking catalysts*, IOP Conference Series: Materials Science and Engineering, IOP Publishing: 2016; pp 1-7.

28. Munir, D.; Piepenbreier, F.; Usman, M. R., Hydrocracking of a plastic mixture over various micro-mesoporous composite zeolites. *Powder Technology* **2017,** *316*, 542-550.

29. Huang, C.; Li, A.; Chao, Z.-S., Heterogeneous catalytic synthesis of quinoline compounds from aniline and C_1–C_4 alcohols over zeolite-based catalysts. *RSC Advances* **2017,** *7* (76), 48275-48285.

30. Thommes, M.; Kaneko, K.; Neimark, A. V.; Olivier, J. P.; Rodriguez-Reinoso, F.; Rouquerol, J.; Sing, K. S. J. P., Physisorption of gases, with special reference to the evaluation of surface area and pore size distribution (IUPAC Technical Report). *Pure Applied Chemistry* **2015,** *87* (9-10), 1051-1069.

31. Wannapakdee, W.; Yutthalekha, T.; Dugkhuntod, P.; Rodponthukwaji, K.; Thivasasith, A.; Nokbin, S.; Witoon, T.; Pengpanich, S.; Wattanakit, C., Dehydrogenation of propane to propylene using promoter-free hierarchical Pt/Silicalite-1 nanosheets. *Catalysts* **2019,** *9* (2), 174.

32. Park, S. H.; Tzou, M. S.; Sachtler, W. M. H., Temperature programmed reduction and re-oxidation of platinum in y-zeolites. *Applied Catalysis* **1986,** *24* (1), 85-98.

33. Ho, L.-W.; Hwang, C.-P.; Lee, J.-F.; Wang, I.; Yeh, C.-T., Reduction of platinum dispersed on dealuminated beta zeolite. *Journal of Molecular Catalysis A: Chemical* **1998,** *136* (3), 293-299.

34. Huang, C.; Li, A.; Li, L.-J.; Chao, Z.-S., Synthesis of quinolines from aniline and propanol over modified USY zeolite: catalytic performance and mechanism evaluated by in situ Fourier transform infrared spectroscopy. *RSC Advances* **2017,** *7* (40), 24950-24962.

35. Martínez, A.; Arribas, M. A.; Concepción, P.; Moussa, S., New bifunctional Ni–H-Beta catalysts for the heterogeneous oligomerization of ethylene. *Applied Catalysis A: General* **2013,** *467*, 509-518.

36. Cruz, S. A.; Zanin, M., Evaluation and identification of degradative processes in post-consumer recycled high-density polyethylene. *Polymer Degradation Stability* **2003,** *80* (1), 31-37.

37. Scientific, T. Thermo Scientific Nalgene Bottles and Carboys Technical Brochure. https://www.scientificlabs.co.uk/handlers/libraryFiles.ashx?filename=Product_Brochures_A_ASP1150_A.pdf (accessed 15/03/2020).

38. Alnaimi, S.; Elouadi, B.; Kamal, I. *Structural, thermal and morphology characteristics of low density polyethylene produced by QAPCO*; 2015.

39. Aguado, J.; Sotelo, J. L.; Serrano, D. P.; Calles, J. A.; Escola, J. M., Catalytic conversion of polyolefins into liquid fuels over MCM-41: comparison with ZSM-5 and amorphous SiO_2− Al_2O_3. *Energy Fuels* **1997,** *11* (6), 1225-1231.

40. Baerlocher, C.; McCusker, L. B.; Olson, D. H., *Atlas of zeolite framework types*. Elsevier: 2007; p 309.

41. Shabtai, J.; Xiao, X.; Zmierczak, W., Depolymerization− liquefaction of plastics and rubbers. 1. Polyethylene, polypropylene, and polybutadiene. *Energy & Fuels* **1997,** *11* (1), 76-87.

42. Venkatesh, K.; Hu, J.; Tierney, J.; Wender, I., Hydrocracking of polyolefins to liquid fuels over strong solid acid catalysts. *Preprints of Papers, American Chemical Society, Division of Fuel Chemistry* **1995,** *40*, 788-788.

43. Fuentes-Ordóñez, E. G.; Salbidegoitia, J. A.; González-Marcos, M. P.; González-Velasco, J. R., Mechanism and kinetics in catalytic hydrocracking of polystyrene in solution. *Polymer Degradation Stability* **2016,** *124*, 51-59.

44. Chica, A.; Corma, A., Hydroisomerization of pentane, hexane, and heptane for improving the octane number of gasoline. *Journal of Catalysis* **1999,** *187* (1), 167-176.

45. Corma, A.; Juan-Rajadell, M.; Lopez-Nieto, J.; Martinez, A.; Martinez, C., A comparative study of O_4^{2-}/ZrO_2 and zeolite beta as catalysts for the isomerization of n-butane and the alkylation of isobutane with 2-butene. *Applied Catalysis A: General* **1994,** *111* (2), 175-189.

46. Bin Jumah, A.; Anbumuthu, V.; Tedstone, A. A.; Garforth, A., Catalyzing the Hydrocracking of Low Density Polyethylene. *Industrial & Engineering Chemistry Research* **2019,** *58* (45), 20601-20609.

47. Lokhandwala, K. A.; Baker, R. W. Hydrogen/hydrocarbon separation process, including PSA and membranes. US6592749B1, 2003.

48. Bart, J. C., *Additives in polymers: Industrial analysis and applications*. John Wiley & Sons: 2005; p 838.

49. Ding, W.; Liang, J.; Anderson, L. L., Thermal and catalytic degradation of high density polyethylene and commingled post-consumer plastic waste. *Fuel Processing Technology* **1997,** *51* (1-2), 47-62.

50. Fuentes-Ordóñez, E. G.; Salbidegoitia, J. A.; González-Marcos, M. a. P.; González-Velasco, J. R., Transport phenomena in catalytic hydrocracking of polystyrene in solution. *Industrial Engineering Chemistry Research* **2013,** *52* (42), 14798-14807.

51. Auras, S. V.; van Lent, R.; Bashlakov, D.; Piñeiros Bastidas, J. M.; Roorda, T.; Spierenburg, R.; Juurlink, L. B., Scaling platinum-catalyzed hydrogen dissociation on corrugated surfaces. *Angewandte Chemie* **2020,** *132*, 21159 – 21165.

52. BASF. Life cycle assessment (LCA) for ChemCyclingTM 2020. https://www.basf.com/global/en/who-we-are/sustainability/we-drive-sustainable-solutions/circular-economy/mass-balance-approach/chemcycling/lca-for-chemcycling.html#:~:text=An%20LCA%20study%20conducted%20by,incineration%20of%20mixed%20plastic%20waste. (accessed 14/04/2021).

6 Replacing Platinum with Nickel Supported on Zeolites Beta and USY for Hydrocracking of Post-Consumer Polymer

6.0 The relevance of the "Replacing Platinum with Nickel Supported on Zeolites Beta and USY for Hydrocracking of Post-Consumer Polymer" paper to the thesis context

The manuscript presented here is in preparation for submission to the *Applied Catalysis A: General*. The focus of this chapter is on further developing the insights of those previous studies by considering the catalyst cost in the hydrocracking system by replacing the noble metal of Pt by Ni. Despite the pollution related, Ni is a common metallic element in hydrocracking catalysts and provides hydrogenation functionality in a number of other industrial processes. It is worth noting that the present strategy of loading Ni instead of Pt into zeolite USY could be useful for designing low-cost, metal-supported catalysts for polymer hydrocracking.

Replacing Platinum with Nickel Supported on Zeolites Beta and USY for Hydrocracking of Post-Consumer Polymer

*Abdulrahman bin Jumah[1,2], Aleksander A. Tedstone[1] and Arthur A. Garforth[1]**

**Corresponding Author: arthur.garforth@manchester.ac.uk*

1) Department of Chemical Engineering and Analytical Science, University of Manchester, The Mill, Sackville Street, M1 3BB, United Kingdom

2) College of Engineering, King Saud University, P.O. Box 800 Riyadh 11421, Saudi Arabia

6.1 Abstract

Bifunctional zeolite catalysts show high performance when converting the environmental problematic post-consumer polymers into more valuable feedstock hydrocarbons. In a previous study, zeolite beta and USY loaded with 1% Pt have demonstrated high conversion of mixed streams of post-consumer polymers under mild batch reaction conditions of 330 ^{o}C, 20 bar H_2 and reaction time of 30 min. Replacing the costly noble metal, platinum, by a much less expensive alternative, such as, nickel would make significant reduction in the total cost of the catalytic system. By substituting the Pt with 10% of Ni supported USY the same level of conversion of mixed post-consumer polymer was achieved (57%), with a remarkable enhancement to naphtha selectivity in gasoline range (C_5-C_{12}) whilst maintaing an iso/normal paraffin ratio of 4:1.

6.2 Introduction

Hydrocracking is a process where high-boiling molecules are cracked into lower molecular weight and more valuable materials, such as, LPG and naphtha, with a high selectivity towards iso/normal paraffins.[1] The process shows high efficiency, in terms of lowering the energy, reaction time and separation requirements, not only in an oil refinery setting but also when considered for use in recycling environmentally problematic post-consumer polymers to produce valuable hydrocarbon feedstock materials.[2-5] Comparing to thermal and catalytic cracking of polymer, hydrocracking requires a lower temperature to achieve a high degradation rate, and the presence of hydrogen contributes to improving the quality and stability of the output stream by yielding saturated paraffins which are preferred commercially, as well as maintaining the catalyst activity by reducing the coke formation.[6] Moreover, hydrocracking is a one-step reaction converting the polymer with high selectivity to alkanes with reduced separation requirements.

A bifunctional catalyst is required in the process, and it consists of acidic sites to accelerate the cracking reactions by forming carbonium ions,[7] and metal sites to facilitate hydrogenation/dehydrogenation reactions. Commonly, a high surface area support of alumina, amorphous silica-alumina, or zeolites are used.[8-11] The hydrogenation/dehydrogenation function can be provided by noble metals, such as Pt or Pd or transition metals such as, Mo, Co, Co-Mo, W, Ni, or Ni-Mo.[9] In particular, a supported Pt catalyst is found to obtain the highest catalyst activity compared with the other metals by achieving high polymer degradation at comparatively lower temperature.[6, 12-14]

Although the Pt supported is typically 1% or less, this small amount of the noble metal still accounts for a significant proportion of the total operational cost.[15, 16] Among the

non-noble, less expensive metals, nickel could be an effective component to functionalise the hydro-/dehydrogenating of different type of reactions.[17, 18] However, the hydro-/dehydrogenation activity of Ni is much lower than that of Pt and is overcome by increasing the Ni loading. Economically, even with the increased loading, Ni remains significantly less expensive relative to Pt (approximately, Ni at 16 $/kg compared to Pt at 37260 $/kg).[19] The main challenge of replacing the Pt by Ni is to achieve high metal dispersion on the zeolite support. Pt is a heavy metal with high polarizability and has Van der Waals interaction with the zeolite pore wall, but, the Ni atoms are smaller with low polarizability and have weak interaction with zeolite pores.[16] The poor or low dispersion of Ni atoms on a zeolite results in the formation of large agglomerates due to the high tendency of the Ni atoms to migrate easily to the external surface of the conventional zeolite.[16]

The hydrocracking of the polymer is known to be limited by mass and heat transfer as well as diffusional issues resulting from the catalyst pores and the high viscosity of the molten polymer.[20, 21] Microporous zeolites incorporated with an active metal have proved to be effective hydrocracking catalysts yielding a significant fraction of saturated paraffins from polymers.[22-24] However, microporous zeolites are highly selective towards gaseous products with smaller proportion of liquids due to hindered diffusion of larger hydrocarbons through the narrow micropores. Thus, the introduction of larger mesopores (2-50 nm) into conventional microporous zeolites (such as, zeolite USY) could increase diffusivity and potentially the yield of liquid products.[4, 25, 26] Zeolite Beta, and USY impregnated with Pt or Ni are used in this study to convert a mixed feed of post-consumer polymers of low and high density polyethylene (LDPE, HDPE), polypropylene (PP) and polystyrene (PS), into small gaseous and liquid hydrocarbons. The effect of replacing Pt by Ni is investigated, with

the key performance indicators being polymer conversion, product distribution, selectivity of liquid stream, and H_2 consumption. This study of post-consumer polymer recycling can supplement mechanical recycling for a circular economy in the hydrocarbon industries, suggesting a method of recapturing the value of this ubiquitous commodity.

6.3 Experimental procedure

6.3.1 Materials

Zeolites Beta and USY were obtained from Zeolyst International. Tetraammineplatinum(II) chloride hydrate supplied by Sigma Aldrich with a purity of 99 and Nickel (II) nitrate hexahydrate supplied by Fisher Scientific. The post-consumer polymer samples were represented by laboratory polymer products of solvent bottles (LDPE) and centrifuge tubes (PP), and, UK consumer products of milk bottles (HDPE, 1L, typical of retailers) and clear drinking cups (PS).

6.3.2 Feed preparation

The post-consumer samples were shredded and reduced in size to 1-10 mm before being loaded to the reactor. The mixed polymer feed was prepared to approximate their presence in European landfill of LDPE, HDPE, PP, and PS with percentage proportions of 34:24:33:10, respectively.[27]

6.3.3 Catalyst preparation

Zeolite in NH_4^+ form was transformed to its protonated form by calcining at 500 ^oC. Pt and Ni-zeolites were prepared following an impregnation method, by diluting the metal salt in deionized water in a solution concentration of 2.17, 2.53, 5.06 and 10.11 g/L for 1% Pt, 2.5% Ni, 5% Ni and 10% Ni, respectively. Next, the zeolite was mixed

with the metal (1 g :10 mL zeolite:solution) solution at temperature of 65 °C for 24 h. After drying at 100 °C, the catalyst was pelleted, crushed and sieved gain particles in the range of 212-500 μm. Finally, the prepared catalysts were activated at 480 ^{o}C for Pt-catalysts or 510 ^{o}C for Ni-catalysts under a hydrogen flow of 50 ml/min for 16 h in a tubular packed bed reactor.

6.3.4 Catalyst characterisation

The Si/Al ratio, as well as, the added metal levels on the catalyst were determined using Energy-dispersive X-ray fluorescence (EDXRF). The metal reduction temperature was obtained using Temperature Program Reduction (TPR, Quantachrome ChemBET Pulsar TPR/TPD analyser). The acidity of the catalysts were quantified using Ammonia Temperature Program Desorption (NH_3-TPD, Quantachrome ChemBET Pulsar TPR/TPD analyser). The modified zeolites were first activated/reduced under hydrogen flow of 40mL/min at 480 ^{o}C and 510 ^{o}C for Pt-catalysts and Ni-catalysts, respectively. Following that, the catalysts were cooled to ambient temperature, then exposed to 5% of NH_3 in and the temperature was increased to 800 ^{o}C. The NH_3 desorbed was recorded against temperature and the curve was integrated to yield acid concentrations. The coke formed on the catalysts during the hydrocracking was quantified using thermogravimetric analysis (TGA, Q5000-IR TA instrument). The used catalyst was heated up gradually to 600 ^{o}C in flowing N_2 (50 ml/min) with ramping rate of 5 ^{o}C/min to evaporate the water and volatile hydrocarbons, as well as, removing all the polymer residues. Finally the gas flow was switched from N_2 to air to oxidise and quantify the coke content.

6.3.5 Hydrocracking reaction

The activities of the prepared catalysts in hydrocracking of mixed post-consumer polymers were tested using a 300 mL stainless steel Parr Reactor, agitated by an 'anchor' style stirrer, reactor configuration was shown in a previous study.[13] A 20 g feed of LDPE, HDPE, PP and PS was mixed with 2 g of activated catalyst and loaded into the reactor. The reactor was sealed and purged with hydrogen gas before charging to the reaction pressure (typically 20 bar H_2). The reaction temperature of 330 ^oC was reached within 45-55 min, and then kept isothermally for 30 min with an agitation speed of 400 rpm. After the reaction was completed, the reactor was cooled quickly to room temperature using flowing air and the products were collected for GC and GC-MS analysis. The overall conversion was calculated using equation 1 where the conversion was considered as solid to fluid and the solid remained was considered as unconverted feed.

$$X_{(wt\ \%)} = \frac{Soild_{out} - Polymer_{in} - Catalyst_{in}}{Polymer_{in}} \times 100 \quad (1)$$

6.3.6 Product analysis

The hydrocarbon gas products were analysed using a Varian CP 3800 GC fitted with a 50 m x 0.32 mm i.d. PLOT Al_2O_3/KCl capillary column and a FID detector and the H_2 concentration was measured using a calibrated Mass Spectrometer (Hiden Analytical). The liquid samples were analysed by GC-MS system using an Agilent Technologies 6890N Network GC fitted with a 100 m x 0.25 mm i.d. PONA CB column.

6.4 Result and analysis

6.4.1 Characterisation results

6.4.1.1 XRF and BET

The elemental analysis of the modified catalysts by EDXRF is listed in Table 6-1. Overall, the Si/Al ratios were in agreement with the ratios reported by the manufacturer which were 12.5 and 15 for zeolite beta and USY, respectively. Platinum and nickel levels were within ±15% error of the targeted amount.

Table 6-1 Characterisation results of XRF and BET of the catalysts used in the study

Catalyst	Si/Al[a]	Metal loaded	Target metal loading (wt. %)	Metal level[a] (wt. %)	Designation
Beta	15.1	Pt	1	1.08	BPt1
		Ni	2.5	2.16	BNi2.5
		Ni	5	5.06	BNi5
		Ni	10	8.79	BNi10
USY	18.6	Pt	1	0.92	YPt1
		Ni	2.5	2.79	YNi2.5
		Ni	5	5.05	YNi5
		Ni	10	9.73	YNi10

[a] As quantified by EDXRF

6.4.1.2 H_2-Temperature Programme Reduction (H_2-TPR)

The H_2-TPR profiles of the four representative catalysts (Figure 6-1) indicated that platinum and nickel could be reduced/activated at 480 and 510 ^oC, respectively. The Pt supported zeolite showed three H_2 reduction peaks at ~290, 470 and 580 ^oC indicating the strong interaction between Pt and the zeolites.[28] Reduction of the Ni catalysts showed different TPR characteristics, where zeolite beta (BNi10) observed one sharp reduction peak at temperature of ~490 ^oC where corresponding to the reduction of the NiO. However, the reduction of the Ni oxide species on the USY

catalyst consisted of one sharp peak at 370 °C and broad multiple reduction peaks over the range of ~400-650 °C. The first reduction peak could be related to the reaction of NiO to Ni°, and the peaks at higher temperatures could be related to the reduction of stabilised Ni^{2+}, which it likely to be ion-exchanged during the impregnation process.[29] Generally, the reduction of the NiO at high temperature indicated a strong interaction of the Ni oxide with the zeolite supports resulting from the Si–O–Ni bond.[16] The Ni oxide was reduced to active metal by the following reaction $NiO + H_2 \rightarrow Ni° + H_2O$.[30]

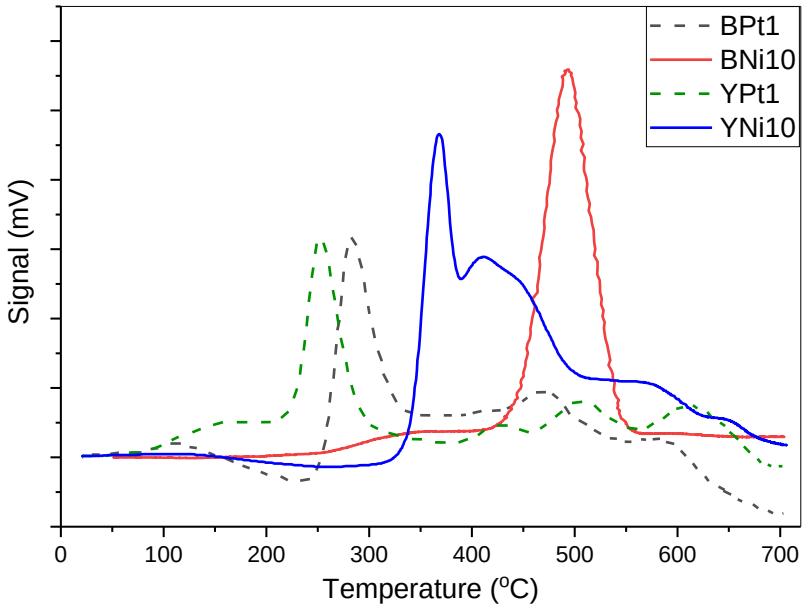

Figure 6-1 H_2-TPR profiles depicting H_2 consumed in arbitrary units as a function of temperature for different metal loading of Pt and Ni on zeolite Beta(12.5) and USY(15).

6.4.1.3 NH_3- Temperature programme desorption (NH_3-TPD)

The strength and concentration of the acid sites of the catalysts tested, determined using ammonia temperature programme desorption are shown in Figure 6-2 and measured in Table 6-2. All catalysts showed weak acid sites represented by the peak in the range of 100-300 °C and strong acid sites in the range of 300-800 °C. Peaks positions did not vary substantially with the different type of metal added or varying

of the metal concentration. Zeolite Beta is a more acidic catalyst comparing to USY and the highest acidity was observed over BNi5 catalyst.

Table 6-2 Quantitative results of NH_3-TPD of the used catalysts

Catalyst	Total acid concentration ($\mu mol_{NH3}.g^{-1}$)	Weak acid concentration ($\mu mol_{NH3}.g^{-1}$)	Strong acid concentration ($\mu mol_{NH3}.g^{-1}$)
BPt1	1393	877	516
BNi2.5	1633	911	722
BNi5	1767	971	796
BNi10	1639	964	675
YPt1	636	453	182
YNi2.5	1627	851	776
YNi5	1550	811	739
YNi10	1747	993	754

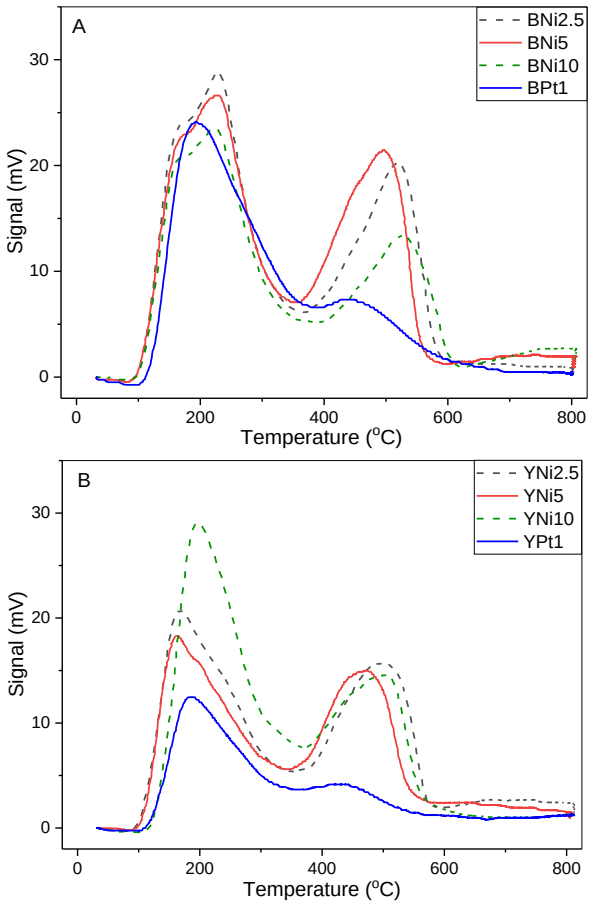

Figure 6-2 NH_3-TPD profile of zeolite (A) Beta and (B) USY both impregnated with 1% of Pt and different levels of Ni.

Overall, the ammonia absorbed was greater at lower temperature (weak acidity) compared to higher temperature (strong acidity). It is also worth noting that the acidity

can be affected by the impregnation of metals due to the possibility of partial blockage of catalyst pores, therefore, lowering the adsorption of ammonia (Table 6-2). The impregnation may result also in partial dealumination of the zeolites framework caused by the replacement of Al in the Si–OH–Al group by Ni,[31] as well as an occupation of some acid sites at higher loading.[29] Adding Ni to both zeolites had different effects on the acidity (Figure 6-2). In the case of Beta, the addition of Ni increased the amount of NH_3 desorbed at higher temperature with similar rates for 2.5 and 5. The acidity also decreased at higher Ni loading (i.e. 10%). Whereas in the case of USY, it showed significant increase in low temperature of NH_3 desorption where Ni loading was at 10%, but little change to the higher temperature desorption was obtained.

6.4.2 Hydrocracking of mixed polymer

Two main challenges of converting post-consumer polymer waste by chemical recycling are the batch variation as the presence of multiple types of polymers may differ and the presence of heteroatoms and metals, which limit the catalyst performance.[27, 32]

BPt1 exhibited higher hydrocracking activity compared to YPt1 (Figure 6-3A) resulting from higher acidity. In addition, zeolite USY with large alpha cages (~15 A°) allowing the formation of bulky molecules, led increased coke formation and potentially rapid deactivation (11.8 wt.% coke on YPt1 compared to 4.8 wt.% on BPt1, Table 6-3). Both Pt loaded zeolites showed high activity with maximum conversion of BPt1 greater than YPt1 (66% and 58%, respectively). The role of Pt in hydrogenation is to dissociate the hydrogen molecule on the active site, increasing its reactivity towards carbocation intermediates, and allowing the formation of

hydrogenated species from the polymer.[33] Since Ni is less active in the hydrogenation reaction compared to Pt, therefore, a lower concentration of dissociated hydrogen is formed on the catalyst surface.[12]

Overall, adding Ni to Beta and USY zeolites had opposite effects, with Beta activity reducing from 48% conversion for BNi2.5 to 37% conversion for BNi10. In contrast adding Ni to zeolite USY increased conversion from 43% (YNi2.5) to 58% (YNi10) equivalent to that of the YPt1 catalyst (58%). The increased activity of YNi catalysts might be explained by the slightly larger pores in USY which may be less likely to be blocked by larger metal loading from (i.e. 10 wt.%). In addition, the TPD data suggested that as Ni loading increased the number of weak acid sites increased. The BNi catalysts did not perform well and conversion decreased with addition of Ni as stated earlier. That reduction in the activity of Beta could be a result of pore blockage and also low dispersion of the Ni.[34]

Overall, the product distributions were different over the two Ni-loaded zeolites with a roughly 50:50 split between gas and liquid selectivity over Beta and a 25:75 split over USY. The overall gas:liquid ratios did not change noticeably with increasing Ni loading from 2.5 to 10 % (Figure 6-3B). Again, the difference suggests the more open structure of the USY (0.74 x 0.74 nm) with α-cage compared to the more confined Beta (0.65 x 0.67, 0.56 x 0.56 nm).

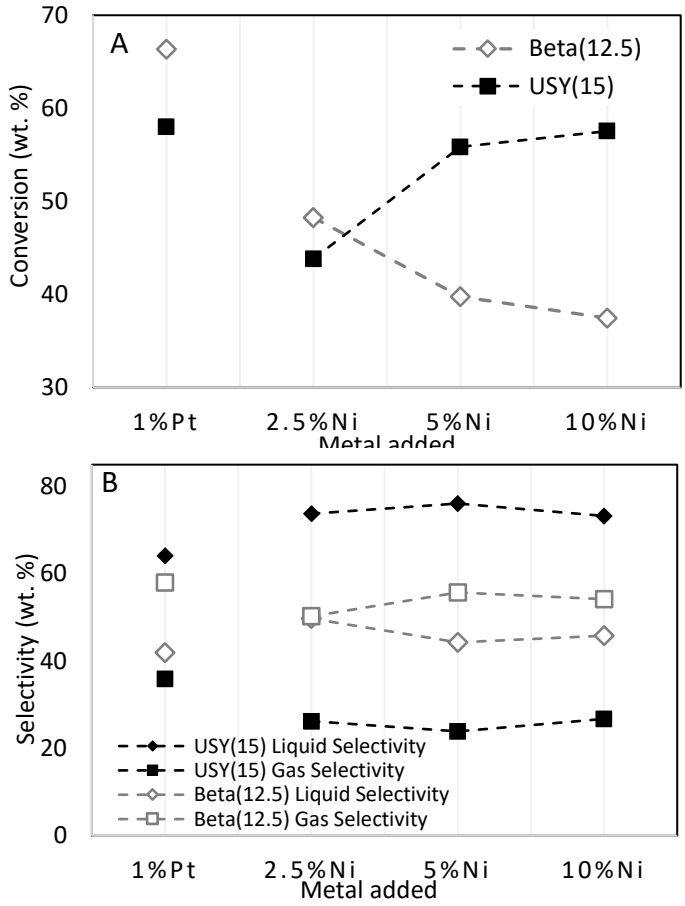

Figure 6-3 (A) Conversion from solid to fluids and (B) selectivity of gas and liquid in the product stream of hydrocracking mixed post-consumer polymers over zeolite Beta and USY impregnating with 1% Pt and different Ni levels at 330 °C and 20 bar.

Table 6-3 Coke deposition content over used catalysts

Catalyst	Coke level (wt. %)	Catalyst	Coke level (wt. %)
BPt1	4.8	YPt1	11.8
BNi2.5	11.5	YNi2.5	12.2
BNi5	9.7	YNi5	12.0
BNi10	8.3	YNi10	10.6

The hydrocracking of post-consumer polymer mixture over zeolite BPt1 was selective more towards gaseous product, mainly C_3-C_4 (Figure 6-4) and may partially resulted from the high proportion of polyethylene (57 wt.% of the feed) in the feed stream, which typically converted into LPG range products, based on a previous study.[13] However, this selectivity decreased with replacing the Pt by Ni (Figure 6-5A). For the USY, the hydrocracking activity increased when the Ni level increased on the catalyst, without significant effect on the product distribution (Figure 6-4). The higher

reactivity on the well dispersed Pt catalysts may have led to secondary reactions (e.g. YPt1, coke content =11.8%),[13] however for BPt1 the coke level was much lower (4.8%). In this case, it may be that pore blockage became more significant and the sites on the surface of the catalyst were less effective, yielding larger fragments and more LPG.

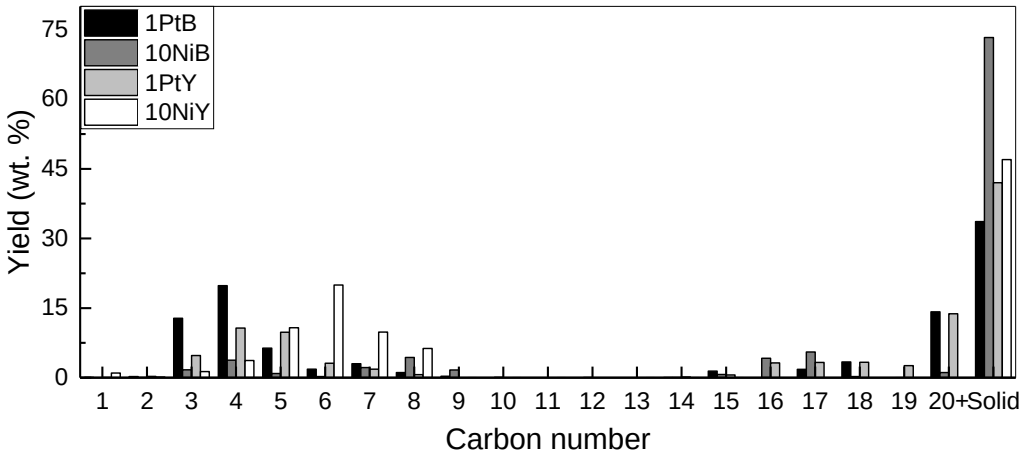

Figure 6-4 Product distribution of hydrocracking mixed post-consumer polymers over zeolite Beta and USY impregnating with 1 wt.% Pt and 10 wt.% Ni at 330 °C and 20 bar.

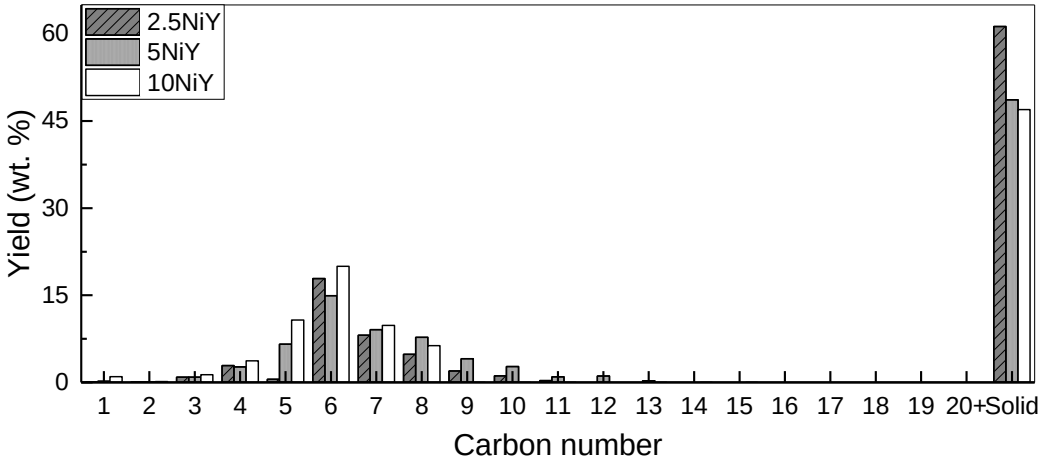

Figure 6-5 Product distribution of hydrocracking mixed post-consumer polymers over zeolite USY impregnating with different Ni levels at 330 °C and 20 bar.

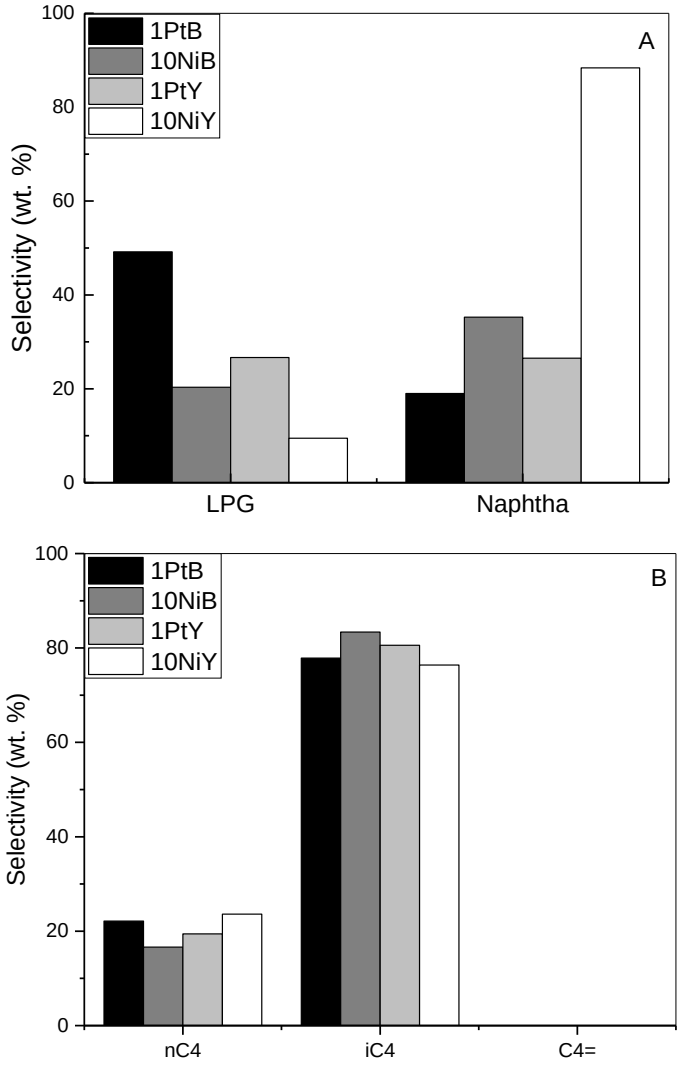

Figure 6-6 Selectivity of (A) LPG (C_3-C_4) and naphtha (C_5-C_{12}) in the overall product stream (B) normal and iso-paraffins, and olifins in the C_4 stream of hydrocracking mixed post-consumer polymers over zeolite Beta and USY impregnating with 1 wt.% Pt and 10 wt.% Ni at 330 °C and 20 bar.

Over all the catalysts used, the ratio of iso/normal alkanes was 4:1, indicating high octane number of the liquid produced (Figure 6-6B). Both metals (Pt and Ni) were highly effective in providing the metal function needed for the hydrogenation reactions, based on the absence of olefins in any of the product streams from the tested catalysts. The role of hydrogen in the hydrocracking system is to maintain the activity of the Pt and Ni, and reduce the coke formation, as well as to hydrogenate the olefins yielded in the earlier stage of the hydrocracking mechanism.[13] Figure 6-7 indicates that the H_2 concentration in the product stream was proportional to the rate the polymer degraded, with the higher conversion, the lower H_2 concentration in the product gas

stream. With the highest conversion obtained over BPt1 there was a surplus of 40% of H_2 concentration in the gas stream.

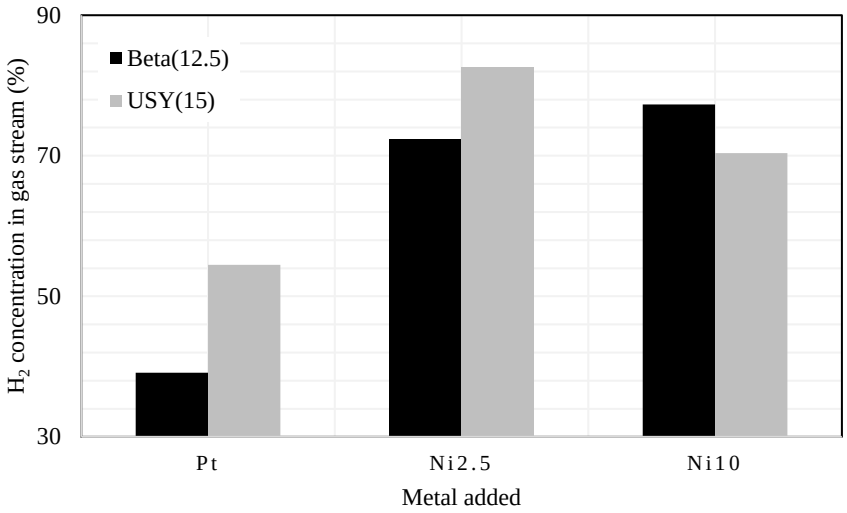

Figure 6-7 H_2 concentration in the gas stream of hydrocracking mixed post-consumer polymers over zeolite Beta and USY impregnating with 1% Pt and different Ni levels at 330 °C and 20 bar.

6.5 Conclusions

Replacing costly Pt with Ni supported zeolite Beta(12.5) and USY(15) was investigated for the hydrocracking post-consumer polymer under mild reaction condition (330 ^{o}C, 20 bar H_2 and 30 min). Generally, both zeolites showed high performance and great potential to yield a rich, highly branched paraffinic stream from polymer waste. The replacement of Pt by Ni negatively impacted on the hydrocracking activity of zeolite beta with increasing Ni content potentially causing pore blockage and preventing the access of reactants to the active sites. However, polymer degradation over USY increased with Ni loading eventually the same level of conversion obtained with YNi10 as with YPt1. Significantly, YNi10 was highly selective catalyst towards C_5-C_8 branched saturated hydrocarbons compared to YPt1 (Figure 6-6).

Although not without its problems environmentally, this work has demonstrated that switching from Pt to Ni achieved similar conversions with enhanced selectivity to one

distillate fraction. As such the replacement of Pt with Ni would reduce overall operational expenditure.

6.6 Acknowledgements

The authors would like to acknowledge the support of King Saud University in Riyadh (KSU) for research funding. In addition, we would like to thank the contribution of Dr. Desmond Doocey and Dr. Sarayute Chansai. Finally, the UK Catalysis Hub is kindly thanked for resources and support for Dr Tedstone via our membership of the UK Catalysis Hub Consortium and funding through EPSRC grant EP/R027129/1.

6.7 References

1. Ding, W.; Liang, J.; Anderson, L. L., Hydrocracking and hydroisomerization of high-density polyethylene and waste plastic over zeolite and silica alumina supported Ni and Ni/Mo sulfides. *Energy Fuels* **1997,** *11* (6), 1219-1224.

2. Munir, D.; Amer, H.; Aslam, R.; Bououdina, M.; Usman, M. R., Composite zeolite beta catalysts for catalytic hydrocracking of plastic waste to liquid fuels. *Materials for Renewable Sustainable Energy* **2020,** *9*, 1-13.

3. Garforth, A. A.; Ali, S.; Hernández-Martínez, J.; Akah, A., Feedstock recycling of polymer wastes. *Current Opinion in Solid State and Materials Science* **2004,** *8* (6), 419-425.

4. Munir, D.; Irfan, M. F.; Usman, M. R., Hydrocracking of virgin and waste plastics: a detailed review. *Renewable Sustainable Energy Reviews* **2018,** *90*, 490-515.

5. Brems, A.; Baeyens, J.; Dewil, R., Recycling and recovery of post-consumer plastic solid waste in a European context. *Thermal Science* **2012,** *16* (3), 669-685.

6. Nakaji, Y.; Tamura, M.; Miyaoka, S.; Kumagai, S.; Tanji, M.; Nakagawa, Y.; Yoshioka, T.; Tomishige, K., Low-temperature catalytic upgrading of waste polyolefinic plastics into liquid fuels and waxes. *Applied Catalysis B: Environmental* **2020,** *285*, 119805.

7. Corma, A.; Planelles, J.; Sanchez-Marin, J.; Tomas, F., The role of different types of acid site in the cracking of alkanes on zeolite catalysts. *Journal of Catalysis* **1985,** *93* (1), 30-37.

8. Ochoa, R.; Van Woert, H.; Lee, W.; Subramanian, R.; Kugler, E.; Eklund, P., Catalytic degradation of medium density polyethylene over silica-alumina supports. *Fuel Processing Technology* **1996,** *49* (1-3), 119-136.

9. Escola, J.; Aguado, J.; Serrano, D. P.; Briones, L., Transportation fuel production by combination of LDPE thermal cracking and catalytic hydroreforming. *Waste Management* **2014,** *34* (11), 2176-2184.

10. Hesse, N. D.; White, R. L., Polyethylene catalytic hydrocracking by PtHZSM-5, PtHY, and PtHMCM-41. *Journal of Applied Polymer Science* **2004,** *92* (2), 1293-1301.

11. Akah, A.; Hernandez-Martinez, J.; Rallan, C.; Garforth, A. A., Enhanced feedstock recycling of post-consumer plastic waste. *Chemcal Engineering Transsactions* **2015,** *43*, 2395-2400.

12. Venkatesh, K. R.; Hu, J.; Wang, W.; Holder, G.; Tierney, J.; Wender, I., Hydrocracking and hydroisomerization of long-chain alkanes and polyolefins over metal-promoted anion-modified zirconium oxides. *Energy Fuels* **1996,** *10* (6), 1163-1170.

13. Bin Jumah, A.; Anbumuthu, V.; Tedstone, A. A.; Garforth, A., Catalyzing the Hydrocracking of Low Density Polyethylene. *Industrial & Engineering Chemistry Research* **2019,** *58* (45), 20601-20609.

14. Celik, G.; Kennedy, R. M.; Hackler, R. A.; Ferrandon, M.; Tennakoon, A.; Patnaik, S.; LaPointe, A. M.; Ammal, S. C.; Heyden, A.; Perras, F. A., Upcycling single-use polyethylene into high-quality liquid products. *ACS Central Science* **2019,** *5* (11), 1795-1803.

15. Deldari, H., Suitable catalysts for hydroisomerization of long-chain normal paraffins. *Applied Catalysis A: General* **2005,** *293*, 1-10.

16. Kim, J.; Han, S. W.; Kim, J.-C.; Ryoo, R., Supporting nickel to replace platinum on zeolite nanosponges for catalytic hydroisomerization of n-dodecane. *ACS Catalysis* **2018,** *8* (11), 10545-10554.

17. Lugstein, A.; Jentys, A.; Vinek, H., Hydroisomerization and cracking of n-octane and C8 isomers on Ni-containing zeolites. *Applied Catalysis A: General* **1999,** *176* (1), 119-128.

18. Karthikeyan, D.; Lingappan, N.; Sivasankar, B.; Jabarathinam, N. J., Activity and selectivity for hydroisomerisation of n-decane over Ni impregnated Pd/H-mordenite catalysts. *Applied Catalysis A: General* **2008,** *345* (1), 18-27.

19. MarketsInsider Nickel price today. https://markets.businessinsider.com/commodities/nickel-price (accessed 05/04/2021).

20. Hassan, H.; Regnier, N.; Pujos, C.; Defaye, G., Effect of viscous dissipation on the temperature of the polymer during injection molding filling. *Polymer Engineering & Science* **2008,** *48* (6), 1199-1206.

21. Griskey, R. G.; Wiehe, I. A., Heat transfer to molten flowing polymers. *AIChE Journal* **1966,** *12* (2), 308-312.

22. Escola, J. M.; Aguado, J.; Serrano, D. P.; Briones, L.; Díaz de Tuesta, J. L.; Calvo, R.; Fernandez, E., Conversion of polyethylene into transportation fuels by the combination of thermal cracking and catalytic hydroreforming over Ni-Supported hierarchical beta zeolite. *Energy Fuels* **2012,** *26* (6), 3187-3195.

23. Garforth, A. A.; Lin, Y.-H.; Sharratt, P.; Dwyer, J., Catalytic polymer degradation for producing hydrocarbons over zeolites. In *Studies in Surface Science and Catalysis*, Hattori, H.; Otsuka, K., Eds. Elsevier: 1999; Vol. 121, pp 197-202.

24. Salmiaton, A.; Garforth, A. A., Multiple use of waste catalysts with and without regeneration for waste polymer cracking. *Waste Management* **2011,** *31* (6), 1139-1145.

25. Munir, D.; Usman, M. R. In *Synthesis and characterization of mesoporous hydrocracking catalysts*, IOP Conference Series: Materials Science and Engineering, IOP Publishing: 2016; pp 1-7.

26. Munir, D.; Piepenbreier, F.; Usman, M. R., Hydrocracking of a plastic mixture over various micro-mesoporous composite zeolites. *Powder Technology* **2017,** *316*, 542-550.

27. PlasticsEurope Plastics –the facts 2017 An analysis of European plastics production, demand and waste data. https://www.plasticseurope.org/application/files/5715/1717/4180/Plastics_the_facts_2017_FINAL_for_website_one_page.pdf (accessed 10/02/2021).

28. Wannapakdee, W.; Yutthalekha, T.; Dugkhuntod, P.; Rodponthukwaji, K.; Thivasasith, A.; Nokbin, S.; Witoon, T.; Pengpanich, S.; Wattanakit, C., Dehydrogenation of propane to propylene using promoter-free hierarchical Pt/Silicalite-1 nanosheets. *Catalysts* **2019,** *9* (2), 174.

29. Fúnez, A.; De Lucas, A.; Sánchez, P.; Ramos, M. J.; Valverde, J. L., Hydroisomerization in liquid phase of a refinery naphtha stream over Pt–Ni/H-beta zeolite catalysts. *Chemical Engineering Journal* **2008,** *136* (2-3), 267-275.

30. Gac, W.; Greluk, M.; Słowik, G.; Millot, Y.; Valentin, L.; Dzwigaj, S., Effects of dealumination on the performance of Ni-containing BEA catalysts in bioethanol steam reforming. *Applied Catalysis B: Environmental* **2018,** *237*, 94-109.

31. Huang, C.; Li, A.; Li, L.-J.; Chao, Z.-S., Synthesis of quinolines from aniline and propanol over modified USY zeolite: catalytic performance and mechanism

evaluated by in situ Fourier transform infrared spectroscopy. *RSC Advances* **2017,** *7* (40), 24950-24962.

32. Ding, W.; Liang, J.; Anderson, L. L., Thermal and catalytic degradation of high density polyethylene and commingled post-consumer plastic waste. *Fuel Processing Technology* **1997,** *51* (1-2), 47-62.

33. Auras, S. V.; van Lent, R.; Bashlakov, D.; Piñeiros Bastidas, J. M.; Roorda, T.; Spierenburg, R.; Juurlink, L. B., Scaling platinum-catalyzed hydrogen dissociation on corrugated surfaces. *Angewandte Chemie* **2020,** *132*, 21159 – 21165.

34. Schreiber, M. W.; Rodriguez-Niño, D.; Gutiérrez, O. Y.; Lercher, J. A., Hydrodeoxygenation of fatty acid esters catalyzed by Ni on nano-sized MFI type zeolites. *Catalysis Science Technology* **2016,** *6* (22), 7976-7984.

7 Conclusions and Future Work

7.1 Conclusions

This research has focused on the hydrocracking of single and mixed streams of pure and post-consumer polymers as a chemical recycling methodology. To achieve sustainable and circular economy when considering polymer recycling, hydrocracking is effectively more favourable than thermal and catalytic cracking routes. Hydrocracking successfully converts key polymer waste to a narrow range of refinery distillation cuts. In addition, this unit preserves the chemical value of polymer waste and reduce the need for landfilling.

In this study, mild reaction conditions of 175-330 °C, 20 bar H_2 and 15-60 minutes of reaction time were used to convert a model compound of squalane and four common different types of polyolefins, namely low and high density polyethylene (LDPE, HDPE), polypropylene (PP) and polystyrene (PS) found in consumer waste. The polymers were converted into valuable petroleum cuts of LPG and naphtha.

The results of hydrocracking of squalane at moderate reaction conditions (275 ^oC and 20 bar H_2) over Pt-USY and Pt-Beta obtained full conversion with a significant selectivity towards light oil stream. Chosen a large chain branched alkane, this suggested the possibility that branched larger polyolefins would to be hydrocracked under similar conditions. The complexity of individual bulkier polymers, however, resulted in very high viscosities on melting where created mass and heat transfer limitations. Batch reactor studies required the use of higher temperatures to achieve full conversion, typically, at 330 ^oC for the virgin polyolefin samples (i.e. Goodfellows).

To help better understand polymer degradation by hydrocracking, a lump model was developed to describe the result of a kinetic study at reduced conversion (temperature range 250-300 °C). Although more experimentation is needed to improve the model, this kinetic study of the hydrocracking of LDPE over 1% Pt-Beta (12.5) suggested that the external mass transfer could be minimised by reducing the catalyst particle size and increasing the agitation speed. However, the internal diffusion limitation cannot be ignored, especially at an earlier stage of cracking process of long chain hydrocarbons.

The hydrocracking of PE and PP streams gave a similar product stream of rich interestingly light and highly branched paraffins, at reaction conditions of 330 °C and 20 bar H_2. PS was converted into aromatic products exemplified by benzene and ethylbenzene suggesting that despite excess H_2 pressure determined at the end of reaction, the conditions were not sever enough to hydrogenate the aromatic ring. Zeolite Beta impregnated with 1% Pt demonstrated high conversion of the all tested polymers streams. Dealuminated USY with 1% Pt, however, was more selective towards liquid products (C_5-C_{20}) based on the wider pore structure. Switching from Pt to the significantly cheaper metal, Ni, was studied and similar activity to 1% Pt-USY(15) catalyst was achieved by impregnating 10% of Ni.

The research presented herein presents the effects of manipulating key process parameters for the production of hydrocarbons from polyolefins. The insights gained will help to overcome the mass- and heat- transfer limitations of heterogeneous catalysis in highly viscous polymer melts in future process design. It will be an important progression from uncatalyzed pyrolysis of municipal solid waste.

7.2 Future work

The last 2-3 years have seen unprecedented developments of technologies (highlighted in Table 1.1 Chapter 1) to regards plastic waste. These technologies include thermal hydrolysis using fluidised bed for small scale converting of polyolefins, and the use of supercritical water to separate, clean and hydrolyse polymers. The research of chemical polymer recycling by hydrocracking is still at early development stages and some further steps are still required to implement this recycling method. Firstly, a study of varying the percentage of each type of polymer in the feeding stream is important to simulate the reality of polymer waste batches using polymers of similar molecular weights used in packaging or other polymer products. Secondly, it will be necessary to investigate the reliability and performance of hydrocracking over different types of polymers, such as polyethylene terephthalate (PET) and polyvinyl chloride (PVC) is essential. Contamination of polyolefin feed would result in presence of O- and Cl- compounds in the system, which undoubtedly would affect the performance of the catalyst and quality of the products.

This work has shown a reliable batch system has been developed but the range of operating temperature and pressure conditions need to be extended. Therefore, catalysts development to selected products is also needed. Third, a further step is suggested of establishing a continuous setup by using melting extruder system to hydrocrack polymers at high hydrogen pressure and applying the optimum conditions obtained by the batch studies. In the continuous process, catalyst life could be studied as well as the influence of regeneration tests on deactivation behaviour. Finally, in-depth economic analysis would be performed to investigate the viability of recycling polymers via catalytic hydrocracking and its economic implications.